

**Novel technologies and process intensification in  
the production of micro-systems with  
pharmacological/nutraceutical activity**

**Annalisa Dalmoro**





Unione Europea



Ministero dell'Istruzione,  
dell'Università e della Ricerca



UNIVERSITÀ DEGLI  
STUDI DI SALERNO

## **FONDO SOCIALE EUROPEO**

**Programma Operativo Nazionale 2007/2013**

**“Ricerca Scientifica, Sviluppo Tecnologico, Alta Formazione”**

**Regioni dell'Obiettivo 1 – Misura III.4**

**“Formazione superiore ed universitaria”**

*Department of Industrial Engineering*

*Corso di dottorato in Scienza e tecnologie per  
l'industria chimica, farmaceutica e alimentare -  
curriculum Ingegneria Chimica  
(XI ciclo)*

**Novel technologies and process intensification in  
the production of micro-systems with  
pharmacological/nutraceutical activity**

### **Supervisors**

*Prof. Matteo d'Amore*

*Prof. Anna Angela Barba*

### **Ph.D. student**

*Annalisa Dalmoro*

### **Scientific Referees**

*Prof. Roland Bodmeier (Freie Universität Berlin)*

*Prof. Nadia Passerini (Università di Bologna)*

### **Ph.D. Course Coordinator**

*Prof. Paolo Ciambelli*



*Una ricerca comincia sempre con la Fortuna del Principiante.  
E finisce sempre con la Prova del Conquistatore.*

*Paulo Coelho, L'alchimista, 1988*



## Publications

*(Inherent the Ph.D. project)*

- **Dalmoro A.**; Barba A.A.; d'Amore M.; Lamberti G.; (2012), "Microparticles production by a single-pot semi-continuous bench scale apparatus", submitted to AIChE Journal;
- Barba A.A.; **Dalmoro A.**; d'Amore M.; Lamberti G.; "Controlled release of drugs from microparticles produced by ultrasonic assisted atomization based on biocompatible polymers", Chem. Biochem. Eng. Q., 26(4) 345-354 (2012);
- Barba A.A.; **Dalmoro A.**; d'Amore M.; (2012) "An engineering approach to biomedical sciences: advanced strategies in drug delivery systems production", Translational Medicine @ UniSa, 4 (1) 5-11 (2012);
- **Dalmoro A.**; Barba A.A.; Lamberti G.; Grassi M.; d'Amore M.; "Pharmaceutical applications of biocompatible polymer blends containing sodium alginate", Advances in Polymer Technology, 31(3) 219-230 (2012);
- **Dalmoro A.**; Barba A.A.; Lamberti G.; d'Amore M.; "Intensifying the microencapsulation process: Ultrasonic atomization as an innovative approach", European Journal of Pharmaceutics and Biopharmaceutics, 80 471-477 (2012);
- **Dalmoro A.**; Barba A.A.; d'Amore M.; Lamberti G.; "Micro-Systems Production: A Promising New Technique with Low Energy Consumption", Scientia Pharmaceutica, 78 (3) 670-670 (2010);





## Proceedings

- **A. Dalmoro**, A.A. Barba, G. Lamberti, M. d'Amore (2012), Sistemi particellari shell-core prodotti via atomizzazione assistita da ultrasuoni, *Convegno GRICU 2012* Montesilvano (PE) ITALY, 16-19 settembre 2012
- S. Cascone, **A. Dalmoro**, G. Lamberti, A.A. Barba (2012), Metodi innovativi di preparazione e testing per sistemi farmaceutici, *Convegno GRICU 2012* Montesilvano (PE) ITALY, 16-19 settembre 2012
- **A. Dalmoro**, M. d'Amore, A.A. Barba, Shell-core particles production by coaxial double channel device, presented to *8<sup>th</sup> World Meeting on Pharmaceutics, Biopharmaceutics and Pharmaceutical Technology*, 19<sup>th</sup>-22<sup>nd</sup> March 2012, Istanbul (Turkey)
- I. Galdi, **A. Dalmoro**, G. Lamberti, G. Titomanlio, A.A. Barba, M. d'Amore, Modeling of the controlled drug release from solid matrices based on swellable/erodible polymeric hydrogels, presented to *19<sup>th</sup> International Congress of Chemical and Process Engineering CHISA 2010 and the 7<sup>th</sup> European Congress of Chemical Engineering ECCE-7*, 28<sup>th</sup> August – 1<sup>st</sup> September 2010, Prague (Czech Republic)
- **A. Dalmoro**, I. Galdi, G. Lamberti, G. Titomanlio, A.A. Barba, M. d'Amore, Targeted oral drug delivery by pH-sensitive microparticles, presented to *19<sup>th</sup> International Congress of Chemical and Process Engineering CHISA 2010 and the 7<sup>th</sup> European Congress of Chemical Engineering ECCE-7*, 28<sup>th</sup> August – 1<sup>st</sup> September 2010, Prague (Czech Republic)
- I. Galdi, **A. Dalmoro**, G. Lamberti, G. Titomanlio, A.A. Barba, M. d'Amore, Swelling, erosion and drug release in hydrogel based solid matrices, presented to *7<sup>th</sup> World Meeting on Pharmaceutics, Biopharmaceutics and Pharmaceutical Technology*, 8<sup>th</sup>-11<sup>th</sup> March 2010, Valletta (Malta).
- Dalmoro, I. Galdi, G. Lamberti, G. Titomanlio, A.A. Barba, M. d'Amore. "PH-sensitive microparticles for enteric drug delivery by solvent evaporation from double emulsion", presented to *7<sup>th</sup> World Meeting on Pharmaceutics, Biopharmaceutics and Pharmaceutical Technology*, 8<sup>th</sup>-11<sup>th</sup> March 2010, Valletta (Malta).



# Contents

<b>Publications.....</b>	<b>iii</b>
<b>Proceedings .....</b>	<b>iii</b>
<b>Contents.....</b>	<b>I</b>
<b>Figures index.....</b>	<b>V</b>
<b>Tables index .....</b>	<b>IX</b>
<b>Abstract .....</b>	<b>XI</b>
<b>Introduction .....</b>	<b>1</b>
<b>1.1 Microencapsulation.....</b>	<b>2</b>
1.1.1 Importance of microencapsulation and applications _____	2
1.1.2 Fundamental steps of microencapsulation_____	3
1.1.3 Scale of production _____	6
<b>1.2 Process intensification.....</b>	<b>9</b>
<b>1.1 Aims of the PhD thesis .....</b>	<b>10</b>
<b>1.2 Outline of the thesis.....</b>	<b>11</b>
<b>State of the art .....</b>	<b>13</b>
<b>2.1 Microencapsulation apparatuses .....</b>	<b>14</b>

---

2.1.1 Patents _____	14
2.1.2 Other literature examples of apparatuses for microencapsulation _____	28
<b>2.2 Apparatuses at low energy consumption (US atomization).....</b>	<b>31</b>
2.2.1 Principles of the ultrasonic atomization and benefits ____	31
2.2.2 Spray-drying using an ultrasonic atomizer _____	34
2.2.3 Coaxial ultrasonic atomizer _____	37
<b>2.3 Remarks about state of the art .....</b>	<b>41</b>
<b>Ultrasonic atomization phenomena.....</b>	<b>43</b>
<b>3.1 Atomization .....</b>	<b>44</b>
3.1.1 Dripping _____	46
3.1.2 Ultrasonic atomization _____	47
<b>Microencapsulation apparatus building.....</b>	<b>51</b>
<b>4.1 General description of the apparatus .....</b>	<b>52</b>
4.1.1 The apparatus: first stage _____	52
4.1.2 The apparatus: final state _____	54
<b>4.2 Criteria of components selection .....</b>	<b>56</b>
4.2.1 Atomizing section _____	56
4.2.2 Feeding section _____	58
4.2.3 Separation/drying section _____	59
<b>4.3 Description of plant operation.....</b>	<b>60</b>
<b>Microencapsulation apparatus testing.....</b>	<b>63</b>
<b>5.1 Process parameters definition .....</b>	<b>64</b>
5.1.1 Operative parameters: feeding _____	64

---

---

5.1.1.a Materials: alginate	64
5.1.1.b Selection of feeding parameters	67
5.1.2 Operative parameters: atomization _____	71
5.1.3 Operative parameters: separation and stabilization _____	71
<b>5.2 Encapsulation of model molecules.....</b>	<b>72</b>
<b>5.3 Materials.....</b>	<b>73</b>
5.3.1 Vitamin B12 selection _____	73
5.3.2 $\alpha$ -tocopherol selection _____	75
<b>5.4 Methods .....</b>	<b>75</b>
5.4.1. Vitamin B12 particles manufacture _____	75
5.4.2 Vitamin B12 loading and release tests _____	77
5.4.3 $\alpha$ -tocopherol particles manufacture _____	77
5.4.4 $\alpha$ -tocopherol particles characterization _____	78
5.4.4.a Image analysis	78
5.4.4.b Dielectric properties	78
5.4.4.c Moisture and temperature measurements	79
5.4.4.d Differential scanning calorimetry	79
5.4.4.e $\alpha$ -tocopherol loading and release tests	79
5.4.4.f Apparatus power consuming	80
<b>5.5 Preliminary results (vitamin B12 encapsulation).....</b>	<b>81</b>
5.5.1 Steps towards atomization _____	87
<b>5.6 Results about final encapsulating tests.....</b>	<b>92</b>
5.6.1 Droplets size prediction by literature correlations _____	101
5.6.1.a Dripping	102
5.6.1.b Ultrasonic atomization	103
<b>Concluding remarks.....</b>	<b>107</b>

---

---

<b>6.1 Concluding remarks .....</b>	<b>108</b>
<b>Appendix A .....</b>	<b>113</b>
<b>A.1 Assay methods: UV-vis spectrometry vs HPLC ...</b>	<b>114</b>
A.1.1 Materials and Methods .....	114
A.1.2 UV-vis spectrometer: method of spectra subtraction__	117
A.1.3 HPLC analysis .....	120
A.1.4 Choice of the most reliable method .....	122
<b>Appendix B .....</b>	<b>125</b>
<b>B.1 Diffusion in a sphere .....</b>	<b>126</b>
<b>References .....</b>	<b>129</b>
<b>CURRICULUM VITAE .....</b>	<b>137</b>

## Figures index

Figure 1. Process intensification toolbox [31] .....	9
Figure 2. Idealization of the intensified plant of microencapsulation.....	11
Figure 3. Apparatus using a hydraulic piston for obtaining a sudden pressure change to achieve microencapsulation [33].....	14
Figure 4. Ultrasonic apparatuses for microencapsulation [33] .....	15
Figure 5. Scheme of the plant for the production of alginate pellets [34] .....	17
Figure 6. Two variations of the process for microspheres preparation [35] .....	18
Figure 7. Equipment configuration for preparing micro-particles using a static mixing assembly [8] .....	20
Figure 8. Scheme of the longitudinal cross-section of a mixing block [36] .....	20
Figure 9. Global scheme of a system comprising a mixing-block [36] .....	21
Figure 10. Different configurations of liquid-liquid extraction apparatus [26] .....	22
Figure 11. Process flow diagram of a system for micro-particles production using a contact tank with recycle, in a continuous process [38] .....	23
Figure 12. Scheme of the apparatus for producing micro-particles containing nucleic-acid [39].....	25
Figure 13. Scheme of three different apparatuses to produce micro-particles, including a freezing zone [38] .....	26
Figure 14. Flow diagram of the continuous spray-capture microencapsulation process [40] .....	28
Figure 15. BRACE microencapsulation process [41].....	29
Figure 16. Apparatus for co-axial electrohydrodynamic atomization [42].....	30
Figure 17. Ultrasonic frequency ranges, kind of applications and ultrasonic atomization mechanism sketch [45] .....	31
Figure 18. Scheme of an ultrasonic atomizer [53].....	35
Figure 19. Sketch of the vacuum spray-dryer (A) with detailed view of the ultrasonic nozzle (B) .....	36

---

Figure 20. Scheme of the ultrasound/spray-drying system [55] .....	36
Figure 21. Schematic description of the microencapsulation system using a coaxial ultrasonic atomizer [58] .....	38
Figure 22. Precision particle fabrication apparatus to produce uniform double-walled microspheres [57].....	39
Figure 23. The three sections of pumping/feeding, atomization and stabilization....	52
Figure 24. A scheme of the initial state of the apparatus .....	53
Figure 25. Scheme of the single-pot semi-continuous bench scale apparatus .....	54
Figure 26. Dimensional features, in mm, of wet-collector, with the details of both fluid dispenser ( <i>B</i> ) and filter ( <i>C</i> ).....	55
Figure 27. Cross-sectional view of a typical nozzle [66].....	57
Figure 28. Dual liquid feed assembly [66].....	58
Figure 29. Apparatus parameters to be controlled and optimized .....	64
Figure 30. Structure of alginate: chemical formula of MM, GM, GG blocks [72] ...	65
Figure 31. Molecular models of two GG dimers (up) and of two MM dimers (down) with Ca <sup>2+</sup> [74].....	66
Figure 32. Coaxial dripping to obtain shell-core systems.....	69
Figure 33. Example of shell-core particles: blue core confined in the transparent shell material.....	70
Figure 34. Shell-core particle and only-core (or matrix) particle .....	72
Figure 35. Vitamin B12 structure [81].....	74
Figure 36. Structure of $\alpha$ -tocopherol [81] .....	75
Figure 37. Parameters for particles manufacture by dripping .....	76
Figure 38. Pictures of fresh particles, both shell-core (up) and only-core (down), and of dried particles (CD: convective; MW: microwave) .....	81
Figure 39. Fraction of B12 released in a phosphate buffer at pH 7.4, particles obtained by dripping, without drying (fresh particles) .....	82
Figure 40. Fraction of B12 released in a phosphate buffer at pH 7.4, particles obtained by first dripping and then drying in a tray-oven with air at 45°C .....	83
Figure 41. Fraction of B12 released in a phosphate buffer at pH 7.4, particles obtained by first dripping and then drying in a microwave cavity.....	84
Figure 42. Mass of B12 released in the phosphate buffer at pH 7.4 for fresh, convective dried, and microwave dried particles.....	85
Figure 43. Fraction of B12 released in two step test, particles obtained by dripping without drying (fresh particles) .....	86

---



---

Figure 44. Fraction of B12 released in two step test, particles obtained by first dripping and then drying in a tray-oven with air at 45°C .....	86
Figure 45. Fraction of B12 released in two step test, particles obtained by first dripping and then drying in a microwave cavity .....	87
Figure 46. Optical microscope picture of shell-core micro-particles obtained by coaxial ultrasonic atomization (P=4W) .....	88
Figure 47. Drop diameter distribution for 25 KHz ultrasonic atomizer (data for water) [66] .....	89
Figure 48. HPLC signals deriving from HPLC analysis of supernatant and washing water of both shell-core and matrix preparations .....	90
Figure 49. HPLC signals of pH 1 solutions (first part of two step release test) after 10 minutes of dissolution of respectively shell-core (dotted line) and only core (solid line) micro-particles.....	90
Figure 50. Optical microscope pictures of shell-core micro-particles: fresh (down) and dried (up) .....	92
Figure 51. Comparison between dielectric properties of water (triangles) and those of produced micro-particles (circles) at room temperature .....	93
Figure 52. UP: DSC scans of pure alginate, cross-linking powder CaCl <sub>2</sub> , physical mix of alginate and CaCl <sub>2</sub> ; DOWN: DSC scans of pure alginate, particles of cross-linked alginate obtained by atomization and then dried by convective drying (CD) or by microwave drying (MW) .....	95
Figure 53. $\alpha$ -tocopherol released (amount of TOC released and measured/theoretical loaded amount of TOC) from alginate matrix and shell-core micro-particles, produced by ultrasonic atomization and stabilized by convective drying (up) or by microwave drying (down) .....	96
Figure 54. $\alpha$ -tocopherol released (amount of TOC released and measured/theoretical loaded amount of TOC) from alginate matrix and shell-core macro-particles (beads), stabilized by convective drying (up) or by microwave drying (down) .....	98
Figure 55. $\alpha$ -tocopherol released (amount of TOC released and measured/theoretical loaded amount of TOC) from alginate matrix micro (stars) and macro-particles (squares), stabilized by convective drying (up) or by microwave drying (down) .....	99
Figure 56. Repartition of power consumed among atomization (2.9%), hardening and separation (1.6%), drying (95.4%). This percentage is defined as the ratio between the specific energies, (joule)/(g of fresh product), of a single section (for example, atomization section) and the sum of the three sections .....	100
Figure 57. Nozzle geometry and relevant dimensions .....	103
Figure 58. Spectra of alginate particles, dried by convective drying (CD) or by microwave drying (MW), and put in three solutions (pH1, bicarbonate buffer	

---

---

and phosphate buffer, both at pH 7.4) at two different concentrations (0.5 g/l; 1 g/l).....	117
Figure 59. Absorbance spectrum (solid line), exponential (dashed line), and curve obtained by subtraction (dotted line), for a system alginate-B12 obtained by dripping it in the cross-linking solution and drying in a tray oven with air at 45°C, and then dissolved in a phosphate buffer at pH 7.4 .....	118
Figure 60. Absorbance spectrum (solid line), exponential (dashed line), and curve obtained by subtraction (dotted line), for a system alginate-B12 obtained by atomizing it in the cross-linking solution, drying in a tray-oven with air at 45°C, and then dissolved in a phosphate buffer at pH 7.4. Top: full spectrum; down: particular of spectrum in the range 300-400 nm .....	119
Figure 61. Signals given by HPLC analysis, using the three different separation procedures.....	121

## Tables index

Table 1. Example of some microencapsulated molecules [1].....	2
Table 2. Main methods for micro-particles preparation [3].....	4
Table 3. A comparison between the features of static and CSTR mixers [20] .....	5
Table 4. Microencapsulation processes and their applicabilities [1] .....	7
Table 5. PLGA based micro-particle formulations available on the market [29] .....	8
Table 6. Variable flow rates, mL/min, according to the combination of drive options and tube diameters [67].....	59
Table 7. Typical properties of alginate Manugel GHB [79] .....	68
Table 8. Polymer (alginate) concentrations (w/w) of both core and shell solutions and their effect .....	70
Table 9. Parameters selected for $\alpha$ -tocopherol particles production .....	78
Table 10. Size mean and standard deviation for both shell-core and matrix particles, fresh and dried (CD or MW); shrinkage percentage for the dried ones ....	81
Table 11. Mean size and standard deviation for both shell-core and matrix micro-particles, fresh and dried; volumetric shrinkage percentage for the dried ones .....	92
Table 12. Physical properties of Manugel GHB alginate solutions [79]: the properties of a solution with a concentration of 1.5% (w/w) are highlighted.....	101
Table 13. Values to insert in correlations for droplet size prediction in ultrasonic atomization .....	103
Table 14. Features of the three different HPLC procedures .....	121
Table 15. Comparison among different ways for detection of vitamin B12 in a system containing alginate (particles obtained by dripping) .....	122
Table 16. Comparison among different ways for detection of vitamin B12 in a system containing alginate (particles obtained by atomization) .....	122

---

---

## Abstract

Purpose of the PhD thesis was to develop a novel microencapsulation process, designing and building a single-pot semi-continuous bench scale apparatus. The novel process is based on the coupling of two emerging techniques, involving ultrasound and microwave, used in atomization and heating operations, respectively. The process has been designed to respond to the needs for process intensification, i.e. improvement of process efficiency and cutting down of energy consumption. With this aim, a review of the main processes used for microencapsulation was first performed: conventional processes showed a number of drawbacks, such as high energy consumption, batch configuration, use of solvents and long times of production. On the basis of the state of the art, the idea of an intensified apparatus for particles production, exploiting alternative resources, such as ultrasound and microwave, was formulated. The apparatus was composed of three main sections: feeding, atomization, separation/stabilization. The feeding and atomization sections were built connecting a double channel ultrasonic atomizer to a system for feeding solutions in a purposely designed separation/stabilization section, thus realizing a semi-continuous apparatus. Separation section consisted of a wet-collector, i.e. a sort of hydrocyclone, which allowed a uniform distribution of the hardening solution and the consequent contact with the atomized drops, a filtering device, and a microwave oven. The wet-collector was placed into the microwave oven to obtain an “on-line” drying. Recirculation of the hardening solution, to renew contact surface between droplets and cross-linker, was guaranteed by a system of centrifugal pumps. In this configuration, when atomization occurred, drops were harvested in the wet-collector. After atomization, the obtained suspension was collected in the cross-linker tank, then the filtering device was inserted in the lower part of the wet-collector, so that hardening solution was recovered and particles

---

settled on the filter, when the suspension was brought again to the wet-collector and after its complete emptying. An eventual following washing step can be done in a similar way to the previous hardening step. Finally, particles were stabilized by microwave drying, and then recovered.

The steps for building the microencapsulation apparatus were accurately shown. Then, criteria used for components selection, in order to obtain the best performances from the plant, were highlighted. After building the plant, the process parameters were defined. First, the research for the best combination of feeding parameters, such as type of materials, composition, concentration and feed rate, that assure the encapsulation of the core material in the shell, was carried out. Then, the parameters of the ultrasonic atomizer (atomization section), essentially power, were tuned. Finally, for stabilization/separation section, fundamental was the relevant stabilization step, where microwave power was set to avoid too high temperatures that could degrade molecules.

The ability of the novel plant to obtain micronized systems, that exhibit a behavior interesting for the pharmaceutical or nutraceutical markets, was tested. Micro-particles characterization showed that it is possible to obtain a shell-core configuration encapsulating two functional molecules, vitamin B12 and  $\alpha$ -tocopherol. Some important results were: 1) high loading and enteric (gastro-resistant) behavior of micro-particles; 2) delayed release for shell-core micro-systems compared to matrix ones; shell-core configuration in macro-scale (beads) able to prevent degradation of  $\alpha$ -tocopherol, instead observed in matrix beads. Moreover, microwave treatment (not harsher for the short irradiation times) caused, especially for shell-core configuration, a little delay in molecule release. Resuming, better release properties for systems produced in the novel apparatus were achieved by the coupling of ultrasonic atomization and microwave drying. Furthermore, the basic transport phenomena occurring in the ultrasonic assisted atomization were investigated, emphasizing the role of operative parameters, and literature correlations, based on forces balance, were also applied for droplets size prediction. All these results endorses the usefulness of the novel plant, based on the combination of two powerful tools of process intensification, ultrasonic atomization and microwave drying, to obtain micro-systems, particularly interesting for specific drug delivery

---

applications. Moreover, working at room conditions and in absence of solvents, improving the energy transfer rate (faster process times), reducing process chambers volume (low particles inertia in ultrasonic atomization, single-pot process realization), enhancing the product quality (micro-particles with tailored features), makes the apparatus more attractive in terms of improved inherent safety and reduced costs.

---

---



---

# Chapter One

---

## **Introduction**

*This chapter outlines the importance of microencapsulation processes, with the related applications and scales of production. Moreover, the concept of process intensification is explained. Then, the aims of the thesis are briefly shown and its organization presented.*

---

## 1.1 Microencapsulation

Microencapsulation is a process by which substances (solids, liquids or gases) may be wrapped in polymeric thin coatings resulting in microscopic particles [1].

### 1.1.1 Importance of microencapsulation and applications

A lot of compounds were incorporated in microcapsules or microspheres by different techniques, in order to stabilize them, convert them into powders, mask undesired taste, or provide modified release properties [2]. Industrial applications for molecules microencapsulation are several: prolonged release of pesticides and herbicides in agriculture's field; spices encapsulation in food industry; incorporation of essences, vitamins and solar filters in the field of cosmetics; modifying release of drugs for oral, buccal, nasal and parenteral use, protection of active principles and cells encapsulation for pharmaceutical industry [3]. Some microencapsulated molecules are shown in Table 1.

**Table 1. Example of some microencapsulated molecules [1]**

Drug/Core material	Characteristic property	Purpose of encapsulation	Final product form
Acetaminophen	Slightly water soluble solid	Taste masking	Tablet
Aspirin	Slightly water soluble solid	Taste masking, sustained release, reduced gastric irritation, separation of incompatibles	Tablet or capsule
Islet of Langerhans	Viable cells	Sustained normalization of diabetic condition	Injectable
Isosorbide dinitrate	Water soluble solid	Sustained release	Capsule
Menthol	Volatile solution	Reduction of volatility, sustained release	Lotion
Progesterone	Slightly water soluble solid	Sustained release	Varied
Potassium chloride	Highly water soluble solid	Reduced gastric irritation	Capsule
Urease	Water soluble enzyme	Permselectivity of enzyme, substrate, and reaction products	Dispersion
Vitamin A pamate	Nonvolatile liquid	Stabilization to oxidation	Dry powder

In particular, in the pharmaceutical field, a well designed controlled drug delivery system can overcome some of the problems of conventional therapies and enhance the therapeutic efficacy of a given drug. To obtain maximum therapeutic efficacy, the molecule has to be

delivered to the target tissue in the optimal amount, in the right period of time, to cause little toxicity and minimal side effects. There are various approaches in delivering a therapeutic substance to the target site in a sustained controlled release way. One of them is using micro-systems as carriers for drugs [1]. Microcapsules can be widely distributed throughout the gastro-intestinal tract, potentially improving drug absorption and reducing side effects due to localized drug on the gastro-intestinal mucosa [4]. Therefore, oral controlled-release multiple-unit dosage forms (pellets, granules or micro-particles) offer several advantages over single-unit dosage forms (capsules or tablets) [5]. Moreover, research in finding new or improving microencapsulation techniques for newly discovered molecules is in constant progress because of the limitations of the current pharmacopeia. The new active molecules, found with the help of advances in biotechnology and therapeutic science, are more often peptides or proteins; they are very active in small doses, sensitive to unfolding by heat or organic solvents, available only in small quantities, and very expensive. Therefore, the stability and the biological activity of the drug should not be affected during the microencapsulation process, yield and drug encapsulation efficiency should be high, microsphere quality and drug release profile should be reproducible within specified limits, microspheres should not exhibit aggregation or adherence, the process should be useful at an industrial scale, and the residual level of organic solvent should be lower than the limit value imposed by the European Pharmacopeia [6]. The realization of the potential that microencapsulation offers involves a basic understanding of the general properties of micro-particles, such as the nature of the core and coating materials, the stability and release characteristics of the coated materials and the microencapsulation methods [1].

### *1.1.2 Fundamental steps of microencapsulation*

The preparation of micro-particles is achieved by both physical-chemical and mechanical processes (Table 2). The choice of the process comes from polymer nature, final particles size and chemical features of drug, especially drug solubility in the polymeric material [4].

**Table 2. Main methods for micro-particles preparation [3]**

Chemical processes	Mechanical processes
Phase separation or coacervation	Spray drying
Interfacial polymerization	Spray cooling
Reticulation in suspension	Fluid bed
Thermal gelatinization	Electrostatic laying
Solvent evaporation	

However, most of the microencapsulation techniques are based on modifications of three basic methods: solvent extraction/evaporation, phase separation (coacervation), and spray drying. For each method, the main steps are [7-8]:

- incorporation of active compounds;
- droplets formation;
- solvent removal;
- micro-particles harvest and drying.

Active compounds may be added to the matrix/coating material (first step) by either co-dissolution in a common solvent, dispersion of finely pulverized solid material, or emulsification if matrix and molecule-containing solution are immiscible [9].

The droplet formation step is fundamental because it determines size and size distribution of the resulting micro-particles, which in turn affect drug release rate and drug encapsulation efficiency. The main procedures used for droplet formation are: stirring, static mixing, extrusion (single pathway system, multichannel system or membranes), and dripping (single droplet formation or jet excitation). In stirring the impeller speed is the main parameter for controlling the droplets size of drug/matrix dispersion in the continuous phase: smaller droplets are obtained by stronger shear forces and increased turbulence when stirring speed increases [10-13]. The extent of size reduction depends on the viscosity of the disperse and continuous phases [5-6, 14-15], the interfacial tension between the two phases [5-6, 14, 16], their volume ratio [16-17], the geometry and number of the impellers, and the size ratio between impeller and mixing vessel [18-19].

Static mixing consists in using baffles or other flow obstacles installed in a tube. The baffle arrangement splits and recombines the stream of

fluid passing through the tube, creating turbulence and inducing back-mixing. There are several advantages of static mixing against continuously stirred tank reactors (CSTR). They are resumed in Table 3.

**Table 3. A comparison between the features of static and CSTR mixers [20]**

Characteristics	Static mixer	CSTR mixer
Process	Continuous	Batch
Mixing efficiency	High	Low
Energy efficiency	High	Low
Particle size distribution	Same	Same
Large-scale production	Easy and predictable	Unpredictable
Cost	Inexpensive	Expensive
Cleaning and maintenance	Easy	Inconvenient

Another mechanism for droplet formation is the extrusion, which consists in feeding the drug/matrix dispersion through a single or a plurality of pathways into the continuous phase. Droplets of the drug/matrix dispersion are formed within the slowly flowing continuous phase, which also provide the droplets transport away from the site of their formation. There are some differences between extrusion and static mixing. In extrusion, the flow is mainly laminar and the droplets are formed directly at the site of introduction of the dispersed phase into the continuous phase and they don't change their dimension thereafter (negligible coalescence). On the contrary, static mixing relies mainly on turbulent flow, which acts on the dispersed phase and thus causes droplets size to change over the whole length of the mixer. Therefore, extrusion gives more uniform and better controlled micro-particles sizes than static mixing [7]. Extrusion can be achieved in single pathway systems, through a continuous injection of a drug/matrix dispersion into a flow of a continuous phase [21], or in multichannel systems, that is micro-mixers consisting of an array of fine channels or microporous membranes.

As concern dripping, jet excitation is powerful in combining productivity and microsphere size control. It consists in the vibration of a liquid jet in order to obtain its disruption into droplets: a longitudinal oscillation imposed on a liquid stream causes periodic surface instabilities, which break up the liquid into uniform droplets [22].

The step that follows the droplet formation is the removal of the solvent of the disperse phase, usually obtained by evaporation or

extraction. Solvent extraction/evaporation neither requires elevated temperatures nor phase separation inducing agents [7]. In both solvent extraction and evaporation, the solvent of the disperse phase must be slightly soluble in the continuous phase so that partitioning into the continuous phase can occur leading to precipitation of the matrix material [23]. The solvent evaporation method is widely used for micro-particles preparation because of its simplicity [3, 6, 23]. The evaporation can be promoted by high temperatures or by reduced pressures [24]: the temperature should be not too high to avoid the damage of the drug; therefore, applying a reduced pressure seems to be a better choice [25].

In solvent extraction, the amount and composition of the continuous phase are chosen so that the volume of the disperse phase solvent can be dissolved. So it may require relatively large amounts of processing fluids and their subsequent recycling [26].

The last step for micro-particles preparation consists in separation, washing and drying. Separation of the solidified microspheres from the continuous phase is usually done either by filtration or centrifugation. Then, washing is required to remove stabilizer or not encapsulated drug: rinsing may involve high temperatures or the use of extraction agents to reduce the amount of residual solvent in the microspheres [27]. Finally, the microspheres are dried either at ambient conditions or under reduced pressure, by heat or by lyophilisation.

### *1.1.3 Scale of production*

The number of encapsulation processes cited in the literature has increased significantly since the 50's, reflecting the growth of research and development in this field [6]: in 2002, over 1000 patents were filed concerning microencapsulation processes. While some new processes are expensive, difficult to be scaled scale up and with a narrow applicability range, others seem to be promising for the encapsulation of active molecules [28]. The first processes developed at an industrial scale were the mechanical ones: spray drying, and pan coating. Today, a large number of microencapsulation processes are identified at different production scales (Table 4). Moreover, examples of micro-particle products, that have entered the market, are shown in Table 5, with the expected manufacturing procedure [29].

**Table 4. Microencapsulation processes and their applicabilities [1]**

<b>Method name</b>	<b>Particle size, <math>\mu\text{m}</math></b>	<b>Production scale</b>	<b>Process reproducibility</b>	<b>Time for preparation</b>	<b>Operation skill required</b>
Air suspension	35-5000	Pilot scale	Moderate	High	High
Coacervation and Phase separation	2-5000	Lab scale	Good	Less	Less
Multiorifice Centrifugal	1-5000	Pilot scale	Moderate	High	High
Pan Coating	600-5000	Pilot scale	Moderate	High	High
Solvent Evaporation	5-5000	Lab scale	Good	Less	Less
Spray Drying and Spray Congealing	600	Pilot scale	Moderate	High	High

In the manufacture of microencapsulated products, industry tends to protect information about scale-up and knowledge about equipment and manufacturing as internal “know how” [6]. The scale-up process will almost always require larger piping and higher flow rates, particularly when the scale factor is very large or the process times have to be kept similar to the smaller scale process. Scale-up into new, larger equipment is often unpredictable and achieved through trial and error experiments, which can be more expensive [8]. Furthermore, the literature concerning microencapsulation processes generally focuses on the methodology used for particles preparation, with the aims of maximum loading and controlled release. Articles describe the influence of formulation parameters (physicochemical) such as the nature and concentration of materials, viscosity of the phases. Process parameters such as stirring rate, addition rate of the coacervation or polymerization agent, and temperature are also studied. However, almost all the published works lead to qualitative or semi-empirical relations between parameters and particles properties. In the cases where no specific methodology has been followed in the lab for producing microcapsules, there is a high risk of uncontrolled evolution of the main characteristics of the capsules (size, structure, and content) produced at larger scales. The only solution is then to adapt the operating process, defined in the laboratory, to the pilot or to the final plant [6].

**Table 5. PLGA based micro-particle formulations available on the market [29]**

<b>Drug</b>	<b>Product</b>	<b>Distributor</b>	<b>Technique</b>
<i>Peptides</i>			
Octreotide acetate	Sandostatin LAR® Depot	Novartis	Coacervation
Leuprolide acetate	Lupron Depot® (North America) Enantone®; Trenantone® (Europe) Prostap SR; Prostap 3 (GB)	TAP Pharmaceuticals Takeda Wyeth	w/o/w emulsion solvent evaporation
Triptorelin acetate	Decapeptyl® Depot Gonapeptyl® Depot (GB) Decapeptyl® SR (GB) Decapeptyl® Neo-Decapeptyl® Decapeptyl® Retard	Ferring Pharmaceuticals Ipsen Technofarma Achè Sidus	Coacervation
Triptorelin pamoate	Telstar®	Pfizer Watson	Hot extrusion, cryogenic grinding
Triptorelin embonate	Pamorelin®	Ipsen Rawfarma	Not available
Lanreotide acetate	Somatuline® LA	Ipsen	Coacervation
Buserelin acetate	Suprecur MP (Japan)	Mochida Pharmaceutical	Spray-drying
<i>Protein</i>			
Human growth hormone	Nutropin® Depot	Genentech	s/o cryogenic spray- congealing (ProLease® , Alkermes)
<i>Small molecules</i>			
Naltrexone	Vivitrol®	Cephalon	o/w emulsion solvent extraction (Medisorb® , Alkermes)
Risperidone	Risperdal® Consta®	Janssen Pharmaceutical	o/w emulsion solvent extraction (Medisorb® , Alkermes)
Minocycline hydrochloride	Arestin®	Orapharma	s/o coacervation
Bromocriptine	Parlodel LA® , Parlodel LAR®	Sandoz (Novartis)	Spray-drying



## 1.2 Process intensification

Process intensification may be defined as a strategy which aims to achieve process miniaturization, reduce the capital cost, improve safety and energy efficiency, and improve product quality. Additional benefits of process intensification include simpler scale-up procedures, and the possibility to allow the replacement of batch processing by using small continuous reactors, which frequently give more efficient overall operation [30]. The philosophy of process intensification has been traditionally defined by four words: *smaller, cheaper, safer, slicker* [31]. Wherever possible, the aim of intensification should be to develop and use multi-functional modules to perform heat transfer, mass transfer, and separation duties. Process intensification may also exploit techniques involving the use of ultrasonic and radiation energy sources. [30]. An interesting example of process intensification is given by ultrasound-microwave coupling for chemical reactors, where the specific advantages of microwave energy and ultrasonic power may become additive when used in combination, promoting both heat and mass transfer [32].

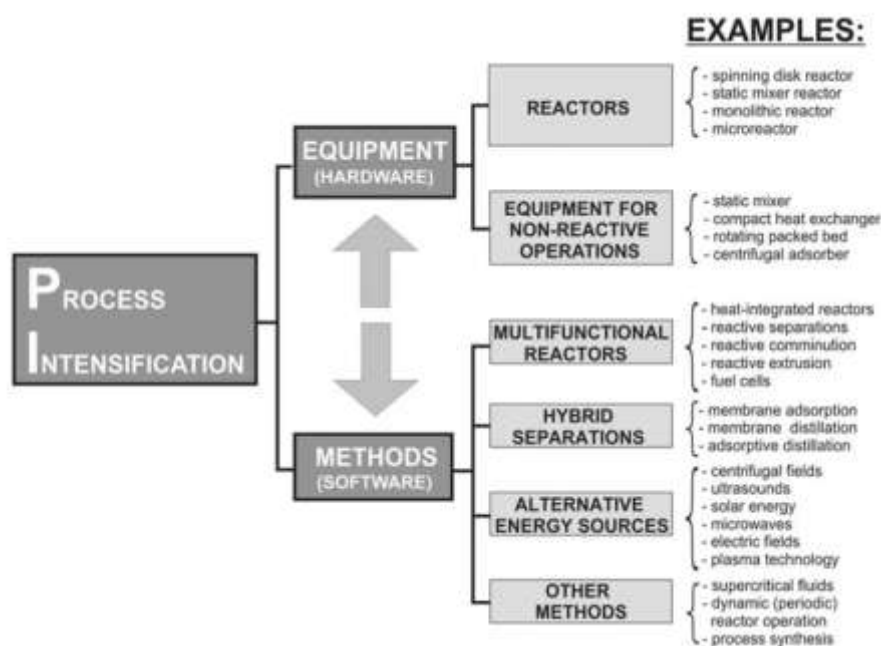


**Figure 1. Process intensification toolbox [31]**

The toolbox for process intensification includes process-intensifying equipment (PI hardware) and process-intensifying methods (PI

software) [31]. Obviously, in many cases overlap between these two domains can be observed because new methods may require novel types of equipment and, vice versa, novel apparatuses sometimes need new, unconventional processing methods. Examples of both hardware and software are shown in Figure 1.

In fine chemical and pharmaceutical industries, process intensification may offer a substantial shortening of the time to market, for instance, by developing a continuous laboratory-scale process, which could be used directly as the commercial-scale process. One must not forget that a liquid flow of only 1 mL/s means, in the continuous operation, about 30 tons/year, which is a quite reasonable capacity for many pharmaceuticals. In such a case, the process development takes place only once, with no scale-up via a pilot plant to the industrial scale. Also, all administrative (FDA) procedures involved in the legal approval of the production technology take place only once: the laboratory-scale technology is the commercial technology. In consequence, start of the production is greatly speeded up, and the patent lifetime of the drug can be much more effectively used [31].

### **1.1 Aims of the PhD thesis**

The research project is focused on the development of a novel microencapsulation process, designing and building a single-pot semi-continuous bench scale apparatus. The novel process is based on the coupling of two innovative techniques, involving ultrasound and microwave, used in atomization and heating operations, respectively, in order to answer to the needs for process intensification, i.e. improvement of process efficiency and cutting down of energy consumption. For the apparatus, whose sketch is on Figure 2, the idea to miniaturize/compact the plant, that is to obtain a single-pot unit, is pointed out. Variation of energy/frequency of ultrasounds may give a particles size distribution more suitable for the final applications. Microwave drying should modify the materials structure giving unique properties to the micro-particles. Finally, the use of an appropriate harvesting/separation systems makes the apparatus semi-continuous.

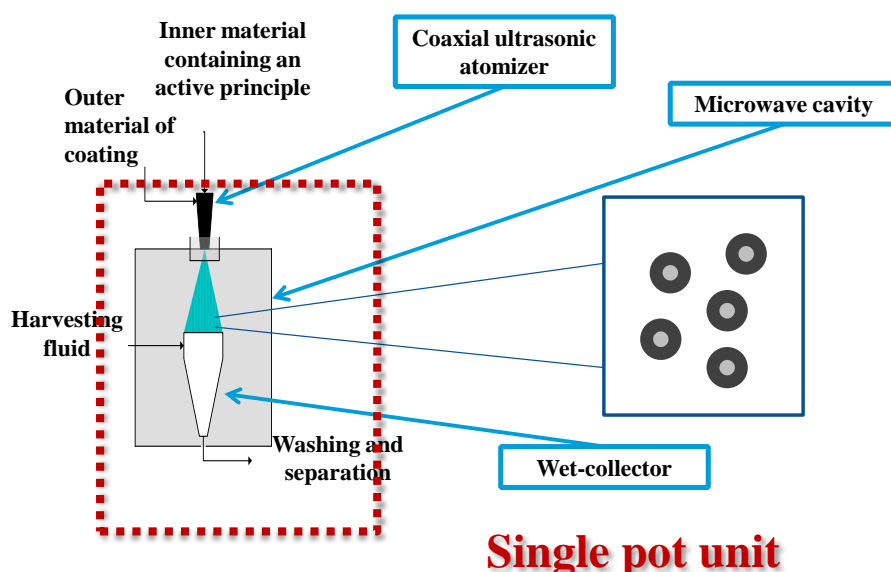


Figure 2. Idealization of the intensified plant of microencapsulation

## 1.2 Outline of the thesis

An introduction on the importance of microencapsulation and process intensification is followed by the review of the literature dealing with apparatuses for molecules microencapsulation. Then, low energy consumption apparatuses, especially those based on ultrasonic atomization, are described. On the basis of remarks on the state of the art, the idea of the novel semi-continuous apparatus for particles production by ultrasound assisted atomization, on a laboratory scale, is pointed out.

The phenomena involved in ultrasonic atomization are first highlighted. In particular, the parameters influencing droplets formation are shown. Then, both the initial stage of the apparatus, without the novel separation/harvesting system, and the apparatus in its final configuration are described. The criteria for selection and design of the most appropriated components for the microencapsulation plant, and the relevant building and working are listed. In particular, a general description of the microencapsulation apparatus is presented focusing on the three important sections: feeding section, atomization section (by coaxial ultrasonic atomizer), and harvesting/stabilization section.

Process parameters definition, with some indications about selection of the materials, apparatuses and tools to be used for the proposed process of microencapsulation, are shown. The built apparatus has been then subjected to tests of encapsulation of model active principles. First of all, the influence of the parameters related to both the inner channel (*core line*) and the outer channel (*shell line*) (such as flow rate, solution concentration and superficial tension) on particles final properties is evaluated. Then the production of systems, both in millimetric and in micrometric scale, encapsulating two model molecules, vitamin B12 as water soluble molecule and  $\alpha$ -tocopherol as water insoluble molecule, is tested. In particular, the results about vitamin B12 encapsulation are preliminary to  $\alpha$ -tocopherol tests and they are carried out in the initial configuration of the apparatus, in order to test the correct working of the plant. Results on particles size analysis, influence of ultrasonic and microwave energy, loading and release tests (despite some difficulties in the control techniques about measure of the model drug concentration in the particles that however were faced and overcome) are shown. Moreover, for the latter system (encapsulating  $\alpha$ -tocopherol), dielectric properties, moisture and temperature measures, as well as apparatus power consuming measure are also reported. The conclusive part endorses the usefulness of the novel plant, based on the combination of two powerful tools of process intensification, ultrasonic atomization and microwave drying, to obtain micro-systems particularly interesting for specific drug delivery applications.

---

## Chapter Two

---

### **State of the art**

*This chapter analyzes the literature related to the different apparatuses for microencapsulation of active molecules. Moreover the features and the advantages of apparatuses using ultrasonic atomization are underlined.*

## 2.1 Microencapsulation apparatuses

The review of literature works is focused on microencapsulation apparatuses, in particular on plants or automated equipments on lab- or pilot-scale first, eventually on industrial scale.

### 2.1.1 Patents

Redding Jr. proposed a microencapsulation apparatus where a sudden pressure change was applied to a dispersion of core and shell material in a liquid carrier in order to obtain the encapsulation of the core material within the shell substance [33]. The sudden pressure change was carried out essentially in two apparatuses. In the first one, a hydraulic piston was driven against the liquid carrier, applying a compressive force to it.

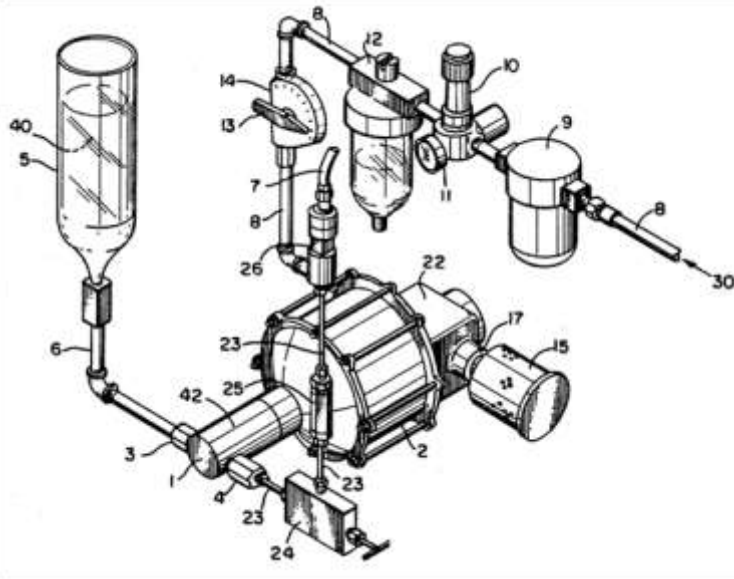


**Figure 3. Apparatus using a hydraulic piston for obtaining a sudden pressure change to achieve microencapsulation [33].**

As shown in Figure 3, the feed tank (5) is connected to an inlet valve (3), that leads into a compression head (1). Pneumatic pump (2) is connected to compression head (1) so that it may drive a piston toward a compression chamber within the compression head (1). Pneumatic pump is driven by high pressure air (30) and its cycling frequency is regulated by adjusting the pump input pressure by rotating the position of the bleeder valve (13). Mixing of shell and core materials was

achieved by conventionally known apparatuses. Then this mixture was fed, under the force of gravity, through a series of valves, to the compression chamber. After that dispersion was subjected to pressure changes (pressure shock waves, shear forces, and perhaps, cavitation), the liquid medium flowed into discharge line (7). The size of produced microcapsules is inversely proportional to the air pressure supplied to pneumatic pump. However, much of the shell material was not used; therefore microcapsules exiting from check valve (4) were confined for a short time in a baffled chamber, called “stabilization tube”, under conditions inducing turbulence, to have thicker microcapsules and more stable shell walls.

In a second apparatus, ultrasound was applied to liquid medium in three different options (Figure 4), giving a narrower size range and a better control of encapsulation process.

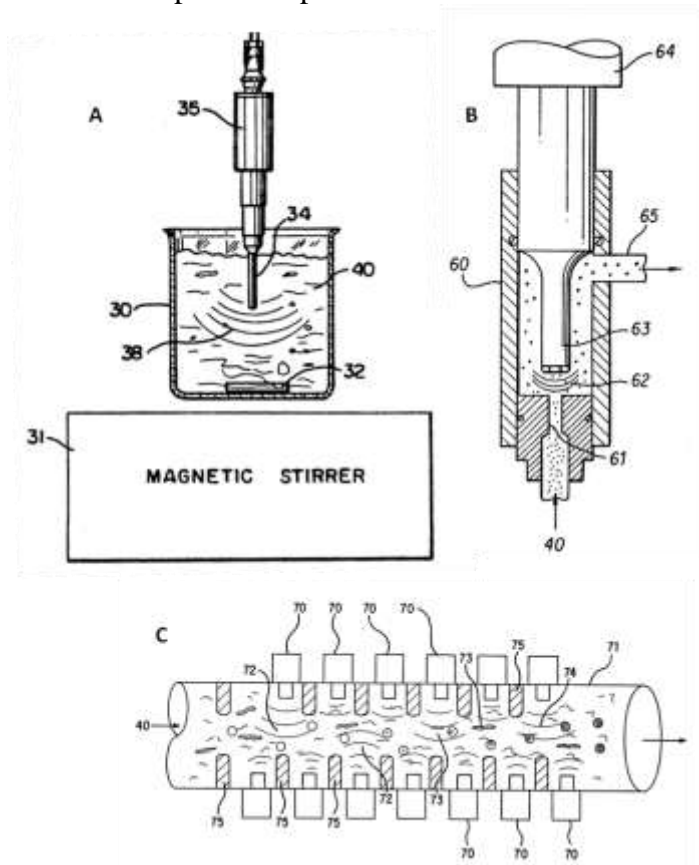


Figure 4. Ultrasonic apparatuses for microencapsulation [33]

In the case A of Figure 4, a treatment container (30) is supported on heater/stirrer (31). Ultrasonic converter (35) is suspended so that a horn (34) may be placed within the container. Ultrasound was applied to the dispersion and stirring was continued to ensure the exposure of both the shell and core material to the ultrasound. An alternative ultrasonic apparatus (B) allows continuous rather than batch encapsulation owing to a flow cell (60) in which the horn (63) of an ultrasonic converter (64) is inserted. Another alternative continuous embodiment (C) consists of a long tube (71) along the sides of which many ultrasonic converters (each of them with a horn penetrating into the flow space of tube) are arrayed.

The main disadvantage of this process is that the capsules are unstable and an additional processing is needed, especially for capsules produced by the piston apparatus. A solution can be a second pass of microcapsules through the apparatus applying the same magnitude or a different magnitude of the pressure change of the first pass. Reasons for recycling can be increasing the shell thickness, changing the composition of the exterior wall, incorporating the capsules as the core of a new capsule, or reducing the size of the resulting capsules.

Several examples showed the features of the previously described apparatuses. First, a combination of partial coacervation, to obtain the pre-mixture, a sudden pressure change in piston apparatus, and a turbulence baffled chamber for hardening, gave capsules ranged in size from 5-15  $\mu\text{m}$ , with an average shell volume of 25%, and a yield of encapsulation of 98%. A higher pressure change gave smaller capsules having more dense shell. The previous procedure was repeated, but the extra hardening in baffled chamber was replaced by a recycling in the compression chamber. The results were the same as those obtained previously, except that the size of microcapsules was reduced to about 3-10  $\mu\text{m}$ . A second recycling further reduced size to 1-5  $\mu\text{m}$ . In the ultrasonic apparatus, type A (Figure 4), spherical capsules were obtained with a size range of 10-30  $\mu\text{m}$ . A re-exposure to ultrasound produced smaller capsules (1-2.5  $\mu\text{m}$ ).

Alisch et al. achieved a process for the production of spherical alginate pellets from drops of alginate solution delivered by a nozzle [34]. The apparatus (Figure 5) consists of a system of feeding and metering (1) an alginate solution that is delivered by a nozzle (3) into a collection device (4), which contains ion solution (preferably calcium chloride solution). The ion solution has a foam layer of a



surfactant to reduce both the interfacial tension of solution and the undesired flattening, due to the impact of droplets on liquid surface.

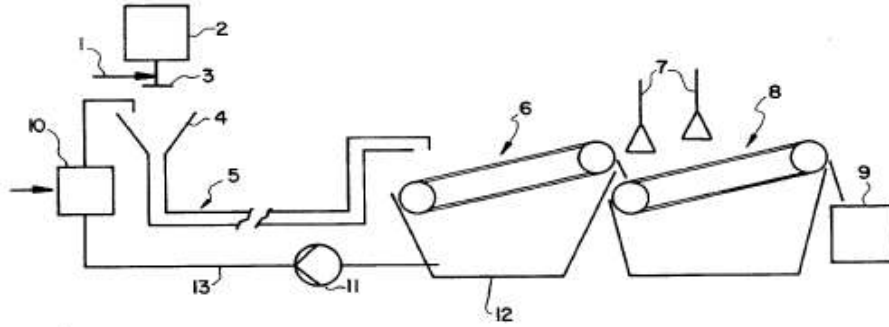


**Figure 5. Scheme of the plant for the production of alginate pellets [34]**

To atomize the alginate solution, mechanical vibrators, magnetic-induction vibrators, pneumatic vibrators, piezoelectric converters, or electroacoustic converters can be used as the vibration exciter (2). The exciter can act directly on the nozzle and cause it to vibrate horizontally or vertically, but it is also possible to impress vibrations on the feed line. Alternatively, it is possible to excite the alginate solution present in a reservoir container. At last, the stream of alginate solution leaving the nozzle can be also acoustically irradiated.

The alginate droplets fall from the collection device (4) through a tubular reactor (5), for such a residence time that the droplets can be consolidated to the desired extent. After leaving the tubular reactor, the alginate pellets are delivered onto a traveling screen (6), from which the calcium chloride solution drips off. Then, the alginate pellets pass onto a traveling screen (8), on which they are washed using wash water nozzles (7). The pellets are collected as products in a collection device (9). The ion solution is recycled, after concentration control (10). The system has to respect some features: viscosities lesser than 200 mPa·s, excitation frequency between 50 and 20000 Hz, and nozzle diameter in the range between 50 and 3000  $\mu\text{m}$ .

Some results obtained in different cases are shown. In Case I, with a nozzle diameter of 280  $\mu\text{m}$ , a frequency of 2100 Hz, residence time (of droplets in ion solution) of 30 min, and lack of surfactant and foam, the diameter of resulting particles was 500  $\mu\text{m}$ . In Case II, with a nozzle diameter of 900  $\mu\text{m}$ , a frequency of 155 Hz, residence time of 1 min, and lack of foam, the size of pellets was 1700  $\mu\text{m}$ . Lastly, Case III, characterized by a nozzle diameter of 1925  $\mu\text{m}$ , a frequency of 50

Hz, residence time of 1.5 min, and presence of foam (20 mm), gave pellets with a diameter of 3400  $\mu\text{m}$ .

Amsden et al suggested another process for the preparation of polymeric micro-particles [35]. The process consists of passing a first solution containing polymer and solvent through an orifice and directly into a second solution containing water and a stabilizing agent. The process scheme (A, Figure 6) shows a polymeric phase (1), held in a tank (2), which is pumped to a needle (5), crossing in turn a conduit (7) at an angle  $\theta$ . Stabilizing (second fluid) phase (8), held in a reservoir (9), is moved through conduit (7) to obtain a fluid containing micro-systems (12).

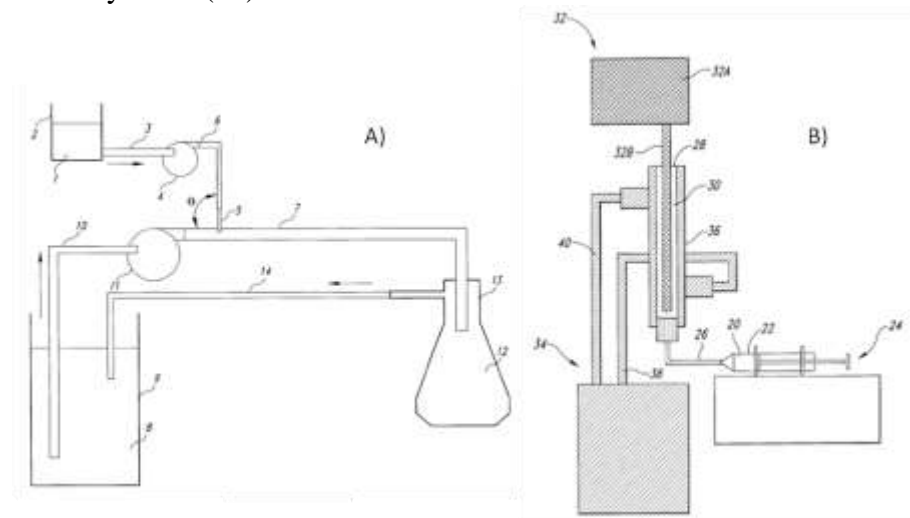


**Figure 6. Two variations of the process for microspheres preparation [35]**

The polymer solution droplets are drawn off the needle tip in a regular and periodic fashion under the shearing action of the stabilizing solution flow. The size and size distribution of the droplets are controlled by the physical properties of the stabilizing solution, the needle outside diameter, and the surface tension between the polymer solution and the needle tip. A plurality of these injection apparatuses can operate in parallel to increase the production rate and level. The configuration B in Figure 6 is another aspect of the process. The polymer-containing fluid (20) is moved by a syringe pump (24) in a mixing chamber (28) (having a column shape and subjected to stirring) which is charged with the stabilizing solution. The control of the temperature in the mixing chamber is achieved by a water-jacket. Here, the first solution, once introduced at the bottom of the column,

meets the second solution and forms droplets. Because the second fluid is kept at a temperature near or above the boiling point of the solvent present in the first fluid, the droplets become almost immediately surrounded by a layer of solvent vapor. Droplets begin to ascend because of the vapor that makes them lighter than the aqueous composition. Droplets shrink until the polymer becomes supersaturated and begins to precipitate, forming the nascent microspheres. Once the microspheres reach the top of the column, the vapor is released and the microspheres become suspended in the first solution. In these systems, the factors influencing the microsphere size are: temperature, nature of the second fluid, and nature and flow rate of the first solution. For example, at lower temperatures the vaporization process occurs more slowly so that the droplets are infused longer, and the microspheres size is larger.

Lyon et al presented an apparatus for preparing micro-particles using a static mixing assembly [8]. There are three different methods, all characterized by a first step of pumping a phase of active molecule and polymer and a stabilizing solution through a first static mixer to form an emulsion. The first method is characterized by flowing the emulsion through a manifold including several static mixers into a quench liquid where emulsion droplets form micro-particles. In a further method, the outflow of the first static mixer is split to form at least two streams, which flow in a second static mixer, and combine them at the end with the quench liquid. The third choice is pumping the emulsion into the quench liquid and adjusting the residence time of the emulsion in the static mixing assembly. A typical scheme for this process is shown in Figure 7. An organic phase (710), polymer/drug solution, and a continuous phase (720), stabilizer-containing solution, are pumped into a static mixing assembly (730). Preferably, static mixing assembly comprises a pre-blending static mixer (732) and a manifold (734) of single static mixers (736). After exiting the static mixing assembly, the oil-in-water emulsion is transferred to a large agitated tank for solvent extraction or quench. The emulsion droplet sizes, and the resulting micro-particle size, are controlled essentially by the flow rate and residence time through the static mixing assembly.

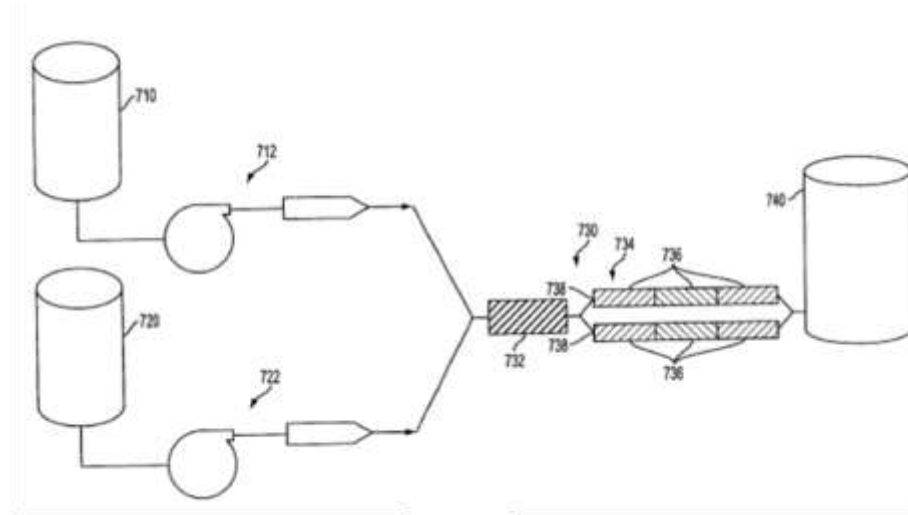


**Figure 7. Equipment configuration for preparing micro-particles using a static mixing assembly [8]**

Bomberger et al presented a system to produce alginate micro-particles loaded with a drug, including a protein, intercellular adhesion molecule ICAM-1, that can be delivered via the nasal way [36]. A typical apparatus includes a mixing block having first and second, axially connected, cylindrical mixing chambers. The diameter of the second chamber is preferably larger than the first one. Referring to Figure 8, a first stream of drug/polymer solution (408) is introduced axially into the first chamber.

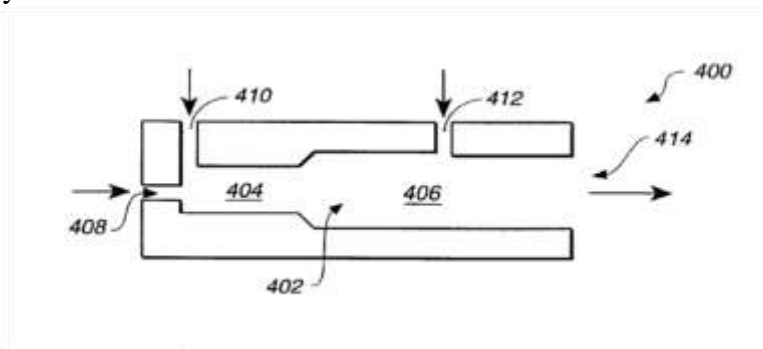


**Figure 8. Scheme of the longitudinal cross-section of a mixing block [36]**

A second stream of emulsifier is introduced into the first chamber through a second port (410), positioned essentially orthogonal to the interior wall of the first chamber (404), to form an emulsion. The emulsifier stream injected tangentially has an axial velocity

component, from the liquid flowing through the chambers, resulting in a helical path, with a consequent turbulence within the first chamber sufficient to create an emulsion of droplets. However, the coaxial introduction of the drug/polymer solution and the emulsifier into the first chamber does not produce micro-particles of the desired size. In the second chamber (406) the droplets are cross-linked by a cross-linking agent that is introduced tangentially (412) to the cylindrical wall of the second chamber (also in this case for creating helical flow of cross-linking agent). Several parameters potentially affect the success of such a system: solvent properties, influencing miscibility and drug loading; flow rates into mixing chambers, affecting micro-particles size; cross-linker concentration, acting on speed of cross-linking step. Washing and filtration processes cause drug leaching, small particle loss, and micro-particles agglomeration.

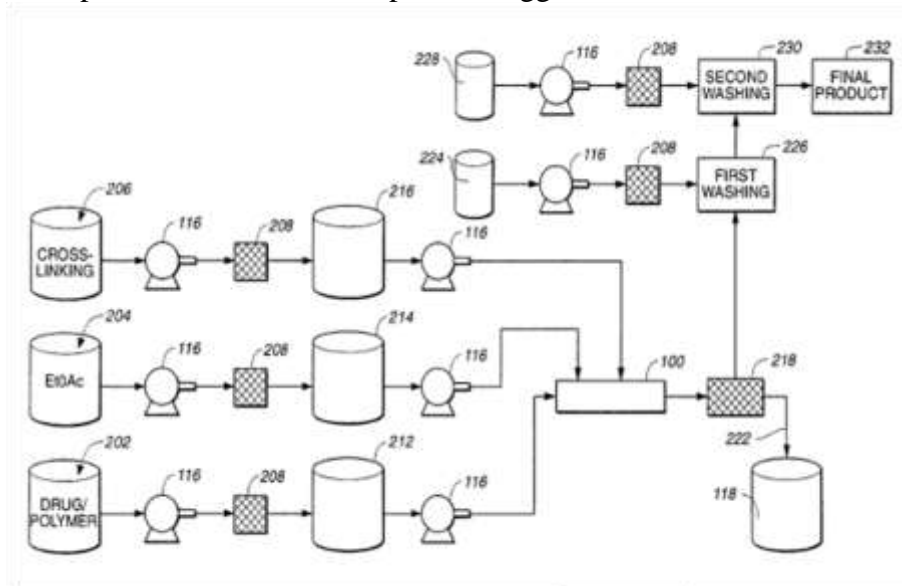


**Figure 9. Global scheme of a system comprising a mixing-block [36]**

In a global scheme, as shown in Figure 9, the drug/polymer solution, emulsifier, and cross-linking solutions are prepared in separated tanks (202, 204, 206, respectively). Each solution is pumped through an appropriate sterile filter (208) and stored in separate sterile holding vessels (212, 214, 216). A second sterile filtration step may be included prior to introduce solutions into the mixing block (100). As the mixture of micro-particles and cross-linking solvent exit the mixing block, the mixture is filtered (218) to catch micro-particles above a predetermined minimum range. Then particles are subjected

to a first wash (226), using a dehydrating solution; then a second wash step (230) is performed to remove the residue of the first wash solution. Micro-particles recovery (232) can be performed by methods known in literature.

A method and apparatus for preparing micro-particles using liquid-liquid extraction was also proposed [26].

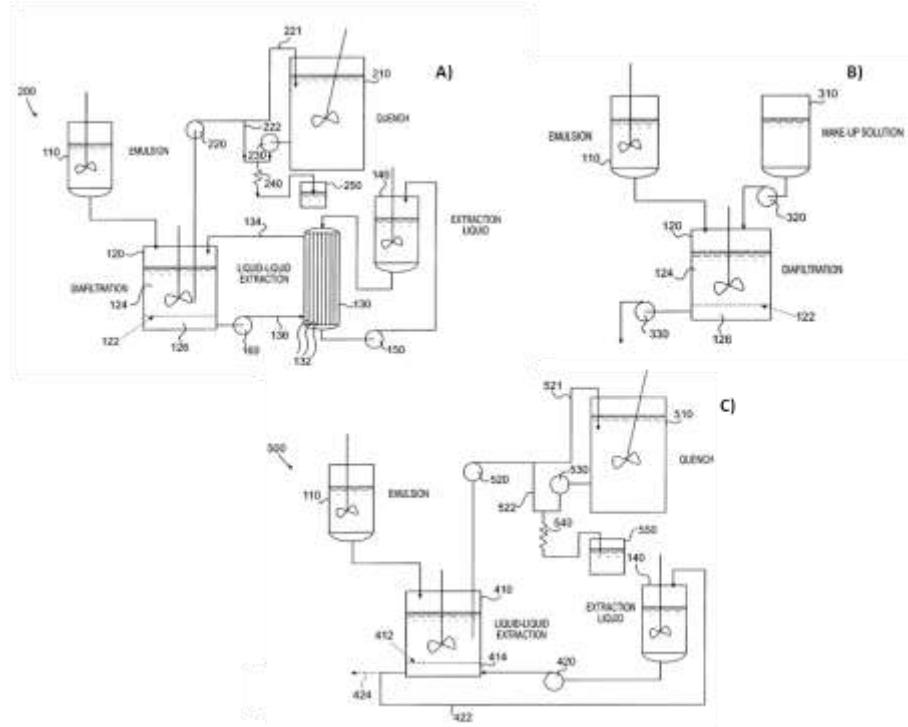


**Figure 10. Different configurations of liquid-liquid extraction apparatus [26]**

Several configurations were presented (Figure 10). The first solution, A, consists of a vessel (110) containing an emulsion, formed previously by traditional techniques, which is transferred to a diafiltration vessel (120). A membrane filter (122) is disposed in the diafiltration vessel so that it is separated into two parts (124 and 126), with the higher part (124) poor of solvent. The solvent rich phase (126) is pumped (160) into a membrane collector (130), with hollow fibers (132), where an extraction liquid coming from a vessel (140), removes the solvent and allows the separated phase to come back to diafiltration vessel. When a selected level of solvent is reached in the emulsion, it can be transferred out of the diafiltration vessel to a quench vessel (210), where a quench liquid complete hardening and

precipitation of micro-particles. The combination of emulsion and quench liquid can be obtained also in a static mixer (240); then the outflow goes into the vessel (250) in which the micro-particles harden and precipitate. In configuration B (Figure 10), the section comprising the emulsion vessel and the diafiltration system is unchanged. However, here the separated solvent reach phase is replaced by a make-up solution (320), preferably an aqueous solution or a solvent-free liquid. The micro-particles harden and precipitate in the diafiltration vessel, from which they can be recovered and dried.

In the alternative scheme C, the diafiltration vessel is replaced by a liquid-liquid extraction (LLE) vessel (410), where emulsion solvent diffuses across membrane (412) into the extraction liquid (flowing from vessel 140). Also in this case, once a selected solvent concentration in the emulsion is reached, the emulsion is transferred from LLE vessel to a quench section, set up as in the case A. Configuration B showed the lowest encapsulation efficiency.

Gibson et al showed an emulsion-based process for making microcapsules [37].

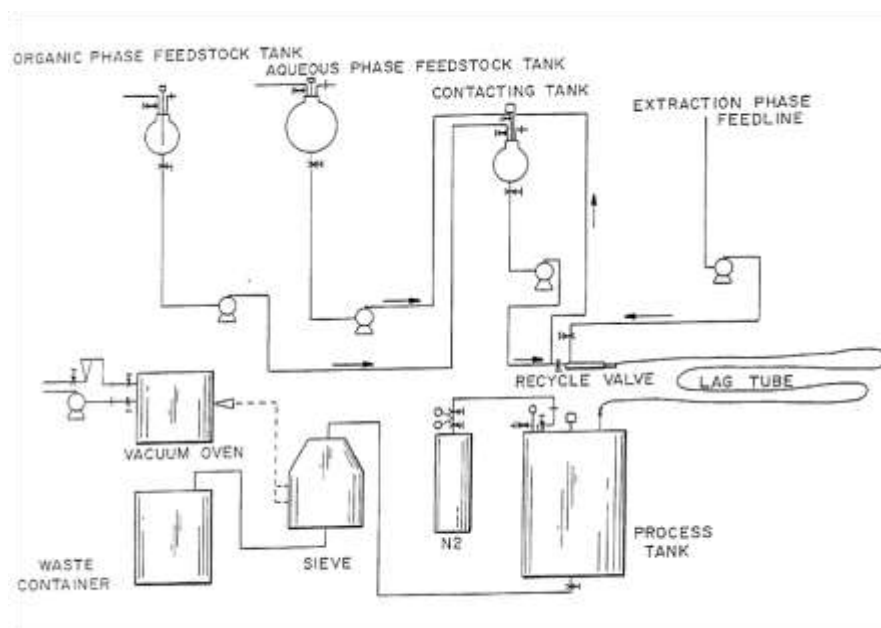


**Figure 11. Process flow diagram of a system for micro-particles production using a contact tank with recycle, in a continuous process [38]**

Emulsion formation derived from combining a dispersed phase (containing polymer, solvent and active agent) with a continuous

surfactant-containing phase. Then extraction and/or solvent evaporation was performed to obtain micro-particles from emulsion droplets hardening. In this patent the microencapsulation process can be performed with some options: using a contact tank with recycle (Figure 11); using a two phase process; or using direct injection of the extraction phase into an emulsion lag tube. The contact tank with recycle is a mean for controlling residence time of emulsion. The pumping rate of the recycle pump and the recycle ratio can be adjusted to produce the desired process conditions. Then, the emulsion is pumped to the extraction step. The solvent removal can include the extraction phase, followed by the evaporation one: the first step of extraction can be skipped, leaving only evaporation, with a consequent reduction in process equipment. In another solution, the evaporation step can be replaced by a membrane separation step. In another configuration, the solvent removal can be performed by an incremental extraction, introducing the extraction phase into the emulsion through multiple feed streams at two or more locations along the lag tube. The incremental addition of the available extraction phase should slow down the extraction process, increasing time to assure micro-particles hardening, and making solvent removal more complete.

A method to prepare micro-particles, containing nucleic acid, was proposed by Tyo et al [39]. Nucleic acid must be protected by minimizing shear forces; limiting sonication, homogenization, and microfluidization; controlling lyophilization, drying, or hardening; limiting the exposure to high temperatures. The first step of this process is the batch formation of a first emulsion: water (containing nucleic acid) in oil (solution of solvent and polymer), W/O (5). A second emulsion is formed by mixing the first emulsion and an aqueous solution by a homogenizer (24). After homogenization, the second emulsion enters a temperature controlled bioreactor chamber (28), that is a solvent removal device, containing a stirrer and an inlet (32) for delivering nitrogen. Washing of micro-particles is performed by introducing water through conduits (41, 42, and 48) to a hollow fiber reservoir (50), connected to a pressure release vent (52), with a filter (54). In the hollow fiber reservoir, the volume is kept constant by continuous removal of solution towards the second washing unit (59). Fluid is circulated from bioreactor to hollow fiber reservoir, then to serially stacked hollow fiber cartridges (59). The size of the hollow fiber membrane's pores is sufficiently small so that the micro-particles



cannot pass through the membranes, unlike reagent and by-products, which are removed by conduit (62). A clamp (70) is opened to collect micro-particles suspension. Moreover, a further washing in the second unit allows increasing yield.

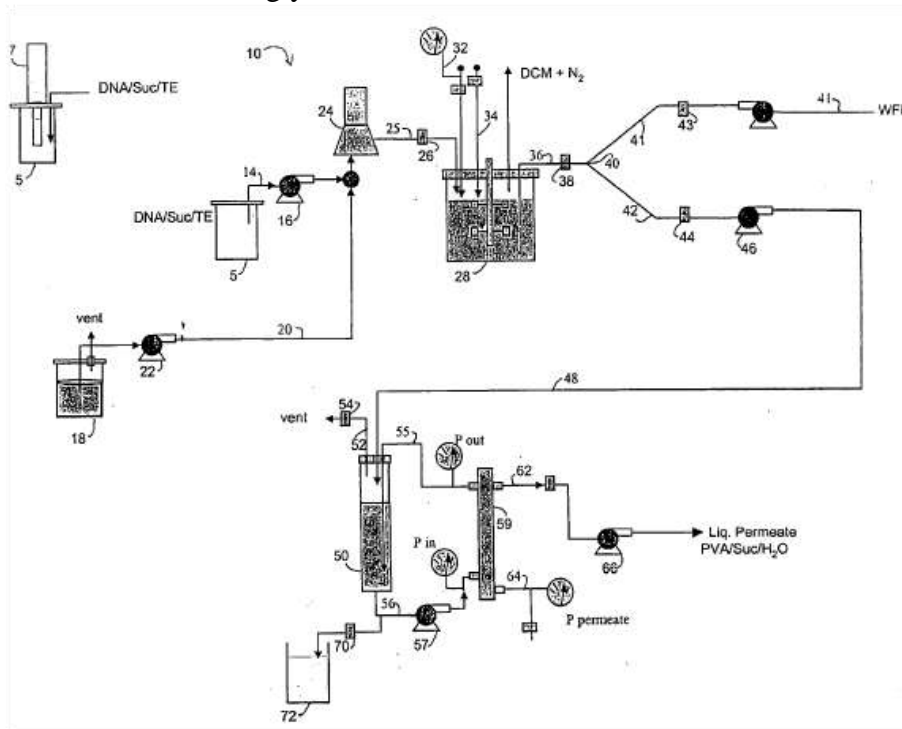


**Figure 12. Scheme of the apparatus for producing micro-particles containing nucleic-acid [39]**

An alternative method, in contrast with the previously described procedure, is characterized by a partial vacuum, replacing the gas overlay, in the solvent removal device. The slurry is then transferred to a filter/dryer, which retains the product and allows the passage of water containing solvent. Inside this unit the micro-particles are washed slowly with water, to promote the diffusion of solvent to water. Finally the product can be rinsed and dried with nitrogen gas, then discharged from the filter/dryer into a sterile tank. The solvent can be recovered from discharged wash water by distillation.

Herbert et al pointed out a method for forming micro-particles, including a freezing zone, surrounded by a liquefied gas, in order to freeze micro-droplets, and an extraction zone, where micro-particles form after solvent removal [38]. A proposed apparatus to obtain micro-particles, shown in Figure 13, A, is made up of a single vessel

(10), divided into a freezing section (20) and an extraction section (22), which has side wall and bottom insulated.

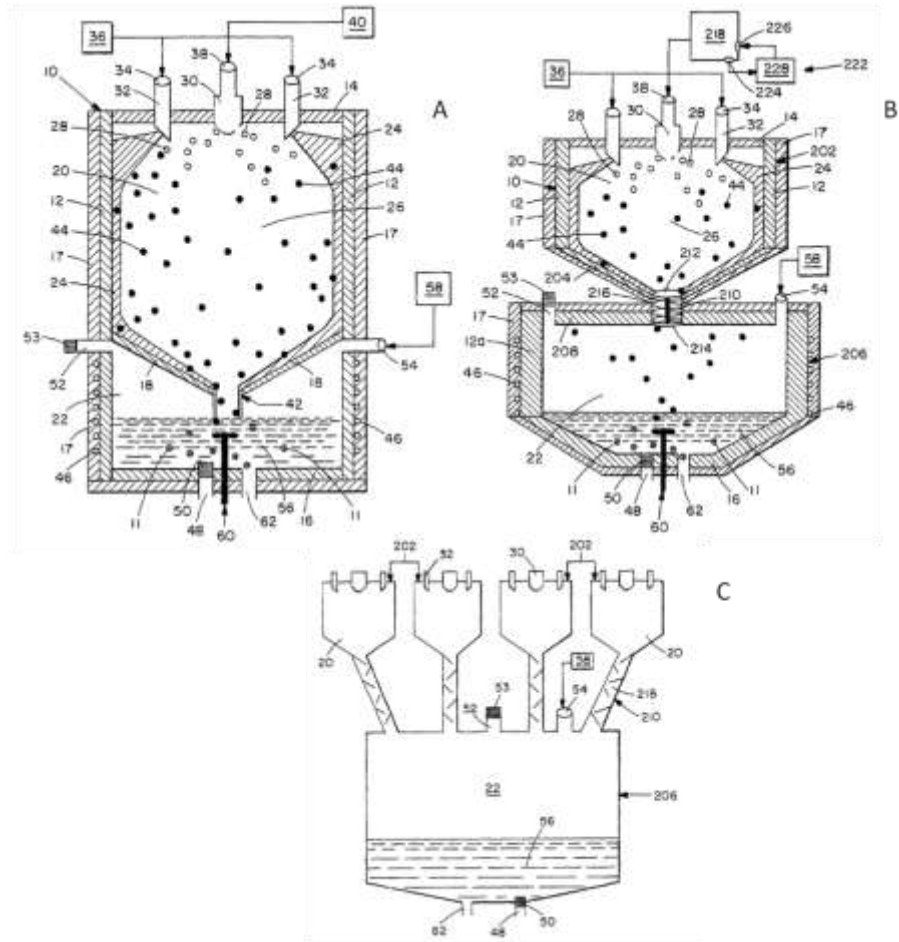


**Figure 13. Scheme of three different apparatuses to produce micro-particles, including a freezing zone [38]**

There are two spray nozzles (32), equally spaced at positions located on a circle centered around the center of the vessel top (14), or centered around micro-droplets forming system (30), for injecting liquefied gas, usually nitrogen, that impinges against side wall (12). Droplets are obtained by an atomizer (30), usually an air atomizer, where micro-particles size depends on pressure of atomizing gas. Then, a three-phase port (42) is sized to allow the flow of a combination of frozen micro-droplets (44), liquefied gas and volatilized gas from freezing section into the extraction one. Extraction section can include a heating system (or partial vacuum) to

volatilize liquefied gas, then to extract the solvent and to collect micro-particles. A bottom tap (48), containing a filter (50), with a size less than one micrometer to allow liquid passage and to retain micro-particles, is present. Gas goes out from a port (52) with a filter (53) to assure sterility. In addition, vessel (10) can optionally include at least one overpressure protection device (rupture disks or pressure relief valves) to protect the integrity of vessel from over-pressurization caused by liquefied gas volatilization. The cold non-solvent liquid enters, as stream, spray or/and extraction bath, from the non-solvent inlet (54) in the extraction section where a low shear mixing device (60) reduces the potential formation of extraction gradients within the extraction bath. The solvent in frozen micro-droplets is taken away to allow solvent extraction into the non-solvent liquid. There is also a bottom tap (62) which is suitable for removing micro-particles and liquids (such as the non-solvent liquid). After extraction, micro-particles are filtered and dried to remove non-solvent. The process can be either batch or continuous. In the solution B, shown in Figure 13, the freezing section and the extraction one are separated; the channel for communication between the two sections includes three-phases mixing means. In another embodiment (scheme C in Figure 13), frozen micro-droplets (44) are formed in different freezing sections and then they are moved to a common extraction section (22).

Lastly, the continuous spray-capture production system proposed by Piechocki et al is shown [40]. Materials used in this process are high viscosity fluids, such as gelatinized starch and alginate. Their atomization is performed by using a spray jet nozzle, which provides hydraulic pressure; an inert gas, pumped into the jet nozzle; a post-nozzle air vortex to disrupt the viscous fluid into fine particles. For higher distances between the jet nozzle tip and the surface of the cross-linking solution, a particles size increase was observed. Moreover, a number of over-sprayers provide a liquid of the same composition as the cross-linking solution, in order to promote contact between aerosols and cross-linking/harvesting liquid. As shown in Figure 14, the product is collected in a separator fitted with two sets of screens, while the filtrate is pumped back to the capture tank by the over-sprayers, after monitoring ion concentrations (to be kept within predefined limits).

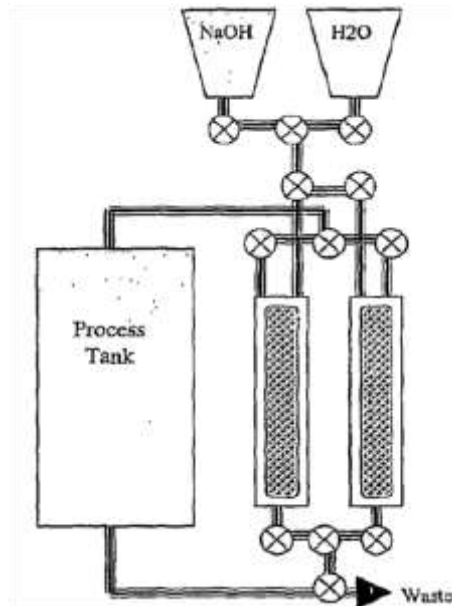


**Figure 14.** Flow diagram of the continuous spray-capture microencapsulation process [40]

### 2.1.2 Other literature examples of apparatuses for microencapsulation

A patented microencapsulation process, named BRACE, was proposed to encapsulate a wide range of materials in micro-spheres or micro-capsules in a diameter range of 50-6000  $\mu\text{m}$  [41]. The process, shown in Figure 15, consists in a feed tank (3), from which a liquid is pumped to a nozzle tip, where a vibrating device (2) causes flow breakup into uniform droplets. The vibrating device can be a magnetic-induction, mechanical, or pneumatic vibrator, piezoelectric or electroacoustic converter. The droplets are solidified during falling through a coagulation line (9), by cooling, chemical reaction or drying, depending on processed material. Feed liquid viscosity has to be lower than 10000  $\text{mPa}\cdot\text{s}$ , emulsions and dispersions have to be stable, dispersed particles should have diameters lower than  $\frac{1}{4}$  of the nozzle size, the coagulation line has not to cause deformation of the particles. Moreover, a number of nozzles can be used to increase the production, for example, shifting the production from 25 Kg/h to 500 Kg/h, the nozzles rise from 12 to 240. Examples of application of this process are agar-agar encapsulating volatile ingredients for cosmetic

use, gelatin and alginates encapsulating oils, fragrances or flavors for food technology.

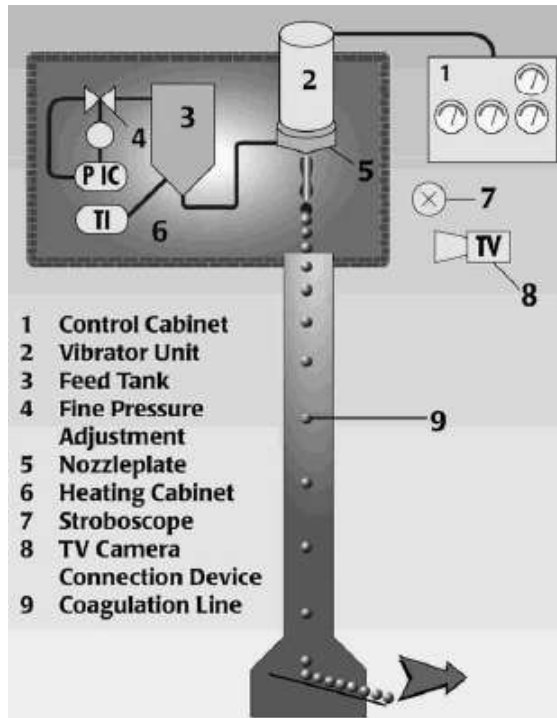


**Figure 15. BRACE microencapsulation process [41]**

Electrohydrodynamic atomization (EHDA) is a process which can generate droplets of size between a few to hundreds of micrometers [42]. A liquid is injected through a capillary tube and a potential difference of several kilovolts is applied between the capillary and the ground electrode: at the capillary exit the liquid assumes a conical shape (commonly named Taylor cone), a thin jet with high charge density exit from the cone apex and breaks down into droplets, independent of the diameter of the capillary tube. Co-axial EHDA (CEHDA) is a variant of conventional EHDA where two concentric capillaries are used, and two different immiscible liquids can be pushed through these two capillaries, obtaining shell-core particles. Size, shape and morphology of particles depend on liquids physical properties, processing conditions, working distance, flow rate and applied voltage [43]. A scheme of the equipment used for the CEHDA is shown in Figure 16. It consists of two syringes to pump the inner and outer liquids to capillaries, an electrical field established between the capillary assembly and a particle collection system (at a fixed

distance). To visualize liquids flow under the influence of the electric field, a video camera is focused on the needle outlet.

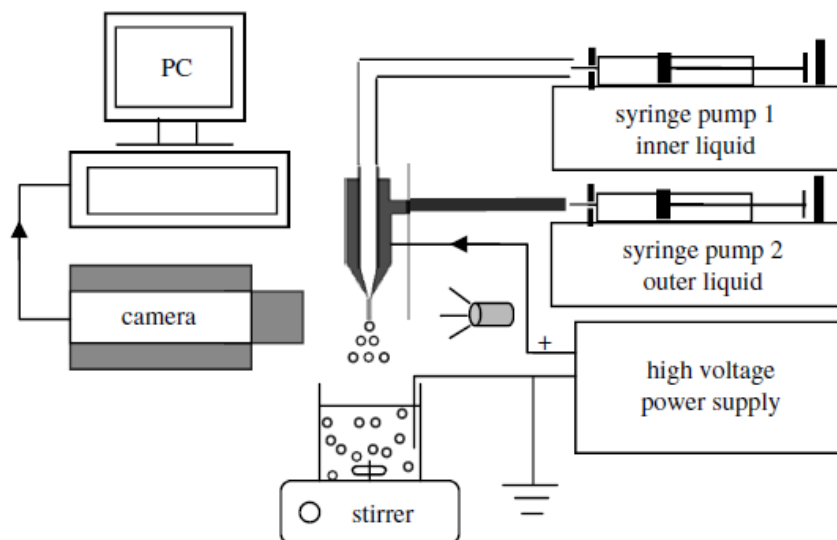


**Figure 16. Apparatus for co-axial electrohydrodynamic atomization [42]**

Here, when Polymethylsilsesquioxane (PMSQ) and perfluorohexane (PFH) were used respectively as shell and core materials, the mean diameter of micro-particles was varied in the range from 310 to 1000 nm (while the corresponding mean shell thickness varied from 40 to 95 nm) by adjusting the flow rate, polymer concentration or applied voltage. For too high polymer concentrations, microspheres were not generated, instead PMSQ fibers encapsulating PFH liquid were obtained [43]. In another work, Budesonide and poly(lactic-co-glycolic acid), (PLGA), dissolved in acetonitrile, were used as the inner drug solution and the outer polymer coating solution, respectively. Through the variation of PLGA concentration and the electrical conductivity of spray solutions, monodisperse PLGA-coated drug particles with sizes ranging from 165 nm to 1.2  $\mu\text{m}$  were prepared, with high encapsulation efficiency (90–95%) at optimal spray conditions [44]. Polymer-coated starch–protein microspheres were also prepared by using this process. A starch and BSA (bovine serum albumin) solution was pumped in the inner capillary and polydimethylsiloxane (PDMS) was pumped in the outer capillary. The microspheres were monodisperse and the protein, BSA, was intact and preserved during the process, showing that this single-step and relatively simple process does not expose proteins to harmful organic

solvents and can be exploited to prepare biodegradable microspheres for protein drug release [42].

## 2.2 Apparatuses at low energy consumption (US atomization)

### 2.2.1 Principles of the ultrasonic atomization and benefits

Ultrasound is defined as mechanical wave at a frequency above the human hearing threshold ( $> 20$  KHz). It continues up to around 1 GHz, where the hypersonic regime starts. The full spectrum is shown in Figure 17, where typical ranges for the phenomena of interest are indicated [45]. Ultrasound can be divided into three frequency ranges: power ultrasound (16–100 kHz), high frequency ultrasound (100 kHz–1 MHz), and diagnostic ultrasound (1–10 MHz) [46].

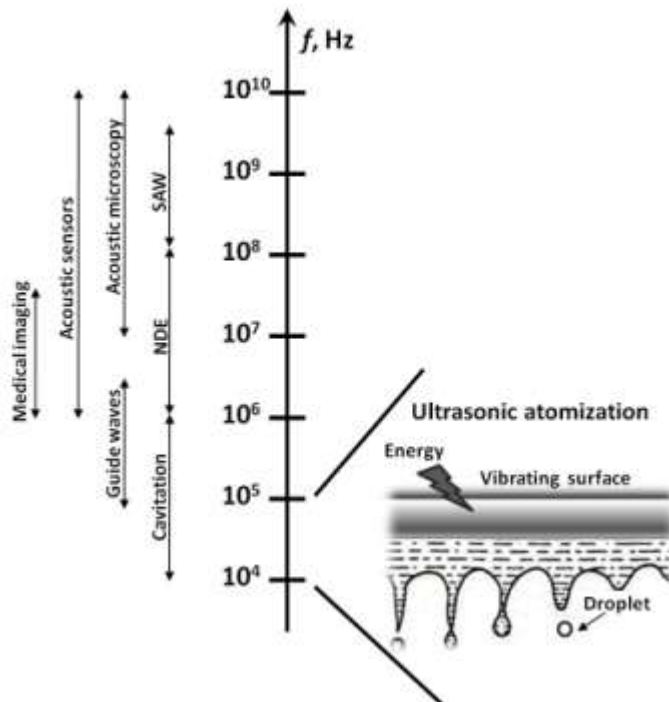


Figure 17. Ultrasonic frequency ranges, kind of applications and ultrasonic atomization mechanism sketch [45]

Ultrasonic energy is mechanical energy and its transmission depends on the elastic properties and densities of the media through which it is propagated. The stresses associated with the propagation of ultrasonic

waves may operate directly; they may be converted into thermal energy by absorption or into chemical energy upon the molecular materials conditions. Examples of the direct effect of ultrasonic stresses are: breaking particles into smaller particles, emulsification, liquids degassing, drying and dewatering of materials, ultrasonic machining, atomization of liquids, and metal forming. Examples of thermal effects are ultrasonic welding of polymers and metals. Chemical effects are ultrasonic cleaning involving chemical attack of contaminants, acceleration of chemical reactions by mixing and curing epoxy materials, and production of new products by accelerating reactions [47]. Ultrasonic atomization is accomplished by several means: by focusing high-frequency ultrasonic energy on the surface of a liquid in a bowl-shaped transducer (0.4–10.0 MHz), by ultrasonically vibrating a surface over which the liquid flows (18–100 kHz), or by feeding the fluid into the active zone of a whistle (8–30 kHz) [47]. Two major hypotheses were proposed to explain the mechanism of liquid disintegration during ultrasonic atomization: *cavitation hypothesis* and *capillary wave hypothesis* [48]. *Cavitation hypothesis* is generally applied to high frequency (16 kHz–2 MHz) and high-energy intensity systems. When the liquid film is sonicated, cavitation bubbles form. During the implosive collapse of these bubbles, especially oscillating bubbles near the surface of the liquid, high intensity hydraulic shocks are generated. These hydraulic shocks start the disintegration of the liquid film and cause direct ejection of the droplets [48-49]. *Capillary wave hypothesis* is based on Taylor instability. The liquid capillary waves are made of crests and troughs. Atomization takes place when unstable oscillations tear the crests (peaks) of surface capillary waves away from the bulk liquid. Thus the drops are produced at the crests whose size is proportional to wavelength. The capillary wavelength decreases with increasing frequency of ultrasound, therefore at higher frequencies finer droplets are obtained [49]. The use of ultrasounds in industrial processes has two main requirements: a liquid medium and a source of high-energy vibrations (the ultrasound). The vibration energy source is a transducer which transfers the vibration (after amplification) to the sonotrode or probe, which is in direct contact with the processing medium. There are two main types of transducers: piezoelectric and magnetostrictive. Piezoelectric transducers are the most commonly used in commercial scale applications due to their scalability: the maximum power per single transducer is generally higher than



magnetostrictive transducers [46]. The process parameters influencing ultrasonic liquid processing are *energy and intensity, pressure, temperature and viscosity*. Both energy and intensity are independent of scale and thus any ultrasonic process will be scalable using these two parameters. An increase of external pressure (also named back pressure) cause the increase of the cavitation threshold and thus the number of cavitation bubbles is reduced. Moreover, it causes also the increase of the pressure in the bubble at the moment of collapse resulting in a more rapid and violent collapse. Therefore, increasing the back pressure can be an effective tool in intensifying the process, without having to increase the amplitude. The temperature affects the vapor pressure, surface tension, and viscosity of the liquid medium: the optimal temperature would give a viscosity so low to allow the formation of cavitation bubbles, but it would avoid dampening effects by a high vapor pressure (if temperature is too high). Despite the numerous process parameters affecting the process output, the ultrasonic processing gives improvements in product quality, process enhancement and cost reduction on a commercial scale, for the following reasons:

1. availability of high amplitude/power units for large commercial operations;
2. high efficiency of ultrasonic transducer (about 85%), with reduction of internal heating (absence of expensive cooling systems);
3. easy to install and/or retrofit systems;
4. competitive energy costs;
5. low maintenance cost, due to the absence of moving parts (the only part requiring replacement is the sonotrode, which is in direct contact with medium) [46].

Moreover, traditional atomizers (rotary, pressure or two-fluid atomizers) use only a fraction of their operating energy (centrifugal, pressure or kinetic energy) to shatter the liquid, while most of this energy is transformed into kinetic energy of the particles. As a consequence, some problems can arise, such as a partial separation of the components in mixtures, or pores and presence of defects on micro-particles surface. Instead, the drops velocity from an ultrasonic atomizer is 1-10% lower than hydraulic or air-atomizing nozzle [50]. The lower velocity of droplets emerging from ultrasonic nozzles

avoids, downstream, drying chambers with large size [51] and, upstream, high pressures or compressed air [52]. Moreover, the mechanical stress caused by the vibration is lower, avoiding the deactivation of bioactive substances [50].

### *2.2.2 Spray-drying using an ultrasonic atomizer*

Spray-drying technique for preparation of micro-systems offers several advantages compared to other microencapsulation techniques. A solution, suspension or emulsion of polymer and drug, is atomized into a stream of warm air: the solidified product, as microspheres, can directly be collected after atomization and further hardening is not necessary. Moreover, spray-drying is, in principle, a continuous process, giving good reproducibility and potential for scale-up. In spray-drying process, the spray is usually generated by pneumatic nozzles. There are some disadvantages associated with these nozzle systems, such as lack of control over the mean droplet size, broad droplet distributions, and risk of clogging in case of suspensions. Despite ultrasonic nozzles have not been routinely used in laboratory scale spray-drying equipment, they can offer the generation of droplets with a uniform size distribution, which leads to more homogeneous size distributions of micro-particles [53], and to the several benefits, previously listed. Therefore, association of ultrasound to spray-drying is a powerful tool, as proved by the following examples.

Bovine serum albumin (BSA) loaded microspheres were prepared using an ultrasonic atomizer with a carrier air stream fitted to a laboratory spray dryer [53]. Since a conventional ultrasonic nozzle was blocked immediately after the atomization beginning, a carrier air design was chosen. The carrier air is necessary to cool the piezo-ceramic element and to flush the embryonic microspheres from atomizer tip. As seen in Figure 18, the ultrasonic atomizer consists of a connection for oscillator (1), a connection for liquid (2), a connection for carrier air (3), a protecting cap (4), and the piezo-ceramic element (5). An emulsion of an aqueous solution of BSA into the organic polymer solution (Poly(D,L-lactide-co-glycolide), PLG, in dichloromethane) was slowly fed to the atomizer using a peristaltic pump. The microspheres were then lyophilized and stored.

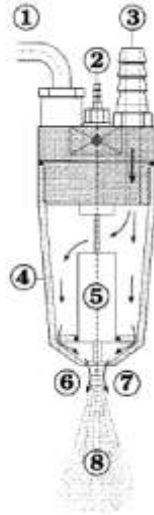


**Figure 18. Scheme of an ultrasonic atomizer [53]**

Different formulation parameters were studied. An increase in both feed's polymer concentration and oscillator power caused nozzle clogging, in the first case for an excessive amount of micro-particles, in the second one for the excessive temperature increase of the atomizer horn, and, accordingly, a reduction in particle yield. The mean particle diameter of all batches was found to be about 10  $\mu\text{m}$ , however a decrease in polymer concentration led to smaller particles. Of course, the release profile was influenced by drug/polymer ratio, feed viscosity and particles size.

Another spray-drying technique, consisting of feeding a fluid through an ultrasonic atomizer, drying the spray under reduced pressure, instead of hot air drying, and collecting the particles in a liquid bath, was evaluated [54]. As shown in Figure 19, a protein/polymer dispersion (BSA solution/ PLA/PLGA in solvent) was fed, by a syringe pump, to a 100 KHz ultrasonic nozzle. The vessel was kept under reduced pressure to allow solvent evaporation from the droplets. A throttle valve was used to avoid an uncontrollable drawn of the protein/polymer dispersion into the vessel. The resulted microspheres, first settled in a surfactant-containing aqueous solution, were then separated from the fluid by filtration, washed with deionized water, and finally dried. Simple particle recovery and use of vacuum instead of hot air for drying made this method well suitable for aseptic micro-systems preparation. However, as final result, the majority of particles

was very porous and exhibited an unacceptably high BSA burst release.

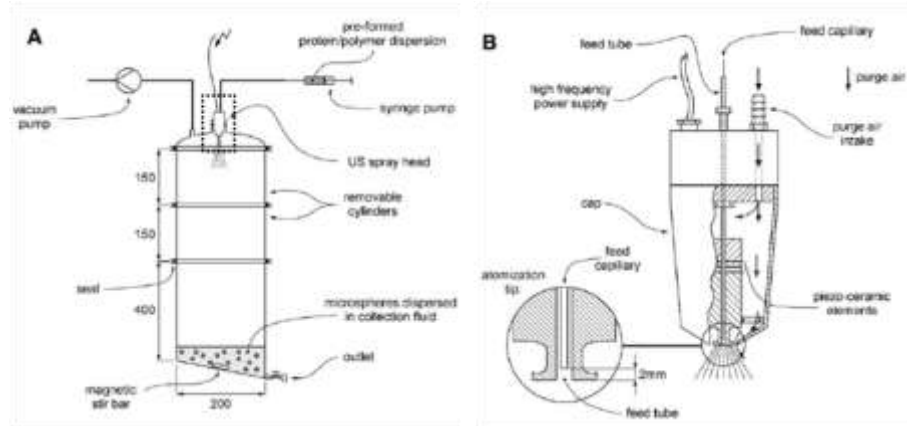


**Figure 19. Sketch of the vacuum spray-dryer (A) with detailed view of the ultrasonic nozzle (B)**

Luz et al proposed the use of a simple and low-cost ultrasonic spray drier system to produce micro-particles [55]. The equipment, shown in Figure 20, consists of an ultrasonic atomizer (1); a tubular furnace with two heating zones, as drying chamber (2); a micro-pored cellulose membrane supported on a sintered plate filter to collect particles (3); a vacuum pump (6) to separate the dried material from air; a filter flask (4) located inside a vessel containing cold water (5) to hold the condensed vapor.

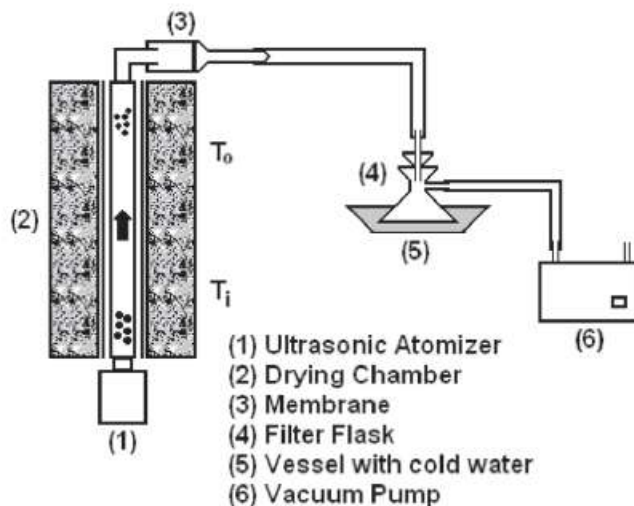


**Figure 20. Scheme of the ultrasound/spray-drying system [55]**

The results showed that 60% of the atomized feed (dextrin aqueous solution) was collected over the membrane in a dried powder form. The micro-particles were spherically shaped, with a diameter ranging from 0.2 to 2.6  $\mu\text{m}$ .

Ultrasonic atomization was an useful tool also in the encapsulation of darbepoetin alfa, a synthetic form of glycoprotein hormone that controls red blood cell production, through spray-freeze drying and spray drying processes at a pilot scale [56]. A suspension of solid protein particles in polymer solution was atomized to form nascent microspheres in each process. In spray freeze drying, the atomized spray was frozen in liquid nitrogen, followed by solvent extraction in cold ethanol for hours to days. In the spray drying, the polymer solvent was removed by evaporation; spray dried micro-particles were further dried using carbon dioxide gas. The ultrasonic nozzles used for both processes produced droplets of about 60  $\mu\text{m}$  or less, depending on the polymer kind, atomization power, and feed flow rate. Encapsulation efficiencies were very high, near 100%. The robustness of the ultrasound assisted process was demonstrated by the excellent reproducibility of physical and chemical characteristics of microspheres as well as of the in-vivo release kinetics.

### *2.2.3 Coaxial ultrasonic atomizer*

Focus is concentrated on the development of precision techniques of particle fabrication to control microsphere architecture as a means to modulate drug release. In particular, the ability to form shell-core micro-systems may offer several additional advantages in drug delivery. Advanced drug release properties, such as delayed or pulsatile release, with the removal of drug “burst”, may be made possible by selectively varying the shell material or its thickness. A coaxial ultrasonic atomizer is employed to produce a coaxial jet made of an annular shell (liquid flowing in the outer nozzle) and of core material (liquid flowing in the inner nozzle), which is acoustically excited to break up into uniform core-shell droplets [57]. As the atomizer vibrates (at a specific frequency), both liquids form a double layered film on the surface of the atomizer tip and are simultaneously fragmented into a large number of drops. Collision occurs among drops in proximity, followed by drops coalescence [50]. There are some examples of methods for fabricating uniform double-walled

microspheres with controllable size and shell thickness, which are shown in the following.

Park and Yeo presented a microencapsulation method using a coaxial ultrasonic atomizer based on interfacial solvent exchange [58]. In this system, shown in Figure 21, a PLGA solution in ethyl acetate, as external phase, and an aqueous solution containing optional solutes, as core phase, were separately fed into an ultrasonic coaxial atomizer. Microcapsules were collected in a water bath containing PVA as stabilizer, then were centrifuged and washed.

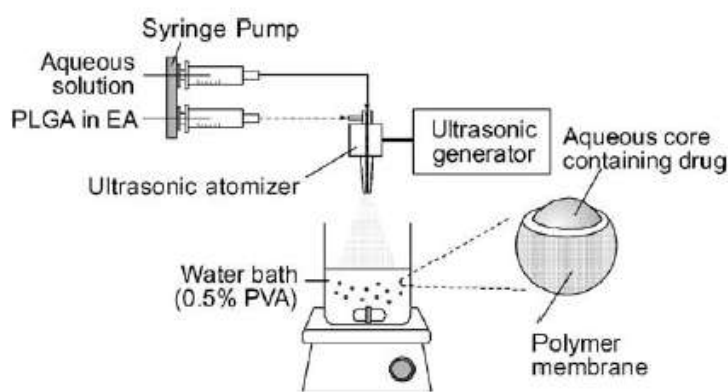


**Figure 21. Schematic description of the microencapsulation system using a coaxial ultrasonic atomizer [58]**

Water bath surface must be agitated (magnetic stirring or bath vibration) to avoid that a polymer layer forms on the surface, obstructing entrance of the micro-systems into the bath. Alternatively, the polymer solvent can be removed first by evaporation combining the solvent exchange method with spray-drying. After the atomization of the feed into the drying chamber, where a stream of warm gas is introduced to evaporate solvent and to solidify micro-systems, the separation of particles and gas can be performed in a cyclone attached to the drying chamber. The polymer solvent can also be removed by direct freeze-drying, when the molecule is sensitive to high temperatures [50]. Some parameters significantly influence the process: among these, the flow rates ratio of the two solutions ( $Q_{pol}/Q_{aq}$ ). When  $Q_{pol}$  is higher than  $Q_{aq}$ , the aqueous drops can easily find the polymer partner, a thicker membrane is produced, and coalescence between aqueous drops is avoided [50, 58]. Moreover, the aqueous drops resist to deformation and are encapsulated within the polymer drops thanks to the higher surface tension. Both extremes values of flow rates should be avoided: if flow rates are too low, the

population density of the micro-drops is not high enough to collide with other drops; if flow rates are high, the size distribution becomes wider. Moreover, a large volume for collection bath is recommended to make a sink condition around the solvent exchange area.

Another example of multiple concentric nozzles to produce shell-core micro-particles was proposed by Berkland et al [57]. The goal of this work was to fabricate uniform double-walled microspheres with PCPH (Poly[(1,6-bis-carboxyphenoxy) hexane]) cores and PLG (Poly(D,L-lactide-co-glycolide)) shells, i.e. PLG(PCPH) micro-particles, as well as PLG cores and PCPH shells, i.e. PCPH(PLG) systems, using the scheme in Figure 22. Thus, a dual polymer jet is formed, pumping the two different polymer solutions (PLG or PCPH in methylene chloride) in the coaxial nozzles. An additional coaxial nozzle supplies a carrier stream, containing surfactant, which surrounds the emerging dual polymer jet: it helps the jet break-up and avoids drop recombination. For each stream, the relative flow can be varied to control core diameter, shell thickness and particle size.

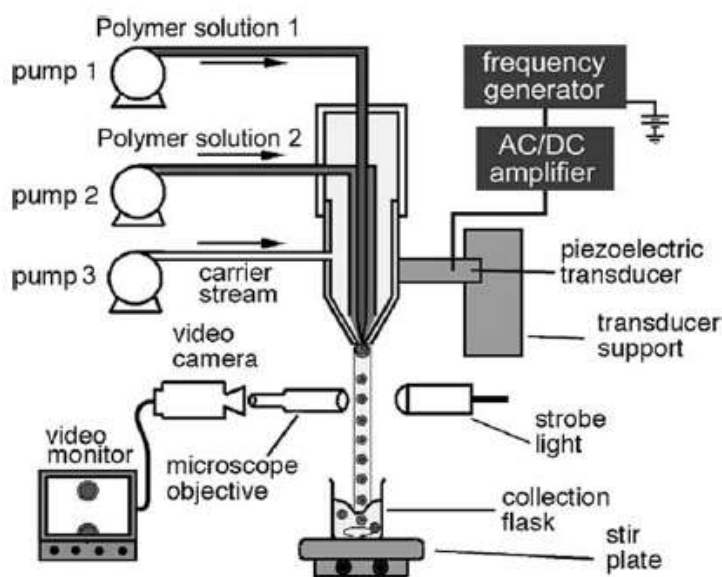


**Figure 22. Precision particle fabrication apparatus to produce uniform double-walled microspheres [57]**

Then, the streams flow into a beaker containing a collecting solution, where drops are stirred, filtered, and finally freeze-dried. This technology allows the production of micro-particles of about 50  $\mu\text{m}$ ,

having a shell thickness from less than 2  $\mu\text{m}$  to tens of microns and a complete and well-centered core encapsulation.

Microencapsulation of indomethacin in PLGA by coaxial ultrasonic atomization was also investigated [59]. Liquid feed in the inner tube consists of a PLGA solution in dichloromethane containing indomethacin, liquid feed through the coaxial outer tube consists of only PLGA solution in dichloromethane. The outer PLGA layer will deposit as a partial coating on the internal droplets containing the drug. The shell-core micro-particles are collected in a surfactant-containing solution bath, under mixing, to allow complete solvent evaporation. Particles are then centrifuged, washed and freeze-dried. The results showed that the presence of a second liquid layer increase the encapsulation efficiency of the drug, preventing drug loss during the solvent evaporation.

Fish oil was also encapsulated in microcapsules: three nozzle types, a pressure nozzle with one liquid channel, a pressure nozzle with two liquid channels, and an ultrasonic atomizer with two liquid channels were compared for their suitability to encapsulate fish oil in isolate whey protein [60]. Microcapsules produced by the double channel ultrasonic nozzle were observed to be more uniform in size and shape if compared to pressure nozzles. The ultrasonic nozzle showed a significantly narrower particle size distribution than the other nozzles. This study demonstrated that new ultrasonic nozzle designs can be a benefit for microencapsulation applications.

An interesting “alternative” apparatus of microencapsulation using ultrasonic atomization was proposed [61]. A tubular housing was coupled to a source of gas flow, such as a fan or a pressurized tank, to obtain laminar flow. The ultrasonic atomizer, in a coaxial configuration too, was assembled in the tubular housing, perpendicularly to the gas flow. The micro-particles were carried to an UV or to both UV and IR curing sections. Then, the cured micro-particles were collected in a collection chamber using either electrostatic attraction or an air filter. The microcapsules transport in the flow could be assisted by applying the same electric charge to the droplets and the walls of the housing channel to prevent both droplet coalescence and deposition on the walls of the flow channel. The apparatus had some benefits over conventional encapsulation technologies, such as the reduction of time and costs, by eliminating collection and hardening baths (filtering, washing and drying become



unnecessary). The use of a gas flow amplifies the capillary waves resulting from the ultrasonic vibrations, leading to tighter droplets size distribution and less consumption of ultrasonic power, thus preventing the degradation of some materials, such as cells and bacteria. Moreover, the UV chamber in the apparatus allows either polymerization of shell material, as monomer, or polymer hardening by solvent evaporation, around a water-soluble core, when water/oil emulsion is atomized. Therefore, thanks to the combination of alternative sources of energy, such as ultrasound and UV, the problem of using high pressures and temperatures is overcome.

### **2.3 Remarks about state of the art**

The review of the state of the art about microencapsulation processes showed first of all that microencapsulation is a matter of continuous investigation owing to its great industrial interest and to the number of possible configurations due to the multiple choices to perform the production of micro-systems and to the large number of parameters influencing each process. Different approaches were therefore followed, concerning both the way of droplets production and the micro-particles harvesting. In all cases the attention is focused on the achievement of micro-particles with the desired dimension and size distribution, according to their specific applications. The great drawbacks of the conventional processes are: high energy consumption; batch configuration, rather than a continuous one (losing all the advantages typical of a continuous process); high use of solvents; large preparation times. The use of ultrasonic devices in many researches highlights the tendency to energy optimization in pharmaceutical manufacturing and the need to move towards intensified preparing methods. In fact, despite the large amount of experimental work done, further researches, devoted both to the design and to the optimization of single-pot ultrasonic assisted processes to produce micro-particles under controlled conditions, could offer a new step of innovation.



---

## Chapter three

---

### **Ultrasonic atomization phenomena**

*In this chapter, the principles of atomization, first conventional, and ultrasonic, are highlighted. In particular, the parameters influencing droplets formation are shown.*

---

### 3.1 Atomization

The atomization is defined as the disintegration of a liquid in drops in a surrounding gas by an atomizer [22]. The resultant suspension (droplets or solid particles) is defined: spray, mist, or aerosol. Atomization occurs owing to the competition between destructive and cohesive forces on the liquid surface, leading to fluctuations and disturbances in the liquid. The cohesive effect of liquid surface tension keeps the fluid in a form showing the lower surface energy, and the stabilizing effect of the viscosity tends to oppose any variation in liquid geometry. Instead, the external forces, such as aerodynamic, centrifugal, and electrostatic forces, act on the liquid surface promoting its disintegration. The initial process of disintegration or break-up is defined *primary atomization*. However a number of larger droplets produced in the primary atomization can be unstable, thus reducing into smaller droplets. This process is usually defined *secondary atomization*.

In the *primary atomization* (because secondary atomization does not necessarily occur), droplets formation depends on the bulk liquid geometry. Thus it is obtained by:

- liquid dripping, the most simple way where drops form under the action of gravity;
- jet breakup, when a liquid jet, leaving a nozzle, is subjected to oscillations and perturbations, as a result of the balance between cohesive and disruptive forces; thus it breaks up into droplets;
- liquid ligament breakup, in rotary or centrifugal atomization, where centrifugal forces cause the detachment of droplets from liquid ligaments on a rotating surface;
- liquid sheet-film breakup, which can occur essentially in three ways, i.e. by contraction of the free edge of the liquid sheet in a thick rim (by surface tension forces), that breaks up in droplets; or by growing surface waves, deriving from instability on the sheet provoked by interaction with the surrounding medium; or, still, by holes generated on the sheet during liquid expansion, that can grow and form ligaments, breaking in droplets;
- liquid free-surface breakup, such as the phenomenon of droplets formation in sea-waves or in waterfalls.

For the *secondary atomization*, instability of the primary droplets is once again caused by the balance of forces acting on the drop (external aerodynamic forces and internal forces due to surface tension and viscosity). If the external forces cannot be balanced by the internal ones, drops break into smaller droplets, which have a higher surface tension, so they remain stable, ensuring an equilibrium state of the droplet. There are two different ways of primary drops breakup, depending on whether the droplets are subjected to steady acceleration (*bag breakup*) or exposed to a gas stream at high speed (*shear breakup*). In the *bag breakup*, the droplet is first flattened, under the constant acceleration, then, once reached a critical relative velocity, it turns in a bag, with a concave surface to the gas flow, which is stretched, and finally breaks (by bag perforation) in the downstream direction. In *shear breakup*, the droplet, under the influence of a high speed gas, is deformed in a way that is opposite respect to the *bag breakup* (convex surface to the gas flow), so that filament and subsequently smaller droplets form.

The effect of the forces acting on the liquid is resumed by dimensionless numbers:

$$Re = \frac{\rho \cdot u \cdot d_p}{\mu} \quad (3.1)$$

$$We = \frac{\rho \cdot u^2 \cdot d_p}{\sigma} \quad (3.2)$$

$$Oh = \frac{\sqrt{We}}{Re} = \frac{\mu}{\sqrt{\rho \cdot \sigma \cdot d_p}} \quad (3.3)$$

Where:

$Re$  = Reynolds number;

$We$  = Weber number;

$Oh$  = Ohnesorge number;

$\rho$  = liquid density;

$u$  = liquid velocity;

$d_p$  = jet diameter (primary atomization) or drop diameter (secondary atomization);

$\mu$  = liquid viscosity;

$\sigma$  = surface tension.

Reynolds number,  $Re$ , is the ratio between inertial and viscous forces. Weber number,  $We$ , is a measure of the relative importance of the fluid's inertia compared to its surface tension. By combining the two dimensionless numbers to eliminate the liquid velocity,  $u$ , the Ohnesorge number,  $Oh$ , that represents the fluid properties, is obtained. Thus, droplets diameter can be predicted by correlations mainly based on liquid properties (density, viscosity, surface tension), on atomizer geometry (orifice size) and on operative parameters, such as liquid flow rate. However, physical phenomena involved in the atomization processes have not been understood yet to such an extent that droplet size could be expressed by equations derived directly from first principles. The correlations proposed are mainly based on empirical studies, even if the empirical correlations proved to be a practical way to determine droplet sizes from process parameters and relevant liquid/gas physical properties [22]. In the following paragraphs, the main correlations for droplets size prediction used for dripping and ultrasonic atomization (matter of this thesis) are described.

### 3.1.1 Dripping

The simplest way of droplet formation is the liquid dripping, which occurs when a liquid is slowly discharged from the end of a thin tube. In particular, due to the low flow liquid velocity, the gravitational and surface tension forces govern the drop formation process. Therefore, the droplet diameter,  $d_p$ , for liquid leaving a thin circular tube, of diameter  $d$ , at low velocity is predicted by the following equation based on the force balance [62]:

$$d_p = \left( \frac{6 \cdot d \cdot \sigma}{\rho \cdot g} \right)^{1/3} \quad (3.4)$$

An approximation for droplet size prediction for small orifices is:

$$\frac{d_p}{d} = 1.6 * Bo^{-1/3} \quad (3.5)$$

Where  $Bo$  is the Bond number defined as:

$$Bo = \frac{d^2 \cdot \rho \cdot g}{\gamma} \quad (3.6)$$

The Bond number is a measure of the importance of surface tension forces on gravity or centrifugal forces. A large Bond number shows

---

that the system is not affected by surface tension, whereas a small Bond number (less than 1) indicates the predominance of surface tension.

### 3.1.2 Ultrasonic atomization

Another way of droplet formation is the jet breakup. In particular, when the liquid flows on a vibrating surface and splits into fine droplets, ultrasonic atomization occurs. A correlation proposed for the size diameter prediction of droplets produced by ultrasonic atomization, mainly based on the frequency  $f$ , was given by Lang [63]:

$$d_p = 0.34 \cdot \left( \frac{8 \cdot \pi \cdot \sigma}{\rho \cdot f^2} \right)^{1/3} \quad (3.7)$$

This correlation is applicable only when the liquid phase viscosity and liquid flow rate have no effect on droplet size, but these parameters were proven to be very important in ultrasonic atomization. The dimensionless numbers, which dictate the droplets size, were modified in order to consider the dependence on physical-chemical properties and ultrasonic parameters. Therefore, the concept of critical Weber, for which inertial and surface tension forces are equilibrated ( $We_c = 1$ ) was extended to ultrasonic atomization, indicating the critical flow rate,  $Q_c$ , as the threshold above which the flow rate influences the droplets size [49]. The critical flow rate was defined as:

$$Q_c = \frac{\sigma}{f \cdot \rho} \quad (3.8)$$

Then, the maximum flow rate, above which dripping takes place forming larger droplets, is considered. The maximum flow rate is the volumetric displacement rate of vibrating surface, given by the product of frequency,  $f$ , the amplitude of sound wave,  $Am$ , and area of vibrating surface,  $A$ . The amplitude,  $Am$ , is defined as:

$$Am = \frac{1}{2\pi \cdot f} \cdot \sqrt{\frac{2I}{\rho \cdot C}} \quad (3.9)$$

where  $I$  is the power surface intensity (defined as the ratio between the power delivered at the surface,  $P$ , and the area of vibrating surface,  $A$ ) and  $C$  is the speed of sound.

The Weber number was thus modified to include the flow rate,  $Q$ , and the ultrasonic frequency,  $f$ :

$$We = \frac{f \cdot Q \cdot \rho}{\sigma} \quad (3.10)$$

The Ohnesorge number was also modified taking into account that in ultrasonic atomization the growth of instability is given by the amplitude,  $Am$ :

$$Oh = \frac{\mu}{f \cdot Am^2 \cdot \rho} \quad (3.11)$$

Another dimensionless number, called Intensity number,  $I_N$ , is defined to take into account the effect of energy density on droplets size:

$$I_N = \frac{f^2 \cdot Am^4}{c \cdot Q} \quad (3.12)$$

From these dimensionless numbers, an universal correlation was proposed by Rajan and Pandit [49]:

$$d_p = \left( \frac{\pi \sigma}{\rho \cdot f^2} \right)^{0.33} [1 + A \cdot (We)^{0.22} \cdot (Oh)^{0.166} \cdot (I_N)^{-0.0277}] \quad (3.13)$$

The exponents in this correlation were chosen from experimental observations in literature.

Ramisetty et al [64] also carried out experiments and developed a correlation applicable in the following ranges:  $f = 20$ -130 KHz;  $\rho = 912$ -1151 Kg·m<sup>-3</sup>;  $\sigma = 0.0029$ -0.073 N·m<sup>-1</sup>;  $Oh = 2.71$ -161.64;  $We = 14.8$ -571;  $I_N = 3.65 \cdot 10^{-13}$  –  $1.92 \cdot 10^{-9}$ . The correlation was:

$$d_p = 0.00154 \cdot \left( \frac{\pi \sigma}{\rho \cdot f^2} \right)^{0.33} \left[ 1 + \left( \frac{\pi \sigma}{\rho \cdot f^2} \right)^{-0.2} \cdot (We)^{0.154} \cdot (Oh)^{-0.111} \cdot (I_N)^{-0.033} \right] \quad (3.14)$$

Avvaru et al [48] made an attempt to include rheological nature, pseudo-plasticity (non-Newtonian behaviour) of atomizing liquid. In particular, they collected data to obtain a correlation for an aqueous solution of carboxy methyl cellulose (CMC), having a shear thinning behavior, with a flow behavior index  $n$ :

$$d_p = \left( \frac{\pi \sigma}{\rho \cdot f^2} \right)^{0.33} + 0.0013 \cdot (We)^{0.008} \cdot (Oh)^{-0.14/n} \cdot (I_N)^{0.28} \quad (3.15)$$

Barba et al [65] proposed a modification of the correlation (3.13) by applying it to the ultrasonic atomization of alginate solutions:



$$d_p = 0.058 \cdot \left( \frac{\pi\sigma}{\rho \cdot f^2} \right)^{0.33} \cdot (We)^{0.151} \cdot (Oh)^{0.192} \cdot (I_N)^{-0.02} \quad (3.16)$$

Therefore, for the atomization of both Newtonian and non-Newtonian liquid, the following observations were done.

1. The droplet size decreases by increasing the frequency,  $f$ . At higher  $f$ , the liquid is subjected to a larger number of compression phases, thus the crest growth is reduced causing the eventual decrease of droplets size.
2. There is a range of liquid flow rate influencing the droplets size. Below a critical flow rate,  $Q_c$ , the liquid cannot cover the whole atomizing surface, thus no effective atomization occurs. Above  $Q_c$ , size is proportional to the liquid flow rate, again basing on film thickness on the atomization surface. Above a maximum flow rate, dripping occurs.
3. An increase in ultrasonic power causes an increase of the vibration amplitude ( $Am$ ), leading to a broader distribution of droplets size. In effect, when power delivered to the tip is low, it can be freely used as soon as liquid spreads on the atomizer surface. Instead, at higher power, the liquid delivered on the surface immediately atomizes causing both a conical pattern of the spray and the exposition of the external part of the atomizer to air, being not wetted by the liquid.
4. The influence of viscosity becomes significant when it is greater than 10 cP [49]. The increase of liquid viscosity was shown to cause a reduction of droplets size. As the liquid viscosity increases, the liquid cannot be immediately atomized as it comes out from the hole. Therefore, the residence time of the liquid on the atomizing surface increases, causing liquid temperature rising, owing to the vibrational energy dissipation, and the consequent decrease of liquid viscosity to a critical value. Thus, the liquid atomizes like a low viscosity liquid giving lower droplets size. The decrease of liquid viscosity is also enhanced by the shear thinning behavior of liquids, such as CMC and alginate: the apparent viscosity on the vibrating surface decreases to the high shear rates. As a result, a pseudo-plastic (non-Newtonian-shear thinning) liquid has a lower droplets size than a viscous Newtonian liquid, with a viscosity equal to the zero shear rate viscosity of the shear thinning liquid.

5. When surface tension decreases, at higher amplitudes the number of capillary waves per unit of vibrating area increases, causing the immediate ejection of droplets from crests. The higher number of droplets ejected from a liquid film for a same liquid flow rate causes a corresponding decrease in droplets size.

Overall, a proper control of the equipment operating parameters (flow rate, frequency, power) and liquid properties (liquid type, viscosity and surface tension) can give the desired droplets size .

---

## Chapter four

---

### **Microencapsulation apparatus building**

*In this chapter, the steps for building the microencapsulation apparatus are shown, the criteria used for components selection are highlighted and, finally, the plant functioning is described.*

---

## 4.1 General description of the apparatus

A semi-continuous apparatus for particles production by ultrasound assisted atomization, on a laboratory scale, was built. It is worth to underline that ultrasonic atomization can be coupled to microwave drying in order to obtain a single-pot, and therefore intensified, plant. The apparatus is composed of three main sections (Figure 23): pumping group or feed section, atomization section, separation and stabilization section. In a first stage, only the sections of feeding and atomization were built, then the separation/stabilization section was improved.

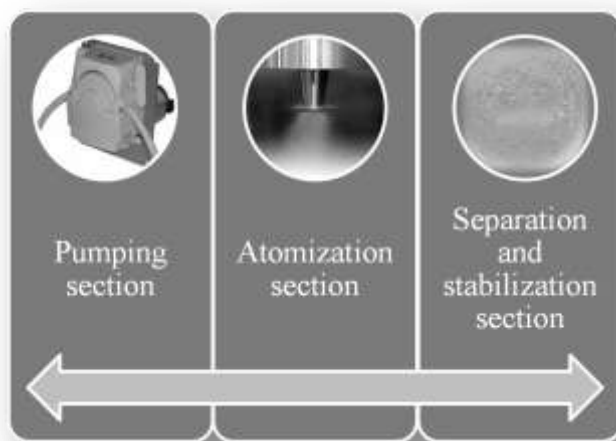


**Figure 23.** The three sections of pumping/feeding, atomization and stabilization

### 4.1.1 The apparatus: first stage

The pumping group is formed by two peristaltic pumps (*Verderflex OEM mod. Au EZ*) controlled by two systems with variable tension (*Long WEI DC power supply PS305D*) to obtain the adjustment of the flow rate. The solutions are withdrawn from stocking tanks by the pumps and are sent to the atomization tip. In particular, the feed circuit is composed of two independent lines, formed by silicon flexible tubes ended by a stretch of plastic, not flexible, tubing.

The atomization section is formed by a coaxial ultrasonic atomizer (*dual liquid feed probe Sono-Tek 025-00010, Sono-Tek corporation*) connected to an ultrasonic generator (*broadband ultrasonic generator mod. 06-05108-25K Sono-Tek corporation*) that converts energy into

vibratory mechanical motion. The atomizing nozzle is connected to the two feed lines, named line 1 (*core line*) and line 2 (*shell line*) to outline the entrance of solutions respectively in the inner and in the outer channel.

The atomization products were collected, in a first stage, in a hardening solution. At this stage, the hardening solution was contained in a beaker and submitted to agitation (*Falco F60*). Features of the initial state of the apparatus can be observed in Figure 24.

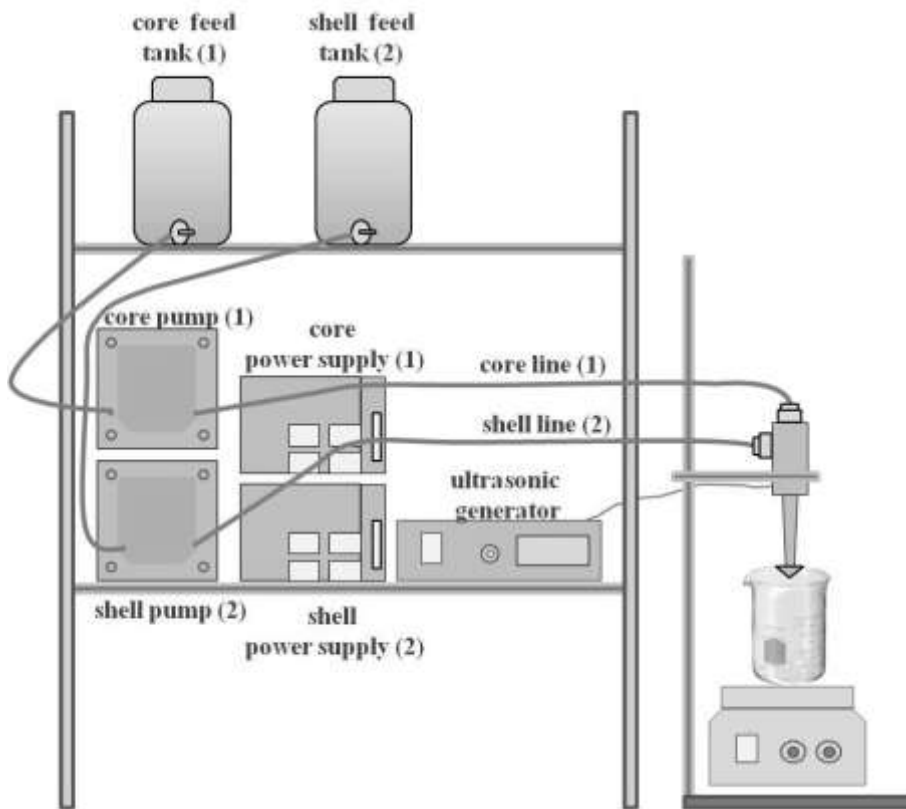


**Figure 24.** A scheme of the initial state of the apparatus

The separation and stabilization section included apparatuses for under-vacuum filtration of particles (*pump KNF Laboport*) and a double line for stabilization operations (drying): tray oven with air (*ISCO mod. 9000*) and microwave multimodal cavity (*De Longhi, Perfecto-Easy MW314*).

4.1.2 The apparatus: final state

In the final state, the apparatus keeps both the configurations of feeding section and atomization section. Modifications were made to the stabilization section in order to obtain a semi-continuous plant. The technical description of the novel semi-continuous apparatus is given in Figure 25.

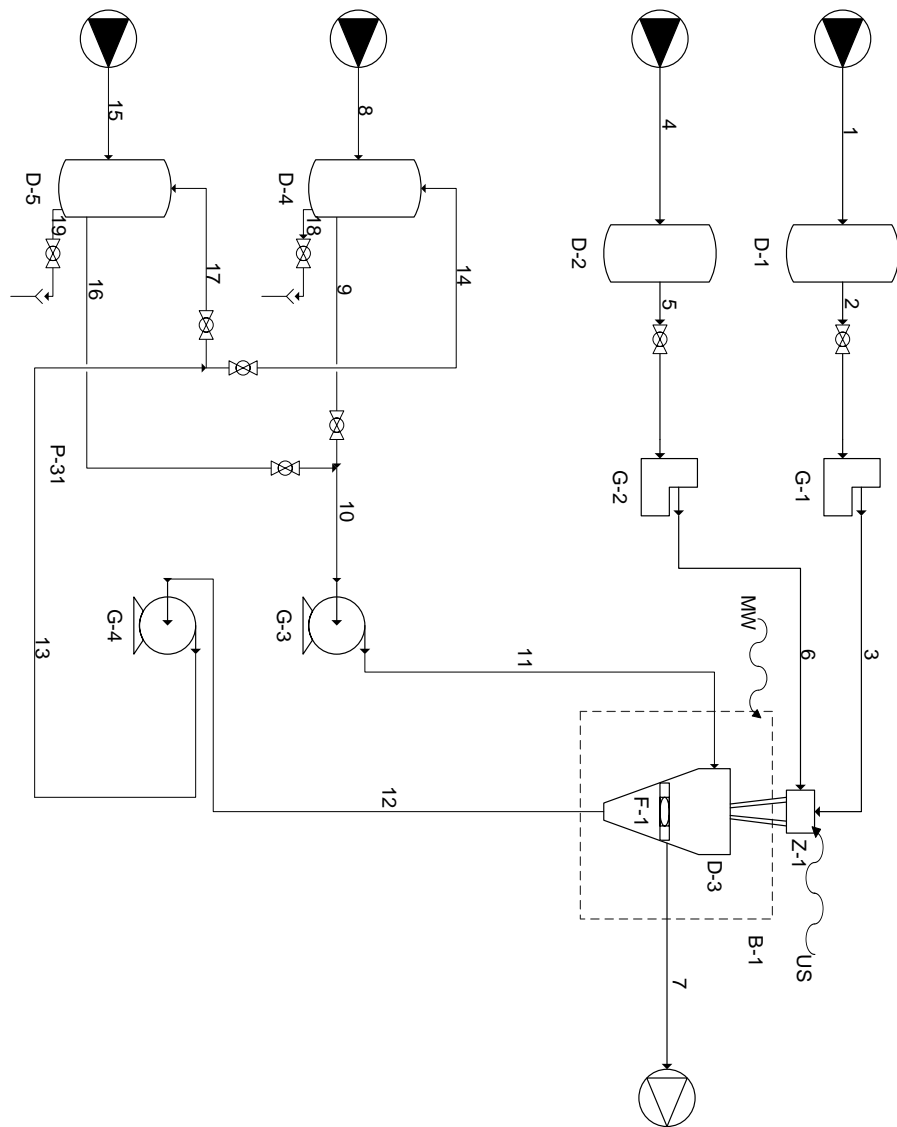
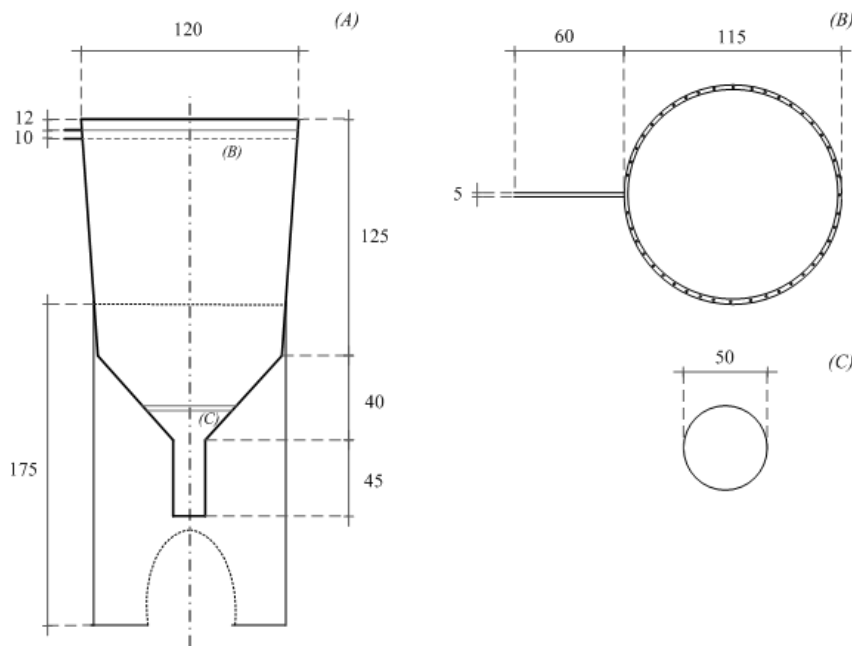


Figure 25. Scheme of the single-pot semi-continuous bench scale apparatus

In particular, the stabilization section is composed of:

- a wet-collector, i.e. a sort of hydrocyclone, that allows the uniform distribution of the hardening solution and the consequent contact with the atomized drops (outgoing from the atomizer, placed at the centre of the wet-collector);
- a filtering device, within the wet-collector, on which the final product is recovered (cross-linked particles);
- a feeding and recirculation circuit of both the hardening solution and the washing water (post-hardening).

The wet-collector, made of glass, shown in Figure 26 (A), is characterized by the entrance of the harvesting fluid in a dispenser (Figure 26, (B)), composed of a pierced circular tube. It is supported by a glass cylinder with an open section for the passage of the tube connecting the bottom of the wet-collector to the pump for recirculation of harvesting fluid (or washing water).



**Figure 26. Dimensional features, in mm, of wet-collector, with the details of both fluid dispenser (B) and filter (C)**

The filtering device is a porous disk (Figure 26, (C)) with the following features: diameter = 50 mm; thickness = 5 mm; porosity grade = 4 (pore size about 5-15  $\mu\text{m}$ ).

The feeding and recirculation circuit is characterized by two centrifugal pumps (*DC15/5 Totton pumps*): the first one provides for feeding the hardening fluid (or alternatively the washing water) to the wet-collector, the latter assures the recycle of the fluid to the tank. The switch from hardening fluid to washing water circulation is made by respectively closing the valve of harvesting fluid's vessel and opening the valve of washing water's vessel. The use of a suitably designed wet-collector allows to carry the process in a semi-continuous rather than in a batch way.

Moreover, a commercial cavity, at low power, is dedicated to the set up of the first prototype of the oven containing the wet-collector. This latter was just designed on the basis of the geometrical features of the multimodal cavity *Perfecto-Easy MW314*. Therefore, the obtained product, settled on the filter, can be subjected to a final microwave drying before recovering by extraction of the filter from the apparatus.

## **4.2 Criteria of components selection**

Selection of components, to be used for construction of the plant, is a fundamental step, as it cannot be a trivial choice from catalogues. Rather, first an accurate analysis of both possible strong and weak points of the future plant and process, then a relevant effort to reach the former and overcome the latter, are done. Therefore, right selections are needed to complete the apparatus and obtain the best performances, from the central unit (in this case the ultrasonic atomizer) to the most insignificant connection tubes, whose neglect (for example about suitable material, size, thickness) could slow down or even stop the apparatus working.

### *4.2.1 Atomizing section*

The crucial component of the apparatus is the ultrasonic atomizer. The search for the most suitable coaxial ultrasonic atomizer gave as result the purchase of a Sono-Tek product [66]. Disc-shaped ceramic piezoelectric transducers receive high frequency electrical energy from the Broadband Ultrasonic Generator and convert that energy into vibratory mechanical motion at the same frequency. The transducers are coupled to two titanium cylinders that amplify the motion. The excitation created by the transducers produces standing waves along the length of the nozzle, whose amplitude is maximized at the atomizing surface, located at the end of the small diameter portion of



the nozzle (Figure 27). In general, high-frequency nozzles are smaller, create smaller drops, and have a lower flow capacity than nozzles that operate at lower frequencies. The vibration amplitude must be carefully controlled. Below the so-called critical amplitude, there is insufficient energy to produce atomization. If the amplitude is too large, the liquid is literally ripped apart, and large “chunks” of fluid are ejected. The amplitude ideal for producing fine, low-velocity, spray is thus located only within a narrow band of input power. The exact magnitude of required power depends on several factors, including nozzle type, liquid characteristics (viscosity, solids content), and flow rate.

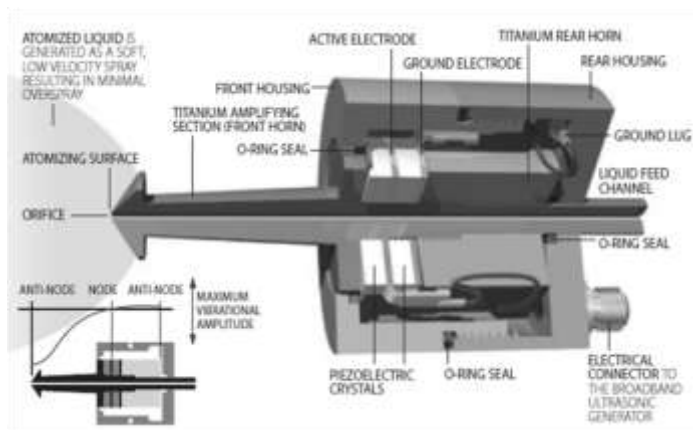


**Figure 27. Cross-sectional view of a typical nozzle [66]**

Depending on nozzle style, the atomizing surface shape is conical, focused, or flat. Focused nozzles are usually recommended for use in applications where flow rates are very low and narrow spray patterns are needed; the cylindrical spray shape (flat) is used in applications where the flow rate can be relatively high, but the width of the spray pattern must be limited. According to these features, a 25 KHz Ultrasonic Nozzle, with conical atomizing surface shape, a tip diameter of 0.46 in (11.684 mm), and an orifice size of 0.040 in (1.016 mm), with a microbore installed in, were selected. The microbore inside has an external diameter of 0.028 in (0.711 mm) and an internal diameter of 0.016 in (0.406 mm). A dual liquid option was selected (selection of the internal microbore), giving greater flexibility to the process and resulting ideal for microencapsulation, as two liquids are mixed right at the nozzle atomizing surface (Figure 28).



**Figure 28. Dual liquid feed assembly [66]**

The selection of the 25 KHz model derives from specifications about the maximum flow rate, the median drop diameter, and the length of the tip that are 3.3 mL/s, 55  $\mu\text{m}$ , and 55 mm respectively. The maximum flow rate of 3.3 mL/s is one of the highest achievable rates (obtainable with a tip diameter of 0.46 in (11.684 mm), and an orifice size of 0.141 in (3.581 mm)) to avoid low productivities. In this case, the selected orifice size gives a maximum flow rate of 0.3 mL/s. The length of the tip of 55 mm is one of the longest to allow the insertion of the nozzle in the microwave cavity and at the center of the wet-collector used as collector. The selection of the conical (against focused or flat) shape for the atomizing surface depends on the need to assure a wide spray pattern distribution of nebulized liquid.

#### 4.2.2 Feeding section

After the selection of the ultrasonic atomizer, the next step was to connect the nozzle to a liquid delivery system. Some recommendations are necessary: choosing the proper liquid delivery system often makes the difference between acceptable and unacceptable performance. First of all, a plastic tube, chemically compatible with the liquid to be sprayed, is preferable. A secure tube insertion in the fitting is fundamental because loose fittings may cause degradation of nozzle performance and may become quite hot owing to the absorption of the ultrasonic energy. Moreover the selection of the best option depends on several factors, such as cost, precision required, needed flow rates and maintenance. Typically, there are six basic methods of liquid delivery that are routinely used with ultrasonic spray nozzles: gear pumps, piston pumps, syringe pumps, pressurized canisters, gravity systems and peristaltic pumps. These latter have some benefits: are excellent with virtually any type of liquid, have only liquid contacting tubing and are flexible in quick tubing changes

and in cleaning. The most suitable pumps are selected to deliver the right flow rate to both the inner and the outer channels and to ensure the desired flow rate ratio to obtain encapsulation of inner material in the outer one. The selected pumps are peristaltic pumps Verdeflex with variable flow capability (Table 6).

**Table 6. Variable flow rates, mL/min, according to the combination of drive options and tube diameters [67]**

Nominal flow rate, mL/min					
<i>Tube (ID)</i>	0.8 mm	1.6 mm	3.2 mm	4.8 mm	6.3 mm
<i>Drive options</i>					
60 rpm	4.6	16	64	140	225
100 rpm	7.7	28	108	235	375
150 rpm	12	42	162	352.5	562.5

However, the solutions to be used in the apparatus have high viscosity, which would cause a reduction of the flow rate. A tube with a greater wall thickness is suggested [68]: a flexible tube with an internal diameter of 1.6 mm and a wall thickness of 1.6 mm was chosen. Moreover, the high viscosity of processed solutions causes the need for stronger end connections in correspondence of the entry in the two channels of the atomizer, where a sudden reduction in section occurs. Therefore, Swagelok fittings were chosen for end connections.

#### 4.2.3 Separation/drying section

In designing the wet-collector, that is similar to a hydrocyclone, a number of parameters have to be considered. The main parameter is the hydrocyclone diameter, i.e. the inside diameter of the cylindrical feed chamber. The second one is the area of the inlet nozzle at the point of entry into the feed chamber. It is usually a rectangular orifice, with the larger dimension parallel to the cyclone axis. The cylindrical section is the next basic part of the cyclone and it is located between the feed chamber and the conical section, with the function to lengthen the cyclone and increase the retention time [69]. In the design of the wet-collector, this cylindrical section is replaced by a conical one at the end of which the filter is placed. Therefore, the liquid is recovered at the bottom of the hydrocyclone and the particles collected on the filter are recovered. The wet-collector was therefore designed on the basis of these suggestions, even if some adjustments were done for both assuring its workability and adapting it to the needs of the novel

plant. For example, the entrance in the wet-collector of the harvesting fluid is not tangential, unlike common hydrocyclones, but there is a dispenser, composed of a pierced circular tube. All the features of wet-collector were already described in Figure 26 in paragraph “4.1.2 The apparatus: final state”. The choice of the two centrifugal pumps for the feeding and recirculation circuit of both the hardening solution and the washing water was done on the basis of two requirements. First of all, there is the need to obtain a uniform distribution of the liquid solution in the wet-collector (to promote contact between hardening and drops). Then, pressure drops, due to the presence of the filter, have to be overcome. It is worth to note that the wet-collector has dimensions just designed on the basis of the geometrical features of the multimodal cavity, for a final “on-line” microwave drying of the obtained product.

### **4.3 Description of plant operation**

The technical description of the novel semi-continuous apparatus is given in Figure 25. Both the solutions, core and shell materials, stocked in separate tanks, respectively D-1 and D-2, are sent by the peristaltic pumps (G-1 and G-2) to the ultrasonic double channel atomizator (Z-1), put at the centre of the wet-collector (D-3), which is in turn placed in the microwave oven (B-1). The feed core line is directed to the inner channel of the nozzle while the shell line is addressed to the outer channel. The two solutions come in contact only at the exit of the two channels, at the atomizer’s tip, where they are nebulized. It is worth to note that in the first operation stage, the filter (F-1) is not present in order to assure a continuous recirculation of hardening solution. Recirculation is essential to renew the surface of contact between droplets and hardening solution and therefore to avoid film formation: feeding (G-3) and recirculation (G-4) pumps are both switched on. Obtained drops come in contact with the hardening solution, (a volume of 300 mL, with a volumetric flow rate of about 37 mL/s), which is uniformly delivered by dispenser. Drops become particles owing to cross-linking with the hardening solution: the obtained suspension is continuously recycled to the storage tank, with the same volumetric flow rate of feed, i.e. 37 mL/s. Therefore, the hardening solution become increasingly concentrated in particles each time it is spread by dispenser (even if it remains always diluted), until the end of atomization process. At this point of the process, when the suspension is stored in the hardening solution tank (D-4), the filter is

placed within the wet-collector. Therefore the suspension is fed back to wet-collector, where all the liquid accumulates owing to the presence of the filter. The feeding pump (G-3) is switched off, while the recirculation pump (G-4) is switched on: at this stage the volumetric flow rate in the recirculation line is of about 1 mL/s due to the filter pressure drops, with a consequent cross-linking time of about 5 minutes. The following washing step, if necessary, is done in a manner similar to the previous hardening step by closing the valve of hardening fluid's vessel and opening the valve of washing water's tank respectively. Particles settled on the filter can be stabilized by microwave drying. Then they are recovered by extracting the filter from the apparatus.



---

## Chapter Five

---

### **Microencapsulation apparatus testing**

*In the chapter, the selection of materials and evaluation of operative parameters are described. Then, a first test about the encapsulation of a model molecule, vitamin B12 is carried out, to check the atomization features of the apparatus. A further test of encapsulation of a molecule with different solubility,  $\alpha$ -tocopherol, is also done in order to validate the final apparatus operation.*

---

## 5.1 Process parameters definition

Each of the three sections has parameters to be first controlled and then optimized (Figure 29).

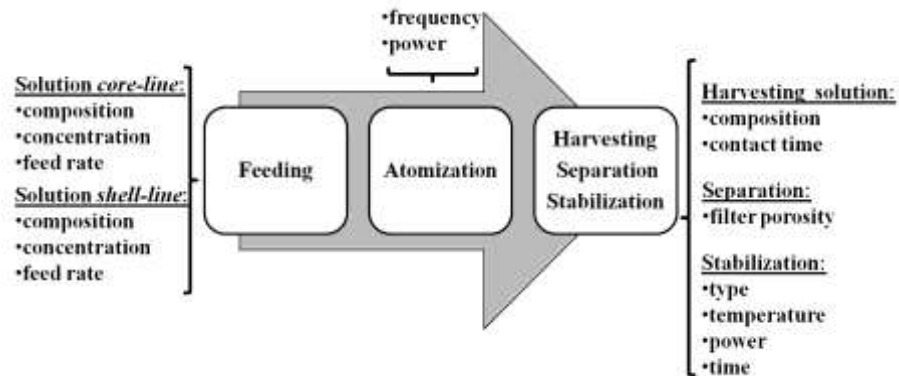


**Figure 29.** Apparatus parameters to be controlled and optimized

Searching for the best combination of feeding parameters, such as type of materials, composition, concentration and feed rate, that assure the encapsulation of the core material in the shell, is highly desired. This phase is achieved by dripping test, keeping the ultrasounds switched off. Then, parameters of the atomization section, essentially power, have to be considered. As concerns the separation and stabilization section, three important parameters have to be defined: 1) properties of harvesting/hardening solution; 2) filter typology; 3) drying conditions.

### 5.1.1 Operative parameters: feeding

#### 5.1.1.a Materials: alginate

As material to be processed in the apparatus, a natural polymer, alginate, was chosen thanks to the possibility to carry out a process in an aqueous environment, without organic solvents or high temperatures.

Alginates, natural biopolymers extracted from brown algae, are anionic linear polysaccharides which contain varying amounts of 1,4'-linked  $\beta$ -D-mannuronic acid (M) and  $\alpha$ -L-guluronic acid residues (G) [70]. The residues may vary in composition and sequence and they are arranged in a pattern of blocks along the chain. Because of the particular shapes of the monomers and their modes of linkage in the



polymer, geometries of the G-block regions, M-block regions, and alternating regions are substantially different (Figure 30). The G-blocks are buckled while the M-blocks have an extended ribbon shape. If two G-block regions are aligned side by side, a hole with a diamond shape is obtained. The M-blocks and G-blocks are interdispersed with regions of alternating structure (M-G blocks). Composition and extent of the sequences and molecular weight determine physical properties of the alginates [71].

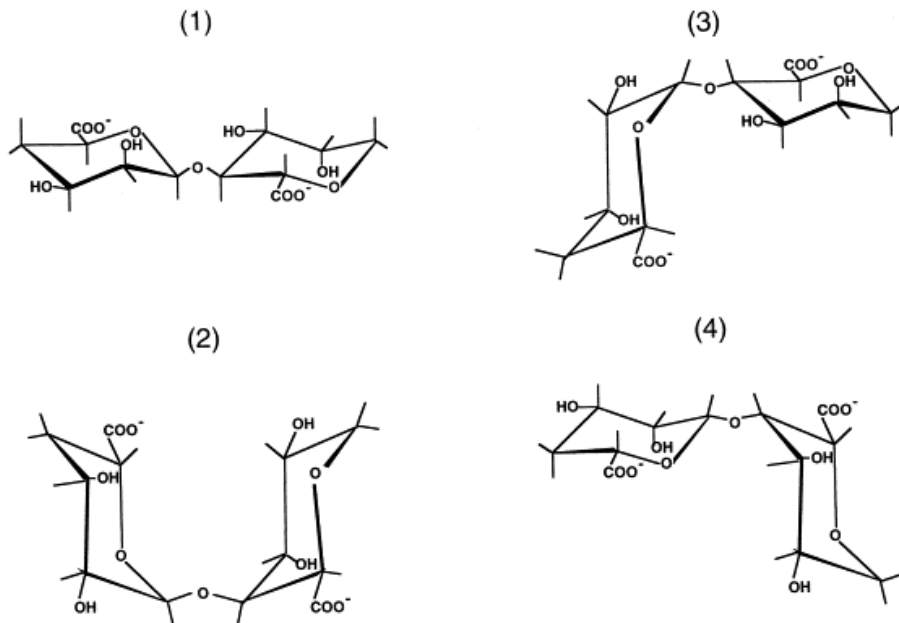


**Figure 30. Structure of alginate: chemical formula of MM, GM, GG blocks [72]**

Alginate has several properties that have enabled its use as a matrix for the entrapment and/or delivery of a variety of biological agents [73]. Among these properties there are: the possibility to carry out a process in an aqueous environment, with a mild room temperature and in absence of organic solvents; a gel porosity that can be controlled by coating procedures in order to modulate the diffusion rate of macromolecules; finally the ability of the system to undergo dissolution and biodegradation under normal physiological conditions. Alginate beads can be prepared by extruding a solution of sodium alginate containing the desired active principle, as droplets, into a divalent cross-linking solution such as  $\text{Ca}^{2+}$ ,  $\text{Sr}^{2+}$ ,  $\text{Ba}^{2+}$ . Monovalent cations and  $\text{Mg}^{2+}$  ions do not cause gelation; while  $\text{Ba}^{2+}$  and  $\text{Sr}^{2+}$  ions produce stronger alginate gels than those produced using  $\text{Ca}^{2+}$ . These

last three ions exhibit positive GG preference. Other divalent cations, such as  $\text{Pb}^{2+}$ ,  $\text{Cu}^{2+}$ ,  $\text{Cd}^{2+}$ ,  $\text{Co}^{2+}$ ,  $\text{Ni}^{2+}$ ,  $\text{Zn}^{2+}$ , and  $\text{Mn}^{2+}$ , would also cross-link alginate gels but their use is limited owing to their toxicity. Since the functional and physical properties of cross-linked alginate beads depend on composition, sequential structure (GG-MM-MG blocks), and molecular size of the polymers, a gel made from a high  $\alpha$ -L-guluronic acid alginate has a higher strength if compared to an alginate rich in mannuronic acid owing to the stronger affinity of guluronic residues (GG) for divalent ions (the diamond shaped hole has dimensions that are ideal for the cooperative binding of calcium ions) [73]. This preference can be explained in terms of the alginate secondary structure. In particular, the type of oxygen atoms involved in binding with the ion may affect the binding preference toward GG or MM groups, as shown in Figure 31.

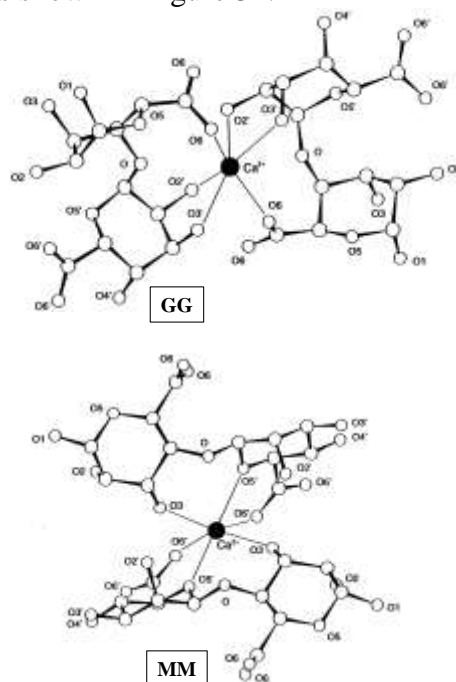


**Figure 31. Molecular models of two GG dimers (up) and of two MM dimers (down) with  $\text{Ca}^{2+}$  [74]**

A total of six interactions between  $\text{Ca}^{2+}$  and alginate oxygens were obtained: the two blocks differ only in the type of oxygens that are in close proximity to the metal ion. In fact, for GG blocks, a carboxylate oxygen (O6) and two hydroxyl oxygens (O2 and O3) in each dimer are involved, while MM blocks involve a ring oxygen (O5) in each

dimer instead of the O<sub>2</sub>. A stronger interaction between Ca<sup>2+</sup> and GG blocks is expected owing to the fact that hydroxyl oxygens (O<sub>2</sub>) are stronger Brønsted-Lowry bases than ether oxygens [74].

Flexibility of the alginate polymers decreases in the order GG < MG < MM, therefore the lowest shrinkage, the highest mechanical strength, the highest porosity, and the best stability towards cations are obtained from alginate with an  $\alpha$ -L-guluronic acid content greater than 70% and an average length of the G-blocks higher than 15 [73]. More rigid gels are also less subjected to swelling and erosion [75].

Key parameter for the entrapment of active principles is the pore size of the gel, which has been shown to be in the interval 5 and 200 nm [71, 76-77]. Therefore, the small molecules diffusion is not affected by the alginate matrix while larger proteins diffusion depends on their molecular weight. Gels made of a high  $\alpha$ -L-guluronic acid have a less open pore structure, exhibiting lower diffusion rates [78]. The porosity can be significantly reduced by partially drying. Moreover, a protein, as much as a low molecular drug, with an overall positive charge can interact with negatively charged alginate, inhibiting diffusion from the gel. Then, degradation of Ca<sup>2+</sup> cross-linked alginate gel can occur by removing Ca<sup>2+</sup> ions, for example by solution containing a high concentration of ions such as a Na<sup>2+</sup> or Mg<sup>2+</sup>. Alginate gels also degrade and precipitate in 0.1 M phosphate buffer solution (in this case the dissolution medium will turn turbid due to the Ca<sup>2+</sup> dissociating from the polymer network and forming calcium phosphate precipitate) and completely dissolve in 0.1 M sodium citrate at pH 7.8 [73]. Furthermore, alginate forms strong complexes with polycations including chitosan, polypeptides and synthetic polymers. These complexes do not dissolve in presence of Ca<sup>2+</sup> chelators and they can be used to both stabilize gel and reduce its porosity. Moreover, alginate has bioadhesive properties, useful when formulating potential delivery vehicles for drugs to mucosal tissues, such as the GI tract. Adherence to mucosal tissues localizes the drug and delays the protein transit time, improving the overall drug effectiveness and bioavailability [73].

#### *5.1.1.b Selection of feeding parameters*

The sodium alginate used was the medium molecular weight Manugel GHB Sodium alginate, purchased from FMC Bio-polymer. It has a high guluronic content: guluronic acid 63%, mannuronic acid 37%. Properties of the alginate are reported in Table 7.

**Table 7. Typical properties of alginate Manugel GHB [79]**

Alginate Manugel GHB	
Molecular weight	~97000
M:G ratio	~0.59
Viscosity at 10 g/l (mPa·s)	50-100
Loss on drying (%)	<13
Ash (dried basis) (%)	18-27
Heavy metals (ppm)	<1.9

The large guluronic content gives more rigid gels, that are less subjected to swelling and erosion [75]. The cross-linking solution was a  $\text{CaCl}_2$  aqueous solution with a concentration, 8.9 g/l, already defined in a previous work [65] and enough high to assure complete cross-linking of particles. Core and shell solutions feeds have to be easily processed: too viscous solutions could lead to the clogging of the channels. Having selected the best concentration for the two streams, the relevant flow rates of each of the inner (core) and outer (shell) streams are varied to control core diameter, shell thickness, and overall particle size [57]. Yeo and Park [58] observed that the encapsulation efficiency decreased by increasing the ratio ( $Q_{\text{Aq}}/Q_{\text{Pol}}$ ) of flow rates of internal aqueous solution ( $Q_{\text{Aq}}$ ) to external polymer solution ( $Q_{\text{Pol}}$ ). In particular, at a relatively high  $Q_{\text{Aq}}/Q_{\text{Pol}}$  ratio (case 1), more water drops would be formed than polymer drops and they would have better chances to grow before collision. At a relatively low  $Q_{\text{Aq}}/Q_{\text{Pol}}$  (case 2), the polymer drops would coalesce into bigger drops before they collide with the aqueous drops. Therefore, the desired shell-core conformation would preferably occur when the size of the polymer drop is larger than that of the aqueous drop (case 2). In fact, authors observed that the encapsulation of one drop by the other was affected not only by the surface tension gradient but also by the size ratio of the participating drops: the contacting microdrops dominating in size, encapsulated the other ones due to the larger inertial force, regardless of the surface tension gradient. In particular, the preferable  $Q_{\text{Aq}}/Q_{\text{Pol}}$  ratio was observed to be 1/4 or lower in order to assure that the size of polymer drops dominate enough the aqueous drops. However different starting conditions lead to a different optimum ratio between inner and outer streams. For example,

Berkland et al [57] produced double walled microspheres of two polymers using a ratio of about 10 to 1 of the outer to the inner polymer solution.

To test the ability of coaxial apparatus to obtain shell-core systems (as in Figure 32) by a dripping test, i. e. keeping the ultrasounds switched off, both the inner (core) and the outer (shell) streams were highlighted using pigments to see the disposition of the internal drop with respect to the external one.

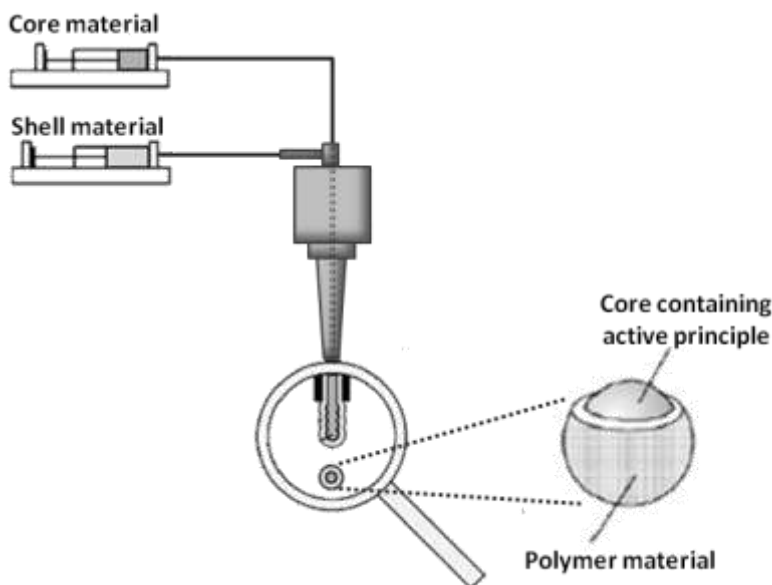


**Figure 32. Coaxial dripping to obtain shell-core systems**

A first dripping test on the apparatus, keeping the ultrasounds switched off, was carried out using water for the core channel and a solution at 1% w/w of alginate as the outer stream. However, under these conditions, for any combination of flow rates, the external shell did not wrap the internal core, producing a shapeless mass. However Berkland et al suggested that increasing the amount of solvent, and thus the fluidity in the shell of the nascent double-walled microsphere, may aid the spreading of the shell phase onto the more highly concentrated and less mobile core phase [57].

Following literature indications about concentration, a system characterized by an inner solution of 1% w/w of alginate and an outer solution of 0.5% w/w of alginate was tested. Even if, having selected the proper flow rate ratio, a shell-core system is obtained, particles

appear to be too weak. Therefore, different combinations of core/shell concentrations of alginate were tested, as shown in Table 8.

**Table 8. Polymer (alginate) concentrations (w/w) of both core and shell solutions and their effect**

(A)	(B)	(C)	(D)	(E)
<b>INT: 1%</b> <b>EXT: 0.5%</b>	<b>INT: 1%</b> <b>EXT: 1%</b>	<b>INT: 1%</b> <b>EXT: 1.5%</b>	<b>INT: 1.5%</b> <b>EXT: 1.5%</b>	<b>INT: 1.5%</b> <b>EXT: 2%</b>
Weak particles owing to the low concentration of alginate in the shell	Good encapsulation, but fast migration outside of inner pigment	An external high concentration gives a greater viscosity to the shell, limiting the migration of the pigment, hence probably of an active principle	Better consistency of particles, delayed migration of pigment	Higher power to pump and then atomize the more viscous shell. Moreover, deformation of the particles toward a non-spherical shape

From notes in Table 8, the best configuration results to be the one with a concentration of alginate of 1.5% (w/w) for both inner and outer solutions (D).



**Figure 33. Example of shell-core particles: blue core confined in the transparent shell material**

A good encapsulation of the internal drop in the external one, as seen by pigments, was obtained for flow rates ratio between the outer ( $Q_{out}$ ) and the inner streams ( $Q_{in}$ ),  $Q_{out} / Q_{in}$ , comprised in a range between 6 and 6.5, with  $Q_{out}$  in the range 4-4.5 mL/min and  $Q_{in}$  in the range 0.65-1.1 mL/min. A picture (Figure 33) of obtained particles in these conditions highlights the confinement of the internal (blue) core in the (transparent) shell. Resuming, a good system for encapsulation can be obtained using a concentration of alginate of 1.5% (w/w) for both internal and external streams in the coaxial nozzle. The optimal flow rate values are:  $Q_{out}$  in the range 4-4.5 mL/min and  $Q_{in}$  in the range 0.65-1.1 mL/min. It is worth to note that concentrations and flow rates above do not endanger the possibility of atomizing the two streams.

#### *5.1.2 Operative parameters: atomization*

The parameters of an ultrasonic atomizer to be tuned are two: frequency and power delivered to the nozzle. The frequency is fixed (already selected in paragraph “4.2.1 Atomizing section”); instead power has to be properly chosen. Below a critical power level, referred to as the “stall point”, there is insufficient energy to produce atomization. At too high power levels, the excess of provided energy causes expulsion of large chunks of material, rather than the characteristic soft spray of fine drops (cavitation). The stall point depends on several factors: nozzle type, liquid features (viscosity, solid content), flow rate, size of atomizing surface. In particular the higher the viscosity or the flow rate, the higher will be the power required. The droplet size distribution is more uniform for low vibrational intensities (power/atomizing surface), whereas and the distribution peak shifts towards higher droplets size. Therefore, power was selected as the minimal power to ensure a uniform distribution of the spray.

#### *5.1.3 Operative parameters: separation and stabilization*

The properties and way of cross-linking, as well as filtering device features, were already described in previous paragraphs. Fundamental is the stabilization step: microwave power was set to avoid too high temperatures that could degrade molecules, especially the thermo-sensitive  $\alpha$ -tocopherol. In particular, a fictitious power level of 245 W, deriving from a duty cycle of the 700 W multimodal cavity (*Perfecto-*

*Easy MW314*) where the magnetron is switched on for 1/3 of total time of operation, was chosen.

## 5.2 Encapsulation of model molecules

Aim of this paragraph is to show the capability of the novel plant to obtain micronized systems that exhibit a behavior interesting for the pharmaceutical or nutraceutical market. In particular, comparison between only core systems (matrix structure) and shell-core systems, both in millimetric and micrometric scale, was done in order to detect loading and releasing of an active principle. In particular, in the shell-core system preparation, the active principle is put in a solution which is fed to the inner channel of the coaxial nozzle, and it is then atomized together with the external solution, containing the polymer, that surrounds the internal one, encapsulating it and, consequently, the active principle. The only-core (matrix) system instead is obtained by atomizing only the internal solution, containing active principle and polymer, in the inner channel, leaving thus empty the external one. As shown in Figure 34, the shell-core system should protect the active principle, thanks to the external coating, differently from the matrix system where the active principle is dispersed in the matrix that should make easier its diffusion from the particle.

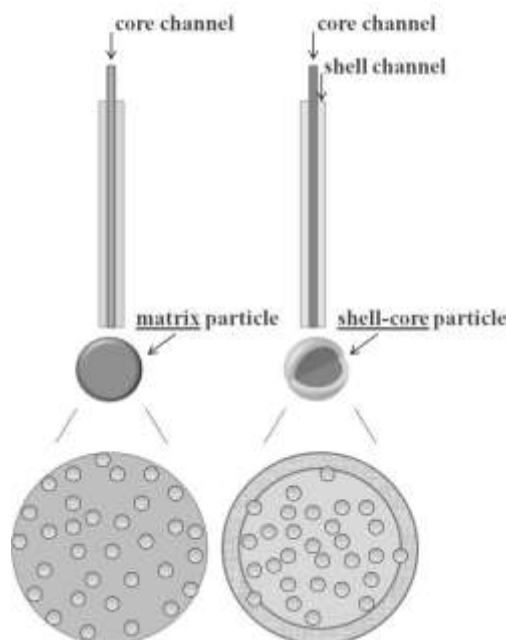


**Figure 34. Shell-core particle and only-core (or matrix) particle**



## 5.3 Materials

Alginate Manugel GHB was used as polymer (for the reasons explained in paragraph 5.1.1.b), with the properties shown in Table 7. Two model active principles were tested: a water soluble molecule, vitamin B12, and a water insoluble molecule,  $\alpha$ -tocopherol. The first molecule (vitamin B12) was used to conduct preliminary experiments in order to test the feasibility to encapsulate a water soluble molecule, therefore using only the assembly of feeding and atomizing sections of the novel plant, without the stabilization section. Tests on  $\alpha$ -tocopherol encapsulation were done in both ways (i.e. with and without stabilization section).

Other chemicals implied in particles preparation were  $\text{CaCl}_2$  in water solution as cross-linker and Tween 80 as surfactant. Moreover, solutions at different pH, simulating the gastrointestinal or physiological conditions, were obtained using hydrochloric acid, sodium phosphate tribasic dodecahydrate, potassium dihydrogen phosphate, sodium hydroxide.

### 5.3.1 Vitamin B12 selection

Selection of vitamin B12, a water soluble molecule, is due to the need to use a not too small molecule, because of the large gel pore size. Pasut et al [80] observed that theophylline has a very low molecule dimension in comparison with network meshes (theophylline van der Waals radius 0.379 nm), therefore its drug release was not influenced by polymer concentration: the experimental theophylline diffusion coefficients in alginate gels were not different from the diffusion coefficient in water. On the contrary, vitamin B12 diffusion was affected by polymer concentration and the diffusion values decreased with increasing polymer concentration. Therefore, B12 size (van der Waals radius B12 of 0.85 nm) is wide enough to make molecule motion influenced by the polymeric network. Nevertheless, the decrease of diffusion coefficient with polymer concentration is not so evident; this would suggest that polymeric meshes are still large if compared to vitamin B12. Finally, they observed a low myoglobin release even over a long time, that leads to conclude that polymeric meshes are comparable to the myoglobin van der Waals radius of 2.1 nm. On the basis of literature considerations [80], B12 was used as soluble active molecule. Moreover, vitamin B12 has a diffusivity in water (37°C) of  $3.8 \cdot 10^{-10} \text{ m}^2/\text{s}$  and a melting point  $>300 \text{ }^\circ\text{C}$ . Vitamin

B12 (whose structure is shown in Figure 35) belongs to the group of vitamins defined cobalamins. It is essential for the body, as together with folic acid contributes to cell division, in particular it is necessary for the necessary for the synthesis of hemoglobin. From the chemical point of view consists of a porphyrin ring that presents a central atom of cobalt, which in turn binds a nucleotide. Several groups organic can bind covalently to the atom of cobalt, forming different types of cobalamins.

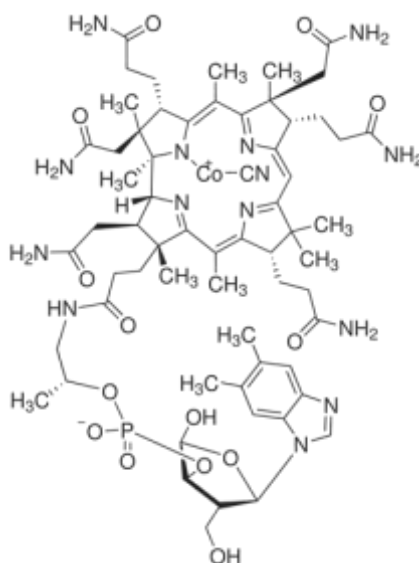


**Figure 35. Vitamin B12 structure [81]**

Vitamin B12 is generally synthesized by bacteria, while it is not produced in animals and plants. Also in humans it is not normally produced, but its intake is associated with diet. Usually it is found in products such as meat (especially liver), eggs and other dairy products due to the microbial activity microbial in them. The therapeutic effects of vitamin B12 vary: from use in the treatment of nervous diseases dependent on its deficiency and in treatment of pernicious anemia (especially in the elderly or in vegetarian people) to lowering, together with folic acid, blood levels of homocysteine (which causes the increase of the incidence of certain cardiovascular and neurological diseases) [82].

### 5.3.2 $\alpha$ -tocopherol selection

The choice of  $\alpha$ -tocopherol (TOC) as further molecule to test encapsulation apparatus is due essentially to its property of insolubility in water, to evaluate its release properties against vitamin B12. It is also a small molecule having a van der Waals radius of 0.43 nm [83].  $\alpha$ -tocopherol is the most biologically active form of vitamin E, that it is not a single molecule but refers to a group of eight fat-soluble compounds including both tocopherols and tocotrienols. The structure of  $\alpha$ -tocopherol is depicted below: it has to be noted the long hydrocarbon chain similar to the tail of a fatty acid.

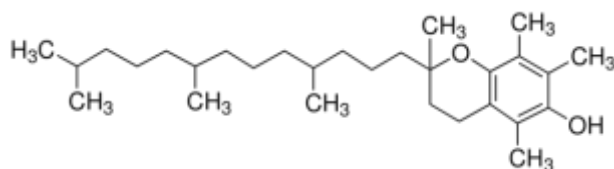


**Figure 36. Structure of  $\alpha$ -tocopherol [81]**

Vitamin E has many biological functions, whose the most important is the antioxidant function [84]. Other functions include enzymatic activities, gene expression and neurological functions. Vitamin E deficiency is not common and it is almost never due to a poor diet. However vitamin E deficiency occurs in three specific situations: in people who cannot absorb dietary fat, in premature, low birth weight infants and in people with rare disorders of fat metabolism. Vitamin E deficiency associated with these diseases causes problems such as poor transmission of nerve impulses, muscle weakness, and degeneration of the retina that can cause blindness.

## 5.4 Methods

### 5.4.1. Vitamin B12 particles manufacture

The process of particles production is characterized by first feeding the internal and the external solutions to the coaxial atomizer, with features reported in 4.1 *General description of the apparatus*, and selected parameters, as shown in the section 5.1.1.b .

In particular, both the internal and external concentrations of alginate are of 1.5% (w/w), with tween 80 (2.5 g/l) as surfactant; the internal concentration of vitamin B12 is 0.525 g/l. Other parameters, as shown in Figure 37, are:

- cross-linking solution features=  $\text{CaCl}_2$ , 8.9 g/l;
- stirring rate of cross-linking solution = 100 rpm;
- distance probe-solution surface = about 2 cm;
- internal flow rate = 0.7 mL/min;
- external flow rate = 4.5 mL/min;
- dripping/cross-linking time = 2 min/5 min (total time: 7 min).

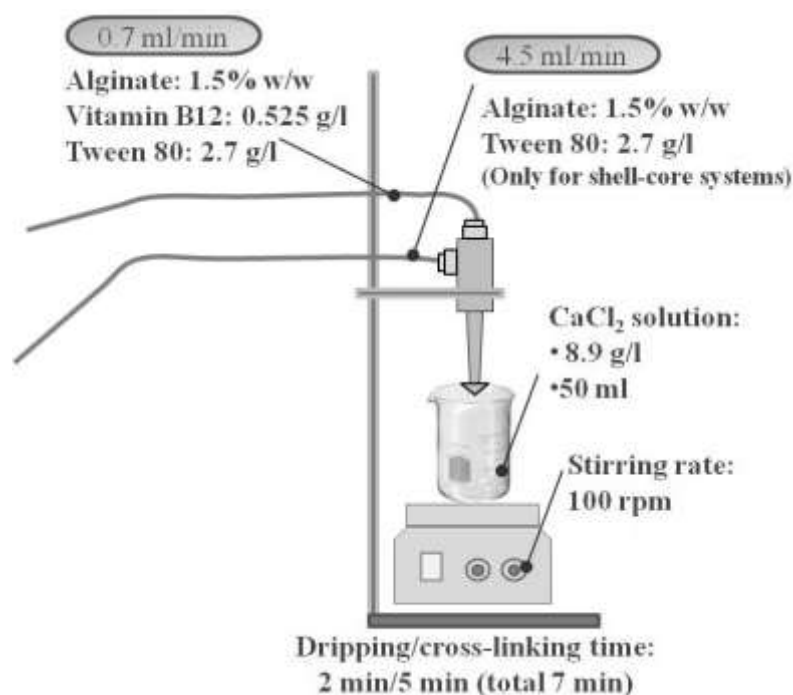


**Figure 37. Parameters for particles manufacture by dripping**

Two types of particles were produced using the parameters above described: shell-core particles and only-core (matrix) particles. For these latter the solution was sent only in the internal channel (core line) of the coaxial nozzle. This means that the quantity of vitamin B12 processed was the same in the two cases, whereas the amount of alginate, and thus the final weight of product, was larger for shell-core particles production.

The particles were then filtered and washed with distilled water. Afterwards, they were directly subjected to loading and release analysis, or they were dried in a tray-oven with air at 45°C (most common literature conditions) or in a microwave cavity (pulsed regime 245 W), until a constant weight was reached.

#### 5.4.2 Vitamin B12 loading and release tests

Tests about loading and release of vitamin B12 from the obtained particles (fresh, convectively dried and microwave dried) were carried out. In particular, the particles were accurately weighed and then put in a given volume (50 mL) of phosphate buffer at pH 7.4, to simulate physiological conditions. To test the enteric nature of particles, these latter were put in 50 mL of an acid solution, 0.1 N hydrochloric acid (pH 1), simulating the pH in the stomach; after a time of 120 min, 0.2 M tribasic sodium phosphate was added to reach pH 6.8, simulating the pH in the intestine, according to Pharmacopeia suggestions. For both tests, samples of 1 mL were taken at predetermined times and assayed for vitamin B12 release by HPLC. The features of HPLC method used to evaluate the vitamin B12 release were the following:

- eluent solution: methanol/water = 30/70 (v/v);
- eluent solution pH = 1.6 (pH was reduced from the initial value of 9 by using HCl);
- eluent flow rate: 1.5 mL/min;
- wavelength of signal acquisition: 361 nm;
- retention time of B12: 3.6 min.

The above described method, used to assay the concentration of vitamin B12 in the dissolution mean (buffer solution at pH 7.4 or two step, pH 1-pH 6.8 solutions), was selected for its greater reliability, carefully evaluated, as described in Appendix A.1 Assay methods: UV-vis spectrometry vs HPLC.

#### 5.4.3 $\alpha$ -tocopherol particles manufacture

$\alpha$ -tocopherol particles production follows the working scheme described in the section “4.3 Description of plant operation”. Parameters for  $\alpha$ -tocopherol particles production are similar to that used for B12 vitamin particles manufacture. In particular, both the internal and external concentrations of alginate are of 1.5% (w/w). The core solution is formed of alginate at 1.5% (w/w),  $\alpha$ -tocopherol at 1% (w/w) and Tween 80 at 0.5% (w/w). The surfactant Tween 80 is introduced in the core solution to reduce interfacial tension, and consequently particles dimensions; moreover a concentration of 0.5% (w/w) is needed to obtain a stable emulsion of the water insoluble  $\alpha$ -tocopherol with the water soluble solution of alginate. The specific flow rate values, concentrations and all the parameters defined for the

apparatus exercise are resumed in Table 9. To compare microwave drying with convective drying, wet particles, just produced in the apparatus, were withdrawn and introduced in a tray-oven with air at 45 °C. It is worth to note that the contacting time between alginate drops and cross-linking solution is the same for both initial and final configuration of the apparatus, thus it does not influence the hardening of nascent micro-particles. Moreover, micrometric particles are quickly penetrated by divalent cations: the cross-linking time of 5 min is more than sufficient for complete hardening [78].

**Table 9. Parameters selected for  $\alpha$ -tocopherol particles production**

Parameters	Core	Shell
Flow rate, mL/min	1.1	4.2
Alginate, % w/w	1.5	1.5
a-tocopherol, % w/w	1	-
Tween 80, % w/w	0.5	-
Atomization/dripping time, min	2	
Cross-linking time, min	5	
Drying type	Microwave (P=245W)/Convective (T=45°C)	

#### 5.4.4 $\alpha$ -tocopherol particles characterization

##### 5.4.4.a Image analysis

Size control of particles was performed by image analysis. It was carried out by the public domain software ImageJ 1.40g (Wayne Rasband, National Institutes of Health, USA, the software is freely available at <http://rsb.info.nih.gov/ij/>). After some modifications of the image color threshold, the software gives the mean size and the ellipses surrounding the particles. The image analysis was performed on fresh particles (before drying treatment) and on dried particles after the stabilization by convective or microwave drying.

##### 5.4.4.b Dielectric properties

Studies on materials dielectric behaviour were performed by measurements using a Network analyzer (Agilent Technologies mod. ES 8753 – coaxial tip, mod. 85070D). A Vector Network Analyzer

(VNA) is connected via coaxial cable to an open-end coaxial probe. To perform the measurements, the technique requires pressing the coaxial probe against the sample material. The microwave signal launched by the VNA is reflected by the sample and, basing on the reflected waves, both dielectric constant and loss factor are calculated. It is worth to note that operative conditions are strict: cable stability (no flexing of the coaxial cable must occur); absence of air gap between probe and samples surface (absence of bubbles in liquid samples and flat surface in solids and semi-solid samples); use of appropriate sample thickness (measurements must be performed on a “semi-infinite” sample).

#### *5.4.4.c Moisture and temperature measurements*

Moisture measurements were carried out by a thermobalance (Ohaus MB45) on both fresh and dried particles to measure respectively the initial and residual percentage of the aqueous solvent.

Temperature measurements, during microwave drying of particles, of both multimodal cavity and sample (particles) were done using a fiber optic thermometer (FISO UMI-8). Infrared pyrometer (Simpson mod. IR-10) was also used to confirm particles' surface temperature.

#### *5.4.4.d Differential scanning calorimetry*

DSC scans of pure alginate, pure  $\text{CaCl}_2$ , a physical mixture of alginate and  $\text{CaCl}_2$ , blank alginate cross-linked particles obtained by atomization and then dried by convective drying (CD), blank alginate cross-linked particles obtained by atomization and then dried in a microwave cavity (MW), were performed. DSC scans were recorded using a differential scanning calorimeter Mettler Toledo DSC-822 (Mettler, Switzerland). Samples were accurately weighed and heated from 25 to 300 °C at a heating rate of 10 °C/min under a nitrogen flow rate of 50 mL/min, as suggested in literature [85].

#### *5.4.4.e $\alpha$ -tocopherol loading and release tests*

Tests about loading and release of  $\alpha$ -tocopherol from the obtained particles (convectively dried and microwave dried) were carried out. To test the enteric nature of particles, these latter were put in 75 mL of an acid solution, 0.1 N hydrochloric acid (pH 1), simulating the pH in the stomach; after a time of 120 min, 0.2 M tribasic sodium phosphate was added to reach pH 6.8, simulating the pH in the intestine,

according to Pharmacopeia suggestions. The temperature was kept at 37 °C. For both tests, samples of 1 mL were taken at predetermined times, mixed with 9 mL of ethanol and centrifuged for 5 min at 6000 rpm (*Remi, R-8C XS Bench Top Centrifuge*) to extract  $\alpha$ -tocopherol (which is not soluble in water). Then  $\alpha$ -tocopherol presence was detected by UV-vis spectrometer (Lambda 25 by Perkin Elmer) by collecting the full absorption spectra in a wavelength range from 200 to 400 nm, and obtaining the peak height closest to 290 nm, in order to avoid incorrect measurements due to shift in  $\lambda_{\max}$ . The procedure of spectra fitting instead of the simple reading of the absorbance at a given wavelength has been proved to be much more effective and in principle to be used to eliminate the interferences due to polymers or other substances, in a previous work [86].

#### *5.4.4.f Apparatus power consuming*

The apparatus power consuming was detected by a power consumption meter (Avidsen), using both the functions of reading the instantaneous consumption in Watt (which allows also the detection of maximum consumption and the time of maximum consumption), and of reading of total energy consumption.



### 5.5 Preliminary results (vitamin B12 encapsulation)

The fresh particles, both shell-core and only-core (matrix) systems, produced by dripping, show a narrow size distribution, as shown in Figure 38.

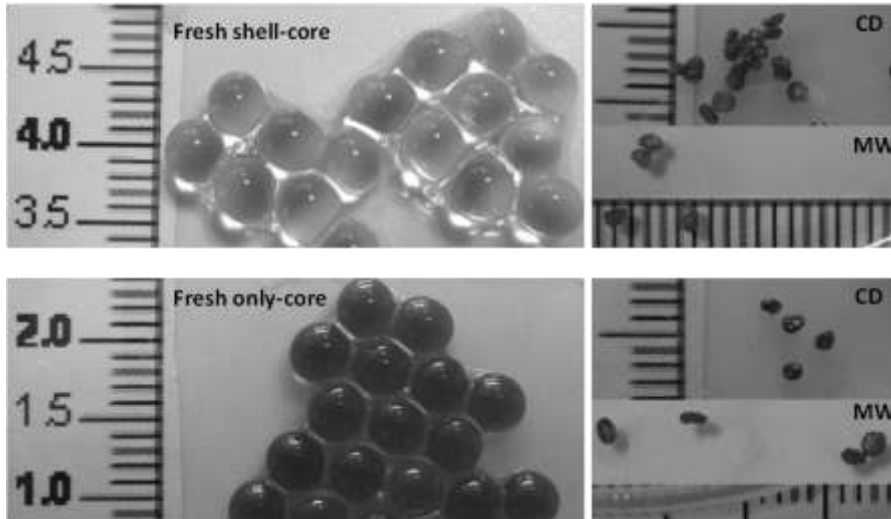


Figure 38. Pictures of fresh particles, both shell-core (up) and only-core (down), and of dried particles (CD: convective; MW: microwave)

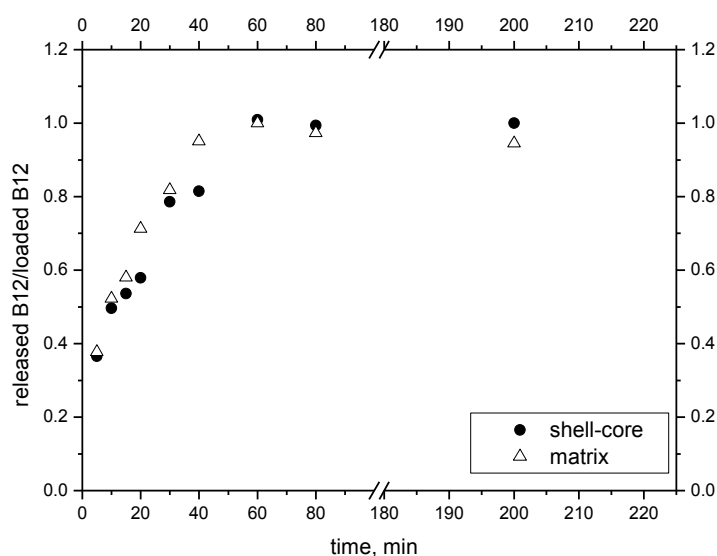
They have an initial size of about 3.8 mm; after drying their volumetric shrinkage is in the range 93-96%, as highlighted in Table 10. The round shape is essentially preserved for convectively dried particles, differently from the microwave dried particles which showed a more elongated shape, even if not too pronounced.

Table 10. Size mean and standard deviation for both shell-core and matrix particles, fresh and dried (CD or MW); shrinkage percentage for the dried ones

	Fresh shell-core	Fresh matrix	CD shell-core	CD matrix	MW shell-core	MW matrix
<b>Mean, mm</b>	3.86	3.81	1.29	1.29	1.43	1.59
<b>Standard deviation</b>	0.01	0.01	0.10	0.15	0.14	0.12
<b>Volumetric shrinkage</b>	-	-	96%	94%	96%	93%

The behaviour of the particles immersed in a buffer solution at pH 7.4 showed that both fresh and dried (CD and MW) particles were

characterized first by swelling and then by erosion. In particular, fresh only-core (matrix) particles showed faster erosion than fresh shell-core particles; in fact their size strongly reduced after 60 min of immersion in dissolution medium, whereas shell-core particles were swollen, but not so much eroded after 80 min. At the end of the test, at 200 min, they were completely dissolved. A lightly delayed release of vitamin B12 from fresh particles (Figure 39) was observed for shell-core particles with respect to the only-core ones, up to 60 minutes: at this time the total amount of B12 was released.



**Figure 39. Fraction of B12 released in a phosphate buffer at pH 7.4, particles obtained by dripping, without drying (fresh particles)**

This behaviour was more evident for particles convectively dried (Figure 40), even if in this case the complete release of vitamin B12 occurred earlier. In particular for matrix particles the release was already complete after 20 min of immersion, whereas shell-core particles showed a full release after 40 minutes, confirming their delaying ability. The early release of dried particles compared to the fresh ones is due to the fact that during the drying, that in the tray-oven with air at 45°C has a duration time of about 6 hours, the vitamin B12 has time to migrate from the internal core to the external shell.

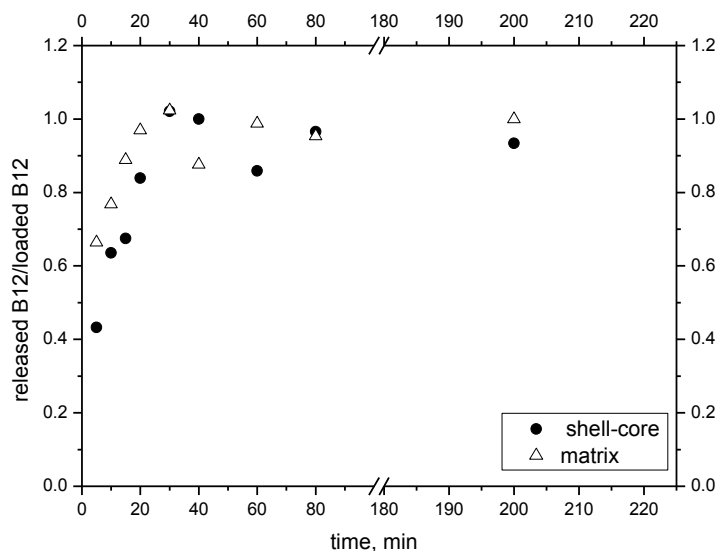


**Figure 40.** Fraction of B12 released in a phosphate buffer at pH 7.4, particles obtained by first dripping and then drying in a tray-oven with air at 45°C

The particles (both shell-core and matrix) dried in a microwave cavity (Figure 41), gave a complete release almost immediately. This can be explained on the basis of literature considerations about microwave technology used to modify the state of molecular interaction between the alginate chains with the aim to delay the release of small molecule drugs [87]. Wong et al observed that the wavenumber of the hydroxyl and carbonyl FTIR peaks of microwave treated blank alginate beads were lower than those of the untreated ones. This indicated that microwave irradiation increased the level of polymer-polymer interaction via hydroxyl and carbonyl moieties, which was expected to delay drug release from the alginate beads. Moreover, intensity of carboxyl and carboxylate peaks of alginate increased with harsher irradiation conditions, suggesting a reduction of interaction between  $\text{Ca}^{2+}$  ions and alginate, and a consequent effect of drug release enhancement. The last phenomenon can be the explanation of the fast release of vitamin B12 from beads due to the combination power-time (245W-about 40 min). Moreover, microwave effects on drug release features of cross-linked alginate were proved to be a function of alginate conformation: high mannuronic content-alginate micro-particles required a shorter period of microwave irradiation to reduce drug release extent (perhaps for its extended chain structure, providing

a higher level of flexibility to interact with the adjacent polymers during microwave irradiation) than high guluronic-alginate micro-particles [88].

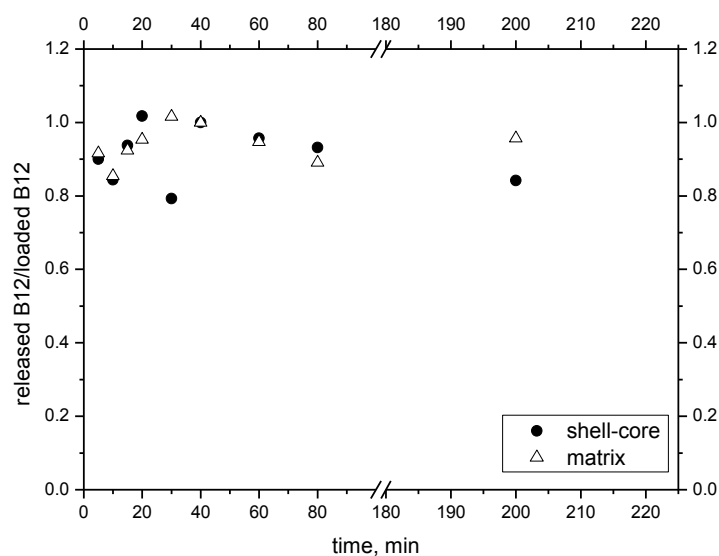


**Figure 41. Fraction of B12 released in a phosphate buffer at pH 7.4, particles obtained by first dripping and then drying in a microwave cavity**

An important advantage of the shell-core particles is the increased loading, as shown in Figure 42, when comparison is made with the loading of the only-core ones. For a theoretical value of vitamin B12 in all the particles of 0.74 mg, shell-core particles have a loading in a range between 0.45 and 0.52 mg, that is a percentage of loading in the range 60-70%; whereas matrix particles have a loading of 0.25-0.35 mg, and a loading percentage of 34-48% (Figure 42). The increased loading is essentially due to the shell coating which acts as a protection for the active molecule.

For matrix system, a theoretical estimation of loaded amount of vitamin B12 is possible by a simple mass balance, considering the mechanism of B12 diffusion through nascent particles, comparable to spheres at uniform initial concentration of B12, during preparation (Appendix B.1 Diffusion in a sphere).

$$R(t) = 1 - \frac{6}{\pi^2} \sum_{n=1}^{\infty} \frac{1}{n^2} \exp(-\mathcal{D}n^2\pi^2t/a^2) \quad (5.1)$$

Where:

$R(t)$  = amount of diffused substance at time  $t$ ;

$\mathcal{D}$  = diffusivity;

$a$  = sphere radius.

So, known the particles diameter, 3.8 mm, and the diffusivity of B12 in alginate gel from literature [80], the calculated percentage loss of B12, by diffusion during preparation (with total time of 7 min), is of 52%, therefore the remaining 48% is the loaded percentage, value in agreement with experimental results.

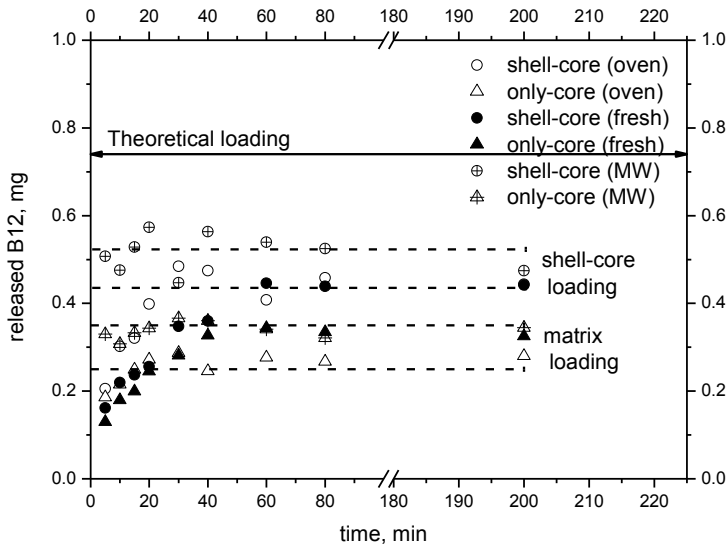


**Figure 42. Mass of B12 released in the phosphate buffer at pH 7.4 for fresh, convective dried, and microwave dried particles**

Enteric tests, founded on a progression of pH from pH1 to pH 6.8, were performed. It is important to underline that particles remained intact during the acid stage (confirming their enteric nature), then, after reaching the higher pH of 6.8, they were subjected to swelling and dissolution similarly to what happens in buffer solution at pH 7.4.

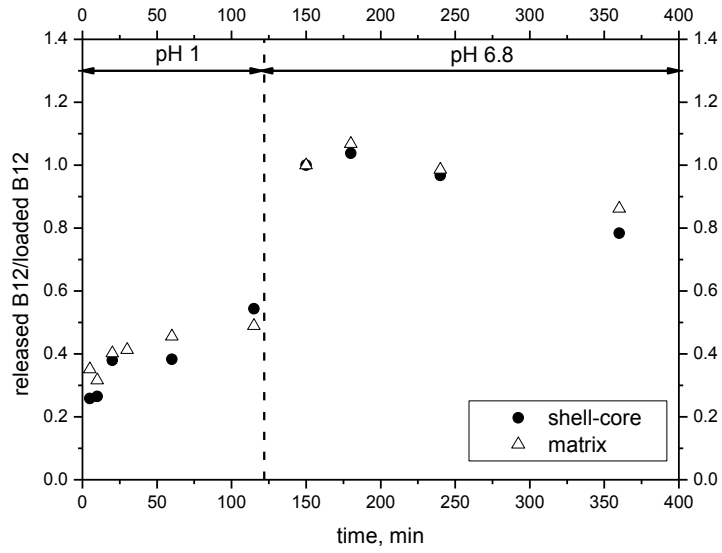


**Figure 43.** Fraction of B12 released in two step test, particles obtained by dripping without drying (fresh particles)

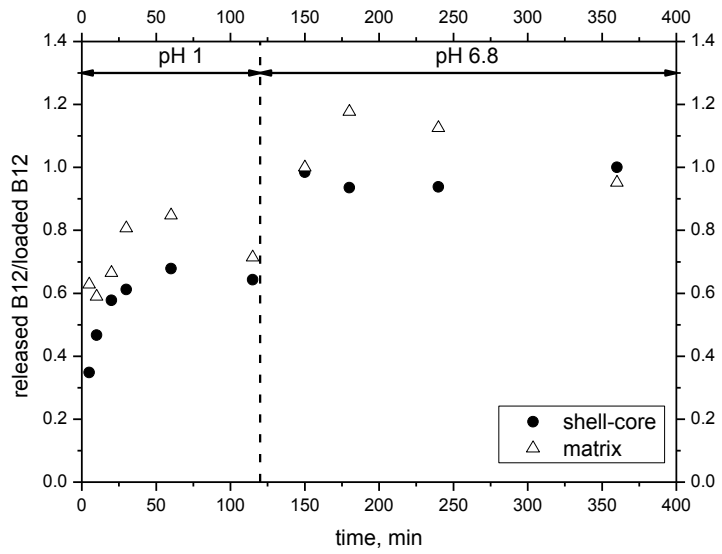


**Figure 44.** Fraction of B12 released in two step test, particles obtained by first dripping and then drying in a tray-oven with air at 45°C

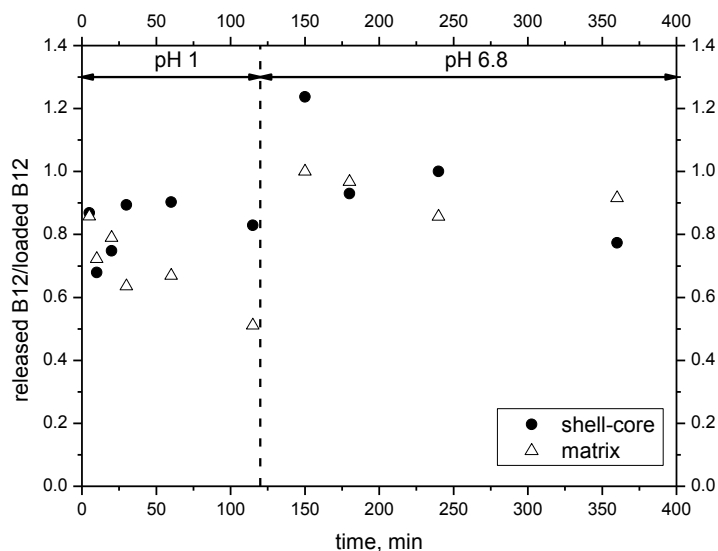


**Figure 45. Fraction of B12 released in two step test, particles obtained by first dripping and then drying in a microwave cavity**

The release from fresh particles shown in Figure 43, was characterized by loss of about half amount of B12 in the acid phase, and by a complete active principle release just after increasing pH to 6.8. A sharp difference between shell-core and matrix particles was not noticed, but only for the first 20 minutes at pH 1. As seen for particles immersed in phosphate buffer at pH 7.4, the convectively dried particles showed a more interesting behaviour (Figure 44). In fact, the greater protection of the active molecule was confirmed by a delayed release during the acid stage. However, in the enteric test too, an early release from dried particles compared to fresh particles was observed, since the drying has such a duration that vitamin B12 can migrate from the internal core to the external shell, and then to the dissolution medium. The particles dried in a microwave cavity (Figure 45) showed the same behaviour observed in the buffer solution at pH 7.4, i.e. they gave a complete release of vitamin B12 almost immediately.

### 5.5.1 Steps towards atomization

Steps towards atomization were done. In particular, keeping the parameters selected for the dripping process (5.4.1. Vitamin B12

particles manufacture), ultrasounds were switched on and a power of 4 W was used to atomize solutions fed to the coaxial atomizer. The particles obtained by atomization (Figure 46) have shown a size of about 54  $\mu\text{m}$ , with a standard deviation of 26. This value is in good agreement with data (related to water) of fine drop diameter distribution given by Sonotek (Figure 47). Drop distribution in Figure 47 is obtained by dividing the drop population into a set of size ranges (channels) and counting the fraction of drops having diameters that fall within each channel. 4 microns was chosen as the channel width. For water atomized by 25 kHz nozzle distribution, 0.7% of all drops falls in the channel that covers the 10-15  $\mu\text{m}$  range, 1.5% falls in the following 15-20  $\mu\text{m}$  range, and so on. The higher percentage of particles falls in a dimensional range between 50 and 60  $\mu\text{m}$ , as well for alginate particles.

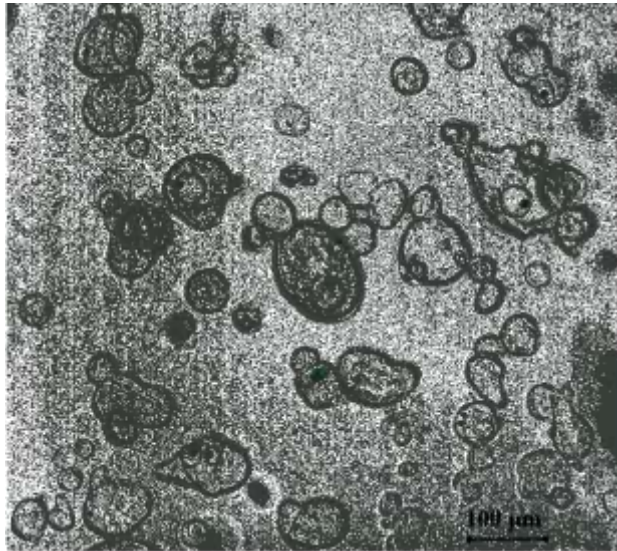


**Figure 46.** Optical microscope picture of shell-core micro-particles obtained by coaxial ultrasonic atomization (P=4W)



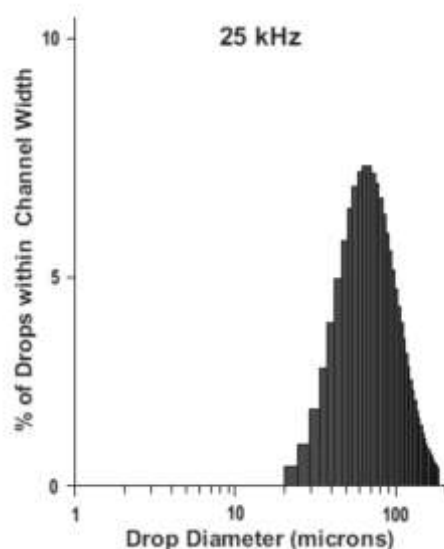


**Figure 47. Drop diameter distribution for 25 KHz ultrasonic atomizer (data for water) [66]**

The superiority of shell-core systems over only-core (matrix) systems in terms of increased drug loading, evaluated for the produced coarse droplets (particles having a diameter of about 4 mm), was detected also in the fine particles, although by an indirect measure. This latter consists in evaluating the sum of B12 lost in supernatant (cross-linking solution) and in washing water and comparing this value to the theoretical one, calculated on the basis of the material fed to the atomizer. HPLC signals of supernatant and washing water of both shell-core and matrix (only-core) micro-particles are given in Figure 48. B12 peak area for washing water of both formulations is similar; instead B12 peak area in supernatant signal of matrix micro-particles is larger than that in the shell-core system supernatant signal, highlighting the ability of shell-core micro-particles to retain a larger amount of B12 during cross-linking compared with matrix (only-core) micro-systems. B12 detected in supernatant and washing water of matrix micro-particles corresponds to the theoretical value of B12, so lack of B12 encapsulation in matrix micro-particles occurred.

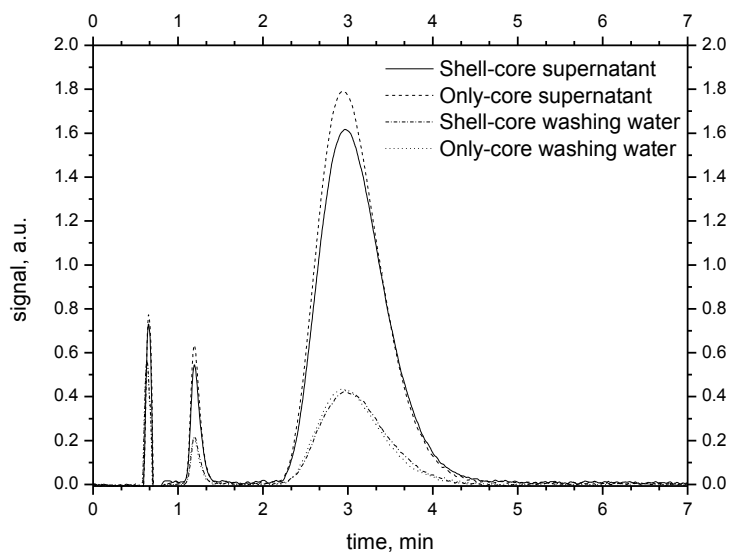


**Figure 48.** HPLC signals deriving from HPLC analysis of supernatant and washing water of both shell-core and matrix preparations

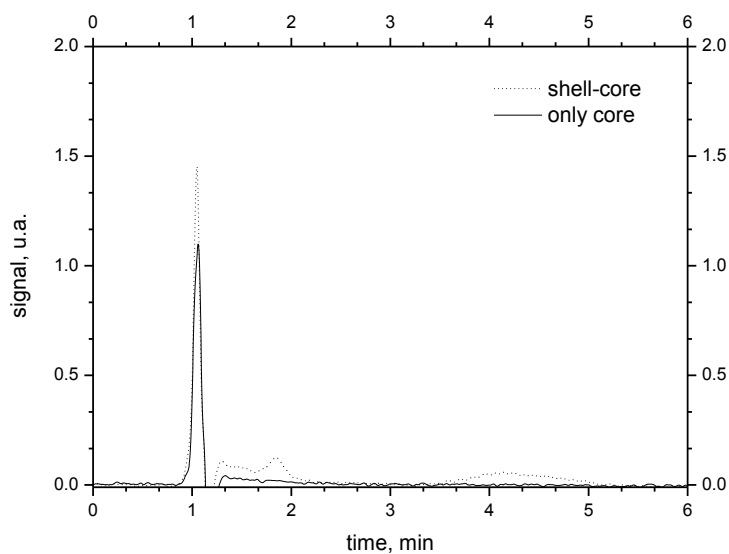


**Figure 49.** HPLC signals of pH 1 solutions (first part of two step release test) after 10 minutes of dissolution of respectively shell-core (dotted line) and only core (solid line) micro-particles

This result is confirmed by the release tests (release tests as described in section 5.4.2 *Vitamin B12 loading and release tests*). In particular, HPLC signals for solutions at pH 1 (initial pH of two step test), containing respectively shell-core and only core micro-particles since 10 minutes, are reported in Figure 49. The signal for matrix micro-particles is flat (this behavior is confirmed after more than 5 hours, data not shown), otherwise the presence of B12, though in very little amount, is detected in shell-core micro-particles through the typical peak of B12 at about 4 min in HPLC signal (dotted line in Figure 49, as before the peak is noticed after 5 hours of dissolution test). However, the lack of B12 loading in matrix micro-particles was confirmed by theoretical evaluation of B12 diffusion, as done for macro-particles in the previous paragraph (details in Appendix B1). In the same equation (4.1), the reduction of particles diameter ( $a$ ) from 3.8 mm to 54  $\mu\text{m}$  causes the complete release of B12 almost immediately after the contact between forming matrix and cross-linking solution, confirming the impossibility to encapsulate B12 in such a matrix micro-system.

Resuming, as well as for coarse droplets, the shell-core conformation on microscopic scale guarantees a better protection of B12. This effect is not so evident because alginate gel pores are still large respect to vitamin B12 molecule size (van der Waals radius: 0.85 nm), therefore this latter is free to diffuse through forming gel. A larger sized molecule (still water soluble), such as BSA (bovine serum albumin) will be affected by the presence of polymer network, however preliminary tests on system alginate/BSA gave as a results a loss of about 70% during preparation. Thus, for final tests of encapsulation in the complete apparatus, a small molecule with different water solubility, nay lypophilic, was tested in order to observe its release behavior from alginate systems.

## 5.6 Results about final encapsulating tests

In this paragraph results about  $\alpha$ -tocopherol particles are showed.

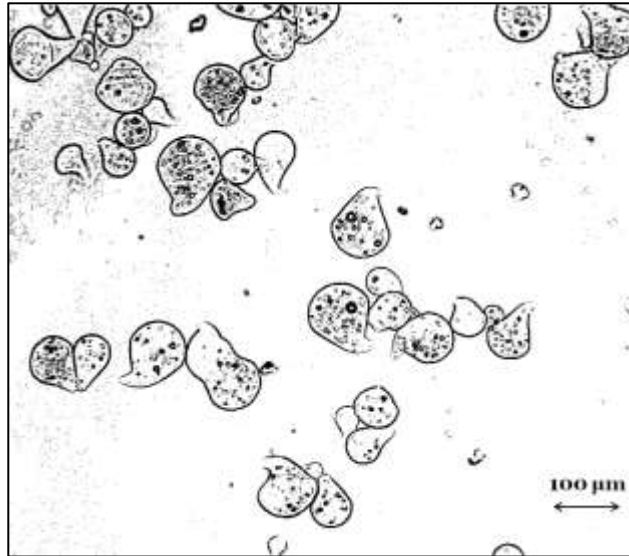


**Figure 50.** Optical microscope pictures of shell-core micro-particles: fresh (down) and dried (up)

Image analysis for size control of both shell-core and matrix micro-particles, done on both fresh and dried product, showed a narrow size distribution (Figure 50).

**Table 11.** Mean size and standard deviation for both shell-core and matrix micro-particles, fresh and dried; volumetric shrinkage percentage for the dried ones

	Mean size, $\mu\text{m}$	S. D.	Shrinkage, %
Shell-core micro-particles-FRESH	78	$\pm 20$	
Matrix micro-particles-FRESH	76	$\pm 20$	
Shell-core micro-particles-DRIED	41	$\pm 12$	86
Matrix micro-particles-DRIED	40	$\pm 12$	85

Shell-core and matrix micro-particles have an initial size of respectively  $78 \mu\text{m}$  and  $76 \mu\text{m}$ ; after microwave drying their size is reduced, by volumetric shrinkage of about 85%, to about  $40 \mu\text{m}$ , as highlighted in Table 11.

Moreover, fresh particles assume a light pendant shape, as showed in Figure 50, because, due to the impact, the spherical drop deforms and keeps the shape owing to the fast cross-linking [65]. This shape is essentially preserved in dried particles.

Then, to evaluate the feasibility and the convenience of stabilization by microwave drying, dielectric properties of fresh micro-particles were compared with those of water (Figure 51), that is a dissipative material, made by natural dipoles which can become easily polarized under application of an electric field orienting the molecules.

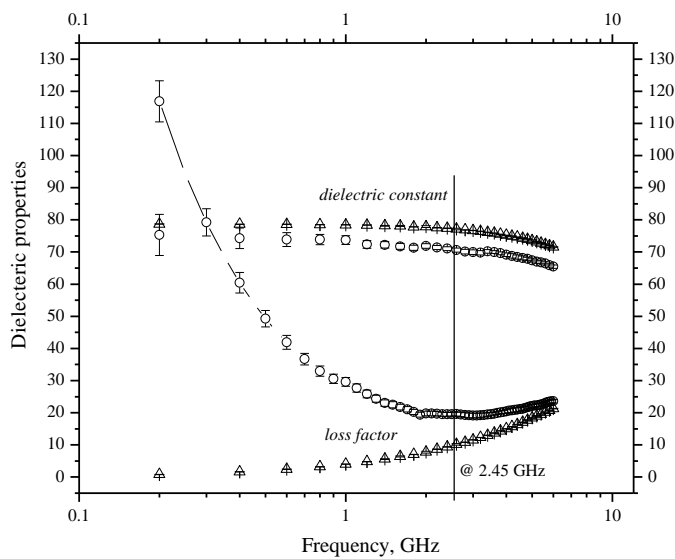


**Figure 51. Comparison between dielectric properties of water (triangles) and those of produced micro-particles (circles) at room temperature**

In fact interactions between materials and electromagnetic energy depend on the ability of the electric field to polarize the charges of the material and on the impossibility of this polarization to follow the rapid changes of the oscillating electric field (dielectric dissipative mechanisms). In presence of an external electric field, different kinds of polarization mechanisms are possible: the electronic polarization, due to modification of electrons position around the nucleus; the atomic polarization, caused by positional shifts of nucleus resulting from a non-uniform distribution of charges within the molecule; the orientation polarization (dipoles rotation), caused by the re-orientation of the permanent dipoles under the influence of the electric field; finally the spatial charge polarization, observed in materials containing free electrons confined on surface (Maxwell-Wagner

effect) [89]. Depending on frequency, one or two mechanisms dominate over the others. In particular, the dipoles rotation is the dominant polarization mechanism in irradiating materials rich in water in the microwave electromagnetic spectrum region.

Therefore, taking into account that the loss factor expresses the loss energy dissipative mechanisms in the material, fresh micro-particles in Figure 51 showed, at the most used frequency of 2.45 GHz for the industrial drying, a loss factor higher than water's loss factor, confirming that they can be easily heated by microwave. The increased loss factor is due to the residual ionic hardening solution, which also involves the decrease of dielectric constant. In effect, decrease of the energy-storage ability is due to subtractions of water dipoles, because solvation effects occur (less dipoles can be polarized); higher loss factor values are due to the enhancement of ionic dissipative mechanism [90].

The feasibility of microwave drying was also confirmed by moisture measurements: from an initial content of about 95 %, microwave drying assures in about 25 minutes a reduction to 3%, acceptable to avoid the impairment of product stability. Moreover, during drying, sample does not reach high or critical values of temperature, owing to the duty cycle that assures to switch on the magnetron for 20 seconds in a minute of operation, even better temperatures decrease with time: in about 25 minutes the sample temperature assume respectively the values of 88°C, 68°C, 59°C, 48°C (while the microwave cavity temperature keeps at 35-42°C).

Furthermore, DSC results endorse the purpose to combine microwave with ultrasounds. DSC scans of pure sodium alginate (Figure 52, UP) showed first a typical endothermic peak to be attributed to the evaporation of water, then an exothermic behavior starting at around 200 °C, with its maximum at about 250 °C, highlighting the polymer decomposition. CaCl<sub>2</sub> has two endothermic peaks at about 145 and 170 °C (all the values coincide with literature data [85]). The physical mixture of pure alginate and CaCl<sub>2</sub> (solid line in Figure 52, UP) showed a combination of peaks typical of the two powders, underlining the absence of physical interaction between the two powders. Scans of atomized particles (both CD and MW), as seen in Figure 52, DOWN, are similar to the scan of pure alginate, with jagged features typical of CaCl<sub>2</sub>.

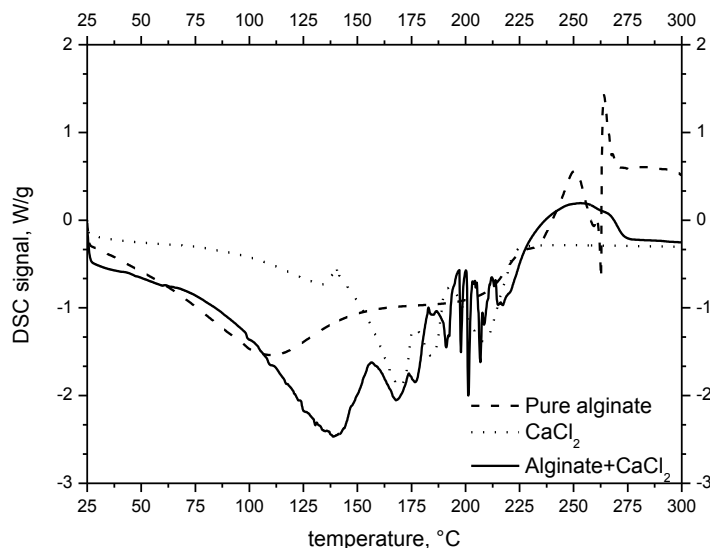


**Figure 52. UP: DSC scans of pure alginate, cross-linking powder  $\text{CaCl}_2$ , physical mix of alginate and  $\text{CaCl}_2$ ; DOWN: DSC scans of pure alginate, particles of cross-linked alginate obtained by atomization and then dried by convective drying (CD) or by microwave drying (MW)**

This implies that neither ultrasonic energy nor microwave drying break the polymer structure. However the endothermic peak is at a lower temperature (about 85 °C) than the pure alginate, due to the evaporation of absorbed water, perhaps for the smaller water content in the dried forms. Moreover, the MW sample shows a more pronounced endothermic peak than the sample CD (the only parameter that distinguishes the two samples is the kind of drying), perhaps because the microwaves cause a faster reorganization of the structure which traps the residual water.

With regard to release tests, the release profiles of both matrix and shell-core micro-particles, are shown in Figure 53. They were stabilized adopting both convective (conventional treatment at 45°C, 220 min) and microwave drying (novel treatment, at pulsed irradiation in about 25 min). For the two kinds of micro-particles, the yield of encapsulation (amount of TOC released and measured / theoretical loaded amount of TOC) was found around 100 %. They had enteric release properties because only at pH 6.8  $\alpha$ -tocopherol was completely released. Shell-core micro-particles show a better gastro-

resistance compared to matrix ones owing to the less amount of  $\alpha$ -tocopherol released at acid pH for both type of drying treatment.

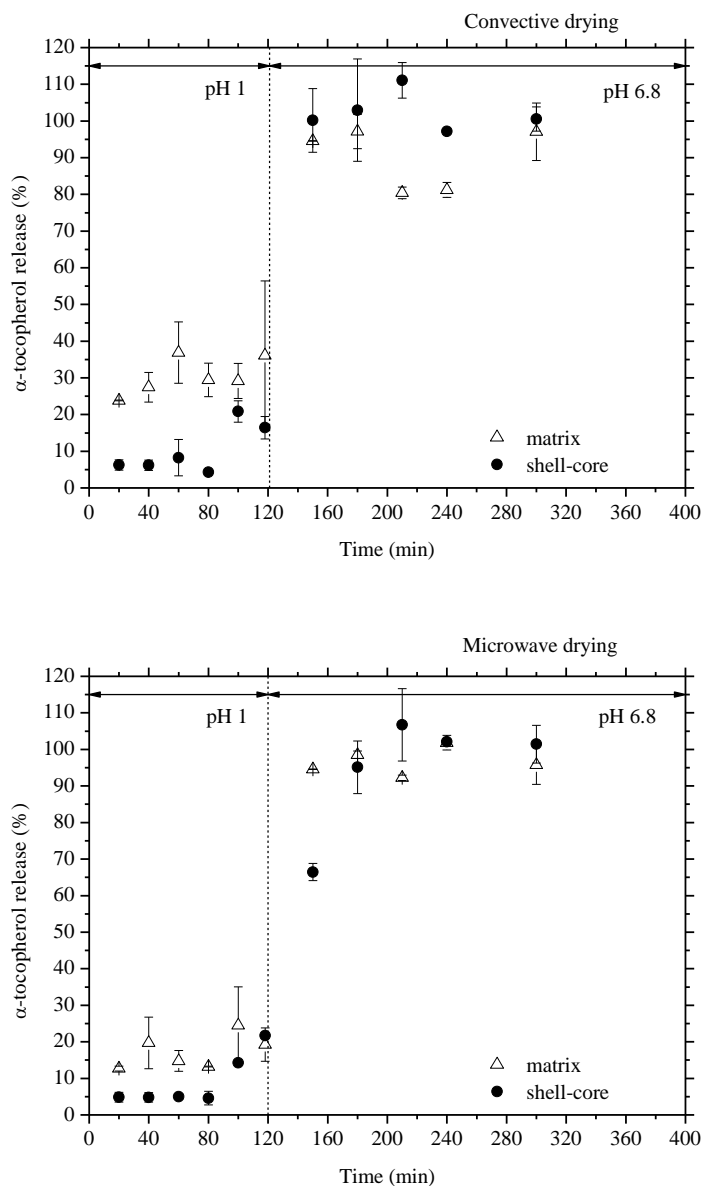


**Figure 53.**  $\alpha$ -tocopherol released (amount of TOC released and measured/theoretical loaded amount of TOC) from alginate matrix and shell-core micro-particles, produced by ultrasonic atomization and stabilized by convective drying (up) or by microwave drying (down)



Moreover, microwave treatment causes, especially for shell-core configuration (Figure 53, down), a little delay in active principle release, unlike the macro-particles (beads) of alginate and vitamin B12 (paragraph “5.5 Preliminary results (vitamin B12 encapsulation)”). The different behaviour can be attributed to the different exposition times to microwave irradiation. In fact Wong et al [87] showed that microwave irradiation increased the level of polymer–polymer interaction in alginate particles, causing a drug release delay, but harder irradiation conditions (as a longer time of irradiation) provoke the reduction of these interactions, promoting faster drug release. Thus, microwave drying usefulness in the controlled drug release was proved: it can affect, by a sort of curing, the polymeric structures.

To confirm benefits deriving from atomization, macro-particles (beads), produced in the same conditions of micro-particles, but switching off the ultrasounds, were tested (Figure 54). Shell-core structures display once again better release properties against matrix systems. In effect shell-core configuration allows avoiding  $\alpha$ -tocopherol deactivation observed instead for matrix beads: for these systems only the 20% of theoretical loaded amount was released and, as no  $\alpha$ -tocopherol was detected in harvesting solution, the remaining 80% undergoes thermal degradation. Therefore, shell-core systems assure a protective barrier against the heat, whose degradation effect on  $\alpha$ -tocopherol, similar to that observed for matrix systems, was stated in literature [91]. Moreover, also for macro-particles, microwave drying (Figure 54, down) gives better release properties: increased loading (for reduced times of exposition to heat, that is the primary cause of TOC degradation, compared to convective drying) and delayed release. Thus, microwave-treated beads encapsulating  $\alpha$ -tocopherol show a different behaviour compared to vitamin B12 beads, despite the same (high) time of exposition to microwave irradiation, that should provoke drug release promotion [87]. The improved drug entrapment and delayed drug release can be explained considering that incorporation of insoluble substances (such as  $\alpha$ -tocopherol) could modify physical properties of calcium-alginate systems, due to hydrophobic property increase and interaction with carboxyl groups of alginate, which can be promoted by microwave irradiation [92].

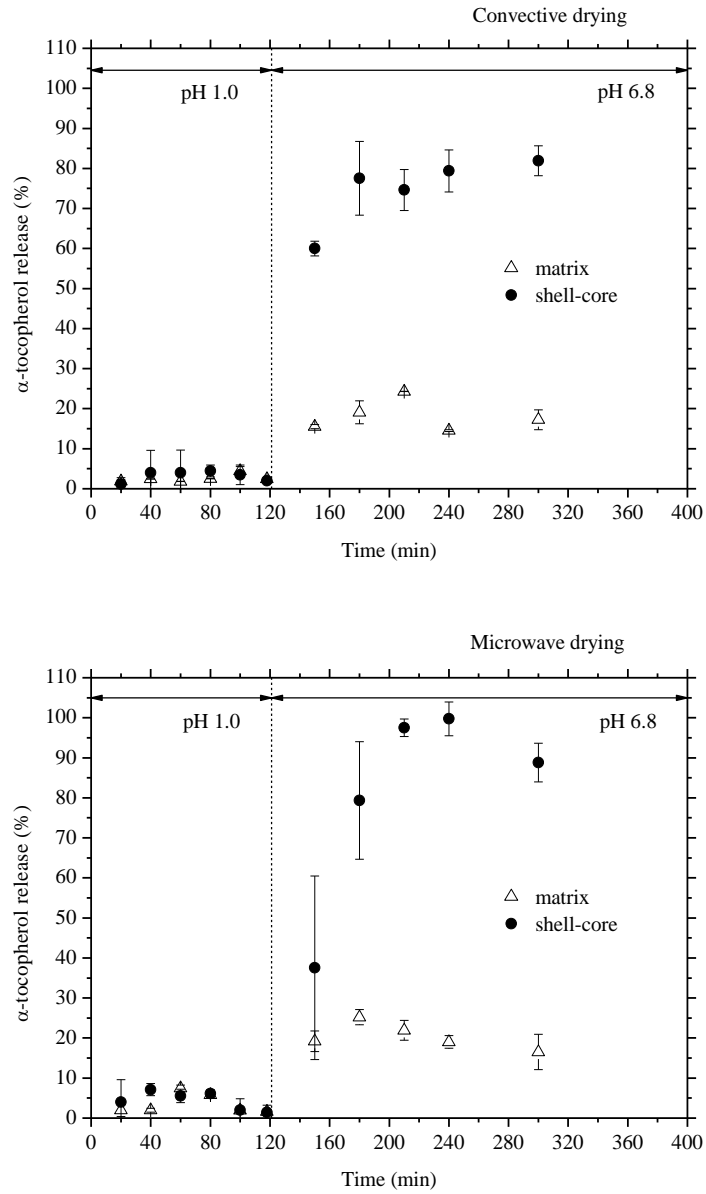


**Figure 54.** α-tocopherol released (amount of TOC released and measured/theoretical loaded amount of TOC) from alginate matrix and shell-core macro-particles (beads), stabilized by convective drying (up) or by microwave drying (down)

Thus, shell-core configuration, in both micro and macro-systems, results to have better release and loading properties for the production of oral pharmaceutical formulations.

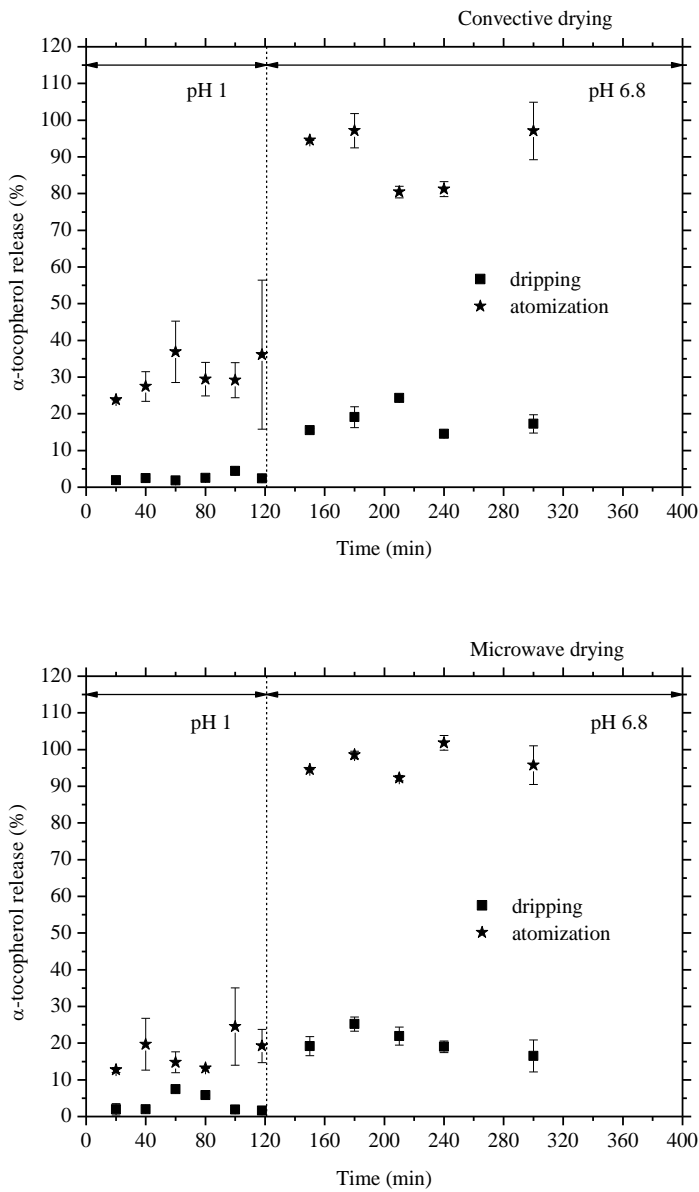


**Figure 55.** α-tocopherol released (amount of TOC released and measured/theoretical loaded amount of TOC) from alginate matrix micro (stars) and macro-particles (squares), stabilized by convective drying (up) or by microwave drying (down)

However, improving release features of matrix particles is possible by exploiting the two fundamental resources of the new apparatus: ultrasonic atomization and microwave drying. Figure 55 shows that ultrasonic atomization avoids the problem of TOC degradation (perhaps thanks to lesser time of heat exposition, to obtain complete drying, for micro-systems compared to beads). Then, coupling microwave drying to atomization allows better gastro-resistance properties, reducing the amount of TOC released at pH 1 from almost 40% (Figure 55, up, stars) to about 20% (Figure 55, down, stars). Resuming, better release properties for systems produced in the novel apparatus are achieved only by the coupling of ultrasonic atomization and microwave drying.

The apparatus power consuming is essentially due to particles drying, as shown in Figure 56, regardless of type (the difference in specific energy consumed between microwave and convective drying is only of some Joules on grams of fresh product), with a percentage on the total consumed energy of about 96%: most of consumed energy depends on particles properties, with an initial moisture of 95%, rather than apparatus' features.

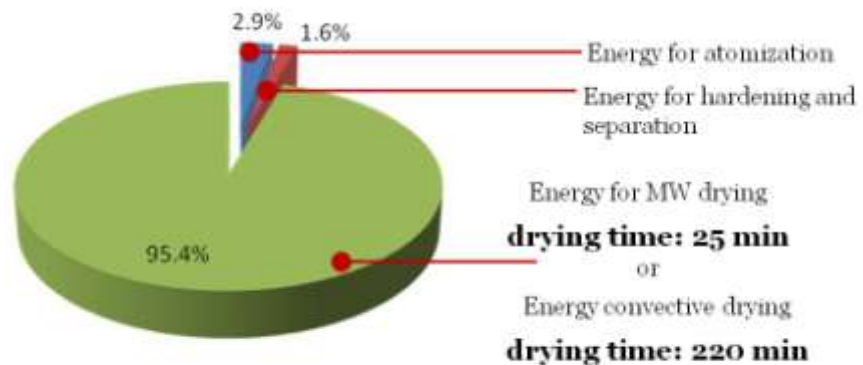


**Figure 56.** Repartition of power consumed among atomization (2.9%), hardening and separation (1.6%), drying (95.4%). This percentage is defined as the ratio between the specific energies, (joule)/(g of fresh product), of a single section (for example, atomization section) and the sum of the three sections

Moreover previous studies of the same research group demonstrated that a laboratory ultrasonic atomizer, working at the highest flow rate allowed by the laboratory system, requires very low volumetric power supply, comparable with the lowest value realized on plant scale using

conventional techniques [93]. Since, usually, the lab scale requires specific energy higher than the plant scale, the ultrasonic assisted atomization is confirmed to be a very promising technique in the intensification of industrial processes.

### 5.6.1 Droplets size prediction by literature correlations

Literature correlations, described in Chapter 3, were applied to predict the size of macro and micro-systems produced in the novel apparatus. The physical properties of alginate solution at 1.5% (w/w) (Table 12) were taken by Chan et al [79]:

**Table 12. Physical properties of Manugel GHB alginate solutions [79]: the properties of a solution with a concentration of 1.5% (w/w) are highlighted**

Alginate concentration, % w/w	Density, Kg·m <sup>-3</sup>	Viscosity, Pa·s	Surface tension, N·m <sup>-1</sup>
0.5	999	0.038	0.071
<b>1.5</b>	<b>1004</b>	<b>0.13</b>	<b>0.07</b>
2.5	1008	0.56	0.069
4.0	1017	2.7	0.057
5.0	1023	4.7	0.047

The alginate solutions have a non-Newtonian behavior; therefore the solution viscosity can be described by the power law:

$$\eta = K \cdot \dot{\gamma}^{n-1} \quad (5.2)$$

The consistency index,  $K$ , and the flow index,  $n$ , are functions of the alginate concentration,  $c$ . Literature fitting equations describe this relationship in a range of alginate concentration between 1% and 3% [65]:

$$K(c) = 0.0619 \cdot c^{2.953} \quad (5.3)$$

$$n(c) = 0.9635 \cdot \exp(-0.08 \cdot c) \quad (5.4)$$

Where  $c$  is in %,  $K$  is in Pa·s <sup>$n$</sup> ,  $n$  is dimensionless.

The shear rate at the wall, for a power-law fluid having a volumetric flow rate  $Q$  flowing in a circular tube of radius  $R$  is given by the following equation [65]:

$$\dot{\gamma}_W = \left[ \left( \frac{1}{n} + 3 \right) \cdot \frac{Q}{\pi \cdot R^3} \right]^n \quad (5.5)$$

For the used alginate solution, at a concentration of 1.5%, the consistency index,  $K$ , and the flow index,  $n$ , were  $0.205 \text{ Pa}\cdot\text{s}^n$  and  $0.854$ , respectively. The calculated shear rate at the wall, from equation (5.5), was  $333 \text{ 1/s}$ ; the consequent viscosity (from equation 5.2) was  $0.088 \text{ Pa}\cdot\text{s}$ .

It is important to highlight some considerations:

- shell-core systems were considered homogeneous owing to the same properties of the material used for both shell and core channels and to the predominance of the shell-channel flow rate;
- actual surface tension is lower than the value reported in literature owing to the presence of the surfactant Tween 80.

#### 5.6.1.a Dripping

First of all, the equation (3.4) was applied to evaluate the theoretical size of beads obtained by dripping (i.e. switching off the ultrasound). It is worth to note that the correlation (3.4) was obtained by considering a liquid flowing from a thin circular tube, of diameter  $d$ . The Sonotek atomizer, as described previously in the paragraph “4.2.1 Atomizing section” has a conical atomizing surface, which influences the detachment of the drop, which first adheres to the walls of the atomizing surface and then falls under the effect of gravity. This phenomenon was observed for both shell-core and matrix particles. In the latter case, even if the liquid flows from the internal microbore, the drop enlarges up to the outer channel, then to the inclined walls, in a similar way to the drop obtained by the shell-core configuration. In effect, experimental drop size is the same for both shell-core particles ( $3.8 \text{ mm}$ ), from a channel with a diameter of  $1.016 \text{ mm}$ , and matrix beads, from a channel with an internal diameter of  $0.406 \text{ mm}$ . Thus, inserting in the correlation (3.4) the diameter of the external orifice,  $d = 1.016 \text{ mm}$ , the predicted drop size is underestimated to  $3.5 \text{ mm}$ . This is due to the fact that the correlation does not take into account the presence of conical surface, which, offering a greater surface of adhesion to the drop, causes a delayed detachment and the consequent increased size. Then, the Bond number (equation 3.6) calculated for this system is  $Bo = 0.14$  (less than 1), highlighting that the drop formation is affected by surface tension. This effect is also confirmed

by the Ohnesorge number (from equation 3.3),  $Oh = 0.26$ , where surface tension force prevails on the viscous one.

5.6.1.b Ultrasonic atomization

Liquid viscosity, atomizer geometry and liquid flow rate have effect on droplet size in ultrasonic atomization, as already discussed in Chapter 3.

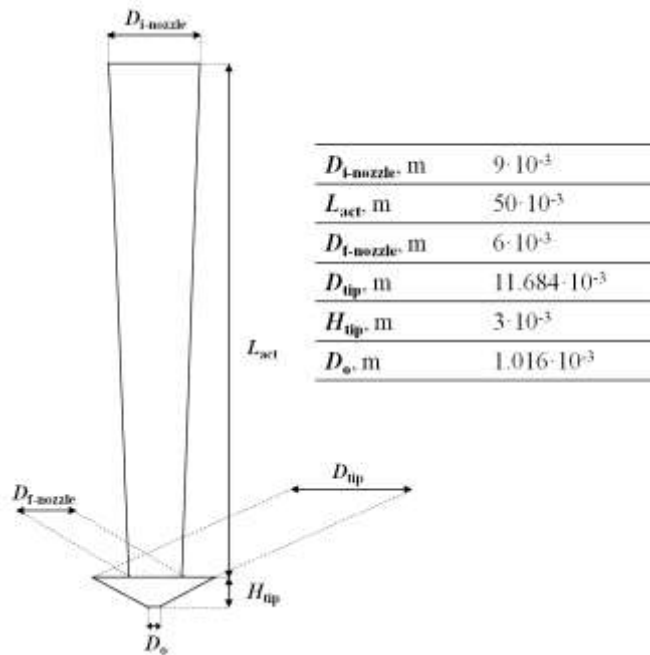


Figure 57. Nozzle geometry and relevant dimensions

Table 13. Values to insert in correlations for droplet size prediction in ultrasonic atomization

Area of vibrating surface, $A$ , $m^2$ (*)	$1.38 \cdot 10^{-3}$
Frequency, $f$ , Hz	25000
Delivered power, $P$ , W	10
Power intensity, $I$ , $W \cdot m^{-2}$ (**)	$7.25 \cdot 10^3$
Speed of the sound (in the water), $C$ , $m \cdot s^{-1}$ (***)	1497

(\*)  $A$  is given by the sum of three areas: 1) the lateral area of a truncated cone having  $D_{i-nozzle}$  and  $D_{f-nozzle}$  as bases and  $L_{act}$  as height; 2) the lateral area of a truncated cone

with  $D_{\text{tip}}$  and  $D_o$  as bases and  $H_{\text{tip}}$  as height; 3) the annulus area with  $D_{\text{tip}}$  and  $D_{\text{f-nozzle}}$ , respectively as external and internal diameter;

$$^{(**)} I = P / A;$$

^{(\*\*\*)} from Barba et al [65]

In effect, in the calculation of modified dimensionless numbers for ultrasonic atomization, a number of parameters related to the nozzle configuration have to be considered.

Nozzle geometry and relevant dimensions are shown in Figure 57; other parameters and combination of some of them are in Table 13.

Therefore, dimensionless numbers assume the following values:

- From equation (3.10):  $We = 25.1$ ;
- From equation (3.11):  $Oh = 8.96 \cdot 10^3$ ;
- From equation (3.12):  $I_N = 9.14 \cdot 10^{-13}$ .

The Weber number is larger than  $We_c (=1)$ , thus spray formation is assured. Moreover, the Ohnesorge number is very high owing to the high value of solution viscosity (0.13 Pa·s against 0.001 Pa·s of water).

Finally, both critical and maximum flow rate were evaluated to compare them with experimental flow rates, that, as described in paragraph “5.1.1.b Selection of feeding parameters”, are  $1.1 \text{ mL} \cdot \text{min}^{-1}$  ( $1.83 \cdot 10^{-8} \text{ m}^3 \cdot \text{s}^{-1}$ ) and  $4.2 \text{ mL} \cdot \text{min}^{-1}$  ( $7 \cdot 10^{-8} \text{ m}^3 \cdot \text{s}^{-1}$ ), respectively for core and shell channels. Calculated critical flow rate was  $Q_c = 2.8 \cdot 10^{-9} \text{ m}^3 \cdot \text{s}^{-1}$  and  $Q_{\text{max}} = 2.2 \cdot 10^{-5} \text{ m}^3 \cdot \text{s}^{-1}$ , thus experimental flow rates are well collocated within the range of good atomization.

Therefore, the three correlations, described in Chapter 3, were applied for droplets, and therefore particles, size prediction.

It is worth to note that experimental shell-core and matrix micro-particles presented the same size, independently from the flow rate. This phenomenon can be explained owing to the high viscosity of alginate solutions (non Newtonian-shear thinning) that avoids the immediate detachment of droplet from the capillary waves formed on the surface, determining a similar droplets size distribution in a no large range of flow rates (in this case  $1.1$  and  $4.2 \text{ mL} \cdot \text{min}^{-1}$ ).

Also, alginate/vitamin B12 micro-particles had a size of  $54 \mu\text{m}$ , alginate/ $\alpha$ -tocopherol micro-particles had a size of  $76\text{-}78 \mu\text{m}$ . This difference in experimental particles size is probably due to the higher concentration of the stabilizer Tween 80 in the first case (alginate/vitamin B12), where Tween 80 is in both shell and core material, compared to alginate/ $\alpha$ -tocopherol micro-particles, where Tween 80 is only in the core (thus less influencing). In effect, the



presence of Tween 80 acts in two ways in the reduction of droplets size. First, it reduces the surface tension. Then, the presence of stabilizer gives a higher liquid viscosity, which causes an increase of duration of liquid contact with atomizing surface. The larger time of contact provokes an increase in liquid temperature and the consequent viscosity reduction. Therefore, the combined effect of reduced surface tension and reduced viscosity leads to the reduction in droplets size. However, these actual values of viscosity and surface tension were not evaluated. Thus, having values in absence of Tween 80 (pure alginate), the correlations were used to only predict size of alginate/ $\alpha$ -tocopherol (with a lower concentration of Tween 80).

The first correlation (3.14) proposed by Ramisetty et al [64], giving a theoretical drop diameter of 58  $\mu\text{m}$ , was not able to predict drop size because the Ohnesorge number is beyond the limits of validity of this correlation ( $Oh = 1.32 \cdot 10^4 \gg 2.71-161.64$ ). In effect the alginate solution has a shear-thinning behavior, that is taken into account in the correlation (3.15) proposed by Avvaru et al [48]. The drop diameter predicted by the correlation (3.15) was of about 71  $\mu\text{m}$ , nearer to the experimental drop size. Furthermore, the third correlation (3.16) [65] gives a predicted particle size of 76  $\mu\text{m}$ , which corresponds to the value experimentally obtained, confirming the goodness of this correlation (3.16) tuned on alginate rather than on CMC, as the previous one (3.15), that is in any case a good interpretation of the phenomena occurring.



---

## Chapter six

---

### **Concluding remarks**

*In this chapter the work done is resumed  
and the main results are highlighted.*

---

## 6.1 Concluding remarks

Purpose of the PhD thesis was to develop a novel microencapsulation process, designing and building a single-pot semi-continuous bench scale apparatus. The novel process is based on the coupling of two emerging techniques, involving ultrasound and microwave, used in atomization and heating operations, respectively. The process has been designed to respond to the needs for process intensification, i.e. improvement of process efficiency and cutting down of energy consumption.

With this aim, a review of the main processes used for microencapsulation was first performed. Attention was mainly focused on equipments, both conventional and innovative, using ultrasonic atomization and a double channel atomizer. The literature analysis pointed out that microencapsulation is still under investigation due to the different available ways to perform the micro-systems production and to the high number of parameters influencing the process. However, conventional processes showed a number of drawbacks, such as high energy consumption, batch configuration, use of solvents and long times of production.

On the basis of the state of the art, the idea of an intensified apparatus for particles production, exploiting alternative resources, such as ultrasound and microwave, was formulated. The apparatus was composed of three main sections: feeding, atomization, separation/stabilization. The feeding and atomization sections were built connecting a double channel ultrasonic atomizer to a system for feeding solutions in the separation section, that, according to the parallel design approach, was meanwhile designed. Thus, in a first stage of preliminary experiments testing the attainability of micronized/shell-core systems, drops produced from the atomizer were hardened in a stirred cross-linking solution contained in a beaker. The separation and the eventual stabilization were performed respectively by an under-vacuum filtration and drying in a microwave cavity or in an oven. Afterwards, purposely the designed separation/stabilization section replaced the conventional system used in the first tests, realizing the final, semi-continuous, configuration. It consisted of a wet-collector, i.e. a sort of hydrocyclone, which allowed a uniform distribution of the hardening solution and the consequent contact with the atomized drops (outgoing from the atomizer, placed at the centre of the wet-collector), a filtering device, and a microwave

oven. The wet-collector was placed into the microwave oven to obtain an “on-line” drying. Recirculation of the hardening solution, to renew contact surface between droplets and cross-linker, was guaranteed by a system of centrifugal pumps. In this configuration, when atomization occurred, drops were harvested in the wet-collector. After atomization, the obtained suspension was collected in the cross-linker tank, then the filtering device was inserted in the lower part of the wet-collector, so that hardening solution was recovered and particles settled on the filter, when the suspension was brought again to the wet-collector and after its complete emptying. An eventual following washing step can be done in a similar way to the previous hardening step. Finally, particles were stabilized by microwave drying, and then recovered.

The steps for building the microencapsulation apparatus were accurately shown. Then, criteria used for components selection, in order to obtain the best performances from the plant, were highlighted. For example, for the main section, i.e. the atomization, the ultrasonic atomizer was chosen with: a not too low frequency to allow processing of viscous materials, a nozzle tip with conical shape to obtain a wide spray pattern, and a large nozzle length to allow insertion of the nozzle itself at the centre of the wet-collector. The feeding section was accessorized with a convenient system of peristaltic pumps, representing the best compromise among cost, precision required, needed flow rates and maintenance.

After building the plant, the process parameters were defined. First, the research for the best combination of feeding parameters, such as type of materials, composition, concentration and feed rate, that assure the encapsulation of the core material in the shell, was carried out. In particular, alginate was chosen as polymer to be processed in the apparatus for the chance to carry out a process in an aqueous environment, without organic solvents or high temperatures and for its properties of biodegradability at physiological pH, which makes it useful for enteric oral formulations. Then, the parameters of the ultrasonic atomizer (atomization section), essentially power, were tuned: power was selected as the lowest value to ensure a uniform spray distribution. Finally, for stabilization/separation section, the properties and way of cross-linking, as well as filtering device features, were defined. Fundamental was the relevant stabilization step, where microwave power was set to avoid too high temperatures that could degrade molecules.

The ability of the novel plant to obtain micronized systems, that exhibit a behavior interesting for the pharmaceutical or nutraceutical markets, was tested. Two model molecules were chosen: a water soluble molecule, vitamin B12, and a water insoluble molecule,  $\alpha$ -tocopherol. In particular, results about vitamin B12 encapsulation preceded  $\alpha$ -tocopherol tests and they were carried out in the initial configuration of the apparatus. Thus, the produced macro-particles (beads) were able to encapsulate vitamin B12 with the following features: shell-core beads with a percentage of loading in the range 60-70%; whereas matrix particles have a loading percentage of 34-48%. Experimental values of B12 loading percentage for matrix particles were confirmed by a theoretical estimation based on a simple mass balance, considering the mechanism of B12 diffusion through nascent particles. Then, in both physiologic pH 7.4 and enteric tests, a delayed release was assured by the shell-core configuration (for fresh and convectively dried particles) compared to matrix configuration. Instead, for microwave dried beads, an immediate B12 release was observed due to the long time of exposition to microwave irradiation (causing a reduction in polymer interactions). As well as for coarse droplets, the shell-core conformation on microscopic scale assured a better protection of B12. This effect was not so evident because alginate gel pores were still large respect to vitamin B12 molecule size (van der Waals radius: 0.85 nm), therefore this latter was free to diffuse through forming gel. A larger sized molecule (still water soluble), such as BSA (bovine serum albumin) will be affected by the presence of polymer network. However preliminary tests on system alginate/BSA gave as a result a loss of about 70% during preparation. Thus, for final tests of encapsulation, a small molecule with different water solubility, nay lypophilic, was tested in order to observe its release behavior from alginate systems.

The latter system, encapsulating  $\alpha$ -tocopherol, produced in the apparatus in its final configuration, showed interesting results. First of all, the feasibility of microwave drying was confirmed by:

- measure of dielectric properties of fresh micro-particles;
- moisture measurements, showing a reduction from an initial content of about 95% to 3%, acceptable to avoid the impairment of product stability, in a short time (about 25 minutes);
- temperature measures during drying, prove that samples don't reach high or critical values of temperature (owing to the duty

cycle); moreover, that is even better for our purposes, temperatures decreased with time.

DSC results endorsed the purpose to combine microwave with ultrasounds: neither ultrasonic energy nor microwave drying broke the polymer structure.

With regard to release tests, shell-core configuration, in both micro and macro-systems, resulted to have better release and loading properties for the production of oral pharmaceutical formulations.

For the two kinds of micro-particles (matrix and shell-core), the yield of encapsulation was found around 100 %. They had enteric release properties because only at pH 6.8  $\alpha$ -tocopherol was completely released. However, shell-core micro-particles showed a better gastro-resistance compared to matrix ones. Microwave treatment (not harsher for the short irradiation times) caused, especially for shell-core configuration, a little delay in molecule release: this effect was also seen for macro-particles. Shell-core macro-particles displayed, once again, better release properties against matrix systems. In effect, shell-core configuration allowed to avoid  $\alpha$ -tocopherol deactivation (by heat), instead observed for matrix beads. Moreover, improving release features of matrix particles (worse than those of shell-core particles) was possible by exploiting the two fundamental resources of the new apparatus: ultrasonic atomization and microwave drying. Ultrasonic atomization avoided the problem of  $\alpha$ -tocopherol degradation, and coupling microwave drying to atomization allowed better gastro-resistance properties. Resuming, better release properties for systems produced in the novel apparatus were achieved by the coupling of ultrasonic atomization and microwave drying.

The power consumption of the apparatus resulted to be essentially due to particles drying, regardless of type; only a little fraction was attributed to the particles production apparatus. Moreover, despite of the slight difference in energy consume between microwave and convective drying, the drying time and the consequent global process time was reduced by microwave stabilization. Furthermore, ultrasonic atomizer required very low volumetric power supply, comparable with the lowest value realized on plant scale using conventional techniques, thus showing its benefit in the intensification of industrial processes.

Furthermore, the basic transport phenomena occurring in the ultrasonic assisted atomization were investigated. Literature correlations, based on forces balance, were also applied for droplets size prediction. A good agreement between experimental and

theoretical data was observed. From this, the role of operative parameters on particles size was emphasized.

All these results endorses the usefulness of the novel plant, based on the combination of two powerful tools of process intensification, ultrasonic atomization and microwave drying, to obtain micro-systems, particularly interesting for specific drug delivery applications. Moreover working at room conditions and in absence of solvents makes the apparatus more attractive in terms of improved inherent safety and reduced costs.



---

---

## **Appendix A**

*In this appendix, a comparison between UV-vis spectrometry and HPLC to detect vitamin B12 concentration in presence of the interfering polymer, alginate, is done in order to select the most reliable method.*

---

### **A.1 Assay methods: UV-vis spectrometry vs HPLC**

To evaluate the encapsulation of a model drug in a system, the most used method is the UV-vis spectrometry, for its operative simplicity and the reduced costs. In particular, the method consists in measuring the absorbance of the model drug at a specific wavelength. Then, through the Lambert-Beer law, absorbance is related to concentration. By a double rays spectrometer, blank and sample solutions should contain the same substances, of course with the exception of drug in the blank solution. During the dissolution of a polymer-matrix pharmaceutical form, the actual quantity of dissolved polymer is unknown, thus the blank cannot be properly prepared. Then, the difficulties in evaluating the drug concentration due to the polymer presence are of a great limitation when studying the drug release from a polymer based pharmaceutical form.

In this particular case, alginate is the polymer that could interfere with the evaluation of drug concentration. Therefore, spectra of alginate in different solutions in the range of 200-400 nm were collected. In particular, cross-linked particles of alginate were analyzed.

With the aim of investigating interferences caused by the alginate dissolution, a more rapid method of particles preparation was used: an atomizer different from the one used in the developing apparatus was used. It was also employed for preliminary activities to test the feasibility of atomization of natural polymers.

#### *A.1.1 Materials and Methods*

VCX 130 PB Ultrasonic Processor (130 W, 20 kHz, Sonics & Materials Inc., CT, USA) and a standard tip for low atomization rate (up to 1 mm<sup>3</sup>/s), code VC 4020 (50 W, 20 kHz, Sonics & Materials Inc., CT, USA) were adopted as sources of ultrasonic vibration and atomizer, respectively. Also a peristaltic pump (Velp Scientifica, IT) and a camera (Canon Digital IXUS 100 IS) were used for the experiments.

These preliminary activities were performed using the following parameters:

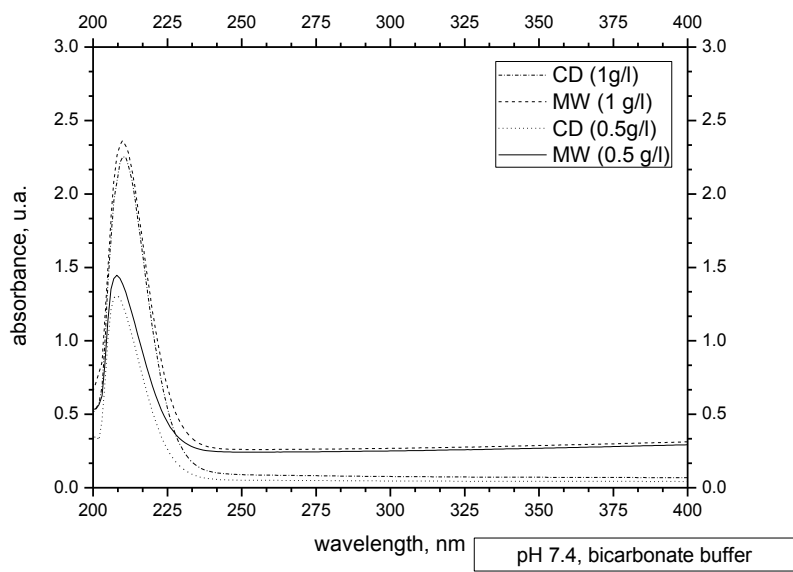
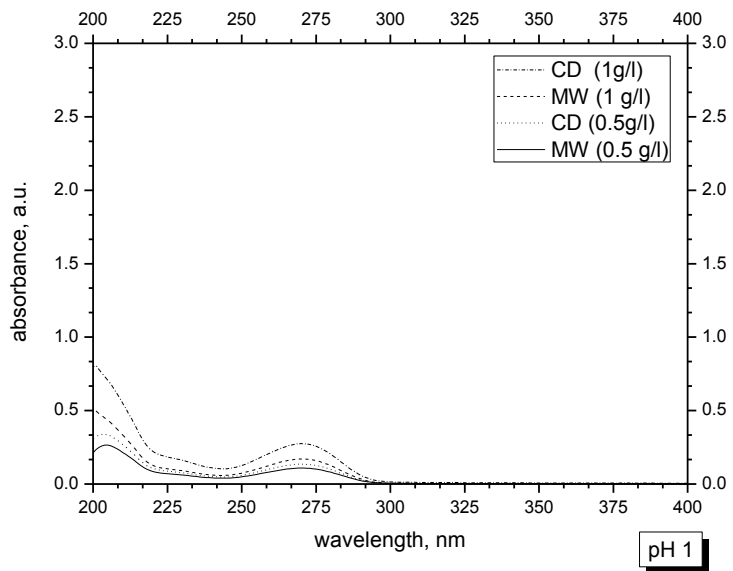
- alginate concentration = 3% (w/w);
- flow rate = 14,5 mL/min;
- atomization amplitude, A=95%;
- atomization/cross-linking time = 40 s;

- cross-linking solution = CaCl<sub>2</sub>, 8.9 g/l, 60 mL;
- washing solution (variable and known volume);
- drying for stabilization: convective or microwave drying (until the mass becomes constant).

The particles obtained in these conditions were put in an acid solution at pH 1 and in two solutions at pH 7.4, bicarbonate buffer solution and phosphate buffer solution.

Spectra (in the range 200-400 nm) of alginate particles in the three solutions are shown in Figure 58. Spectra at pH 1, where particles remain undissolved, highlight that alginate particles have a peak of absorbance at a wavelength of 270 nm. Therefore, it is hard to check the presence of model drugs, such as theophylline and diclofenac sodium, which absorb in the same wavelength range of alginate particles, in acid conditions. Presence of alginate in both the solutions at pH 7.4 is detected only at low wavelengths, especially for bicarbonate buffer. However, adding the model drug (B12) to the starting solution of alginate and then dissolving the obtained particles in a phosphate buffer (where the alginate seems to be not influencing on the range of wavelength typical of B12, 361 nm, as shown in Figure 58), the value of total B12 (encapsulated and lost in cross-linking solution and washing water) measured by UV-vis spectrometer doesn't agree with the theoretical one (as calculated from the volume of solution dripped or atomized). The conclusion is that presence of alginate causes interference, especially for low drug concentration in the solution. It is therefore wrong to measure the amount of B12 evaluating the absorbance at the wavelength of 361 nm. Thus a comparison among different ways for detection of vitamin B12 in a system containing alginate was carried out. Parameters, such as alginate concentration, flow rate, time of cross-linking, type and concentration of cross-linking solution were kept unchanged. Particles were obtained by dripping (in this case the amount of drug encapsulated is larger if compared to atomized particles owing to the greater size) or by atomizing, and were stabilized only by convective drying. Then they were put in a volume of phosphate buffer solution at pH 7.4, where alginate dissolves, to evaluate the amount of vitamin B12 encapsulated in alginate particles.

Appendix A



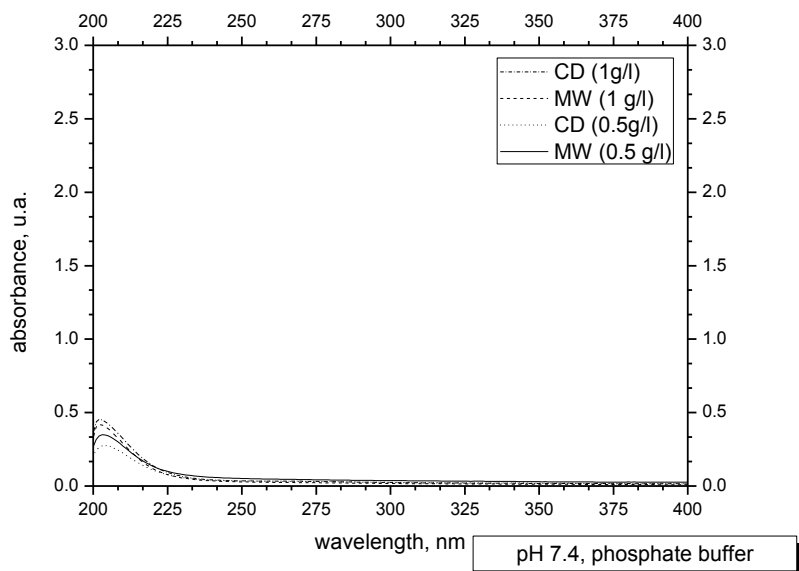


**Figure 58.** Spectra of alginate particles, dried by convective drying (CD) or by microwave drying (MW), and put in three solutions (pH1, bicarbonate buffer and phosphate buffer, both at pH 7.4) at two different concentrations (0.5 g/l; 1 g/l)

The absorbance based method was compared to the method of spectra subtraction using UV-vis spectrometer, and to a different analytical technique, HPLC. Also, three different methods were compared in this last technique because the influence of alginate was noticed.

#### *A.1.2 UV-vis spectrometer: method of spectra subtraction*

The absorbance based method was compared to the method of spectra subtraction using UV-vis spectrometer, and to a different analytical technique, HPLC. Also, three different methods were compared in this last technique because the influence of alginate was noticed.

The method of spectra subtraction, using UV-vis spectrometer, consists in a subtraction of an exponential curve from the spectrum in the range of absorbance of the drug (in this case between 325 nm and 400 nm). The curve obtained is fitted with a Gaussian curve of the following type:

$$G(A) = b_1 \cdot \exp \left( -4 \ln 2 \cdot \left( \frac{\lambda - b_2}{b_3} \right)^2 \right) \quad (3.1)$$

where  $b_1$ ,  $b_2$ ,  $b_3$  are respectively the height of the Gaussian curve, the wavelength corresponding to the maximum of the curve and, finally, the width at half height of the curve. The values are optimized using the least squares methods. In this way, the parameter that replaces the absorbance value, to be considered for the measure of drug concentration is the height of the fitted Gaussian curve. Obviously, the proportionality constant necessary to correlate absorbance to concentration, is obtained by a calibration curve where the ordinate values are not absorbances, but the heights of the fitted Gaussian curves at given concentrations. An example is shown in Figure 59, where a system of alginate particles containing B12, obtained by dripping the alginate-B12 system in the cross-linking solution and then stabilizing it by convective drying, was dissolved in a phosphate buffer at pH 7.4.

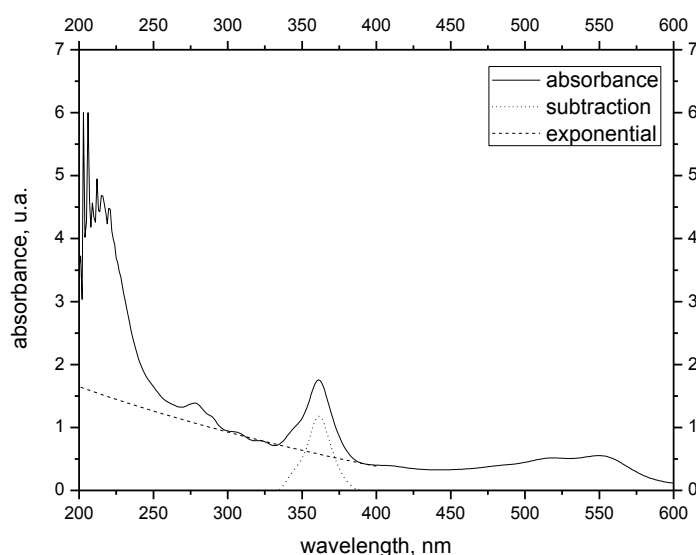


**Figure 59.** Absorbance spectrum (solid line), exponential (dashed line), and curve obtained by subtraction (dotted line), for a system alginate-B12 obtained by dripping it in the cross-linking solution and drying in a tray oven with air at 45°C, and then dissolved in a phosphate buffer at pH 7.4

The resulting spectrum gave an absorbance, at the wavelength of 361 nm, of 1.76 if the first method is used. Instead, the value of the height of the Gaussian curve, obtained by spectra subtraction method, is 1.18. The difference between the two method results to be more pronounced for atomized particles because in this case the amount of drug

encapsulated is lower, owing to the smaller size of particles, and thus the interference of alginate is more evident.

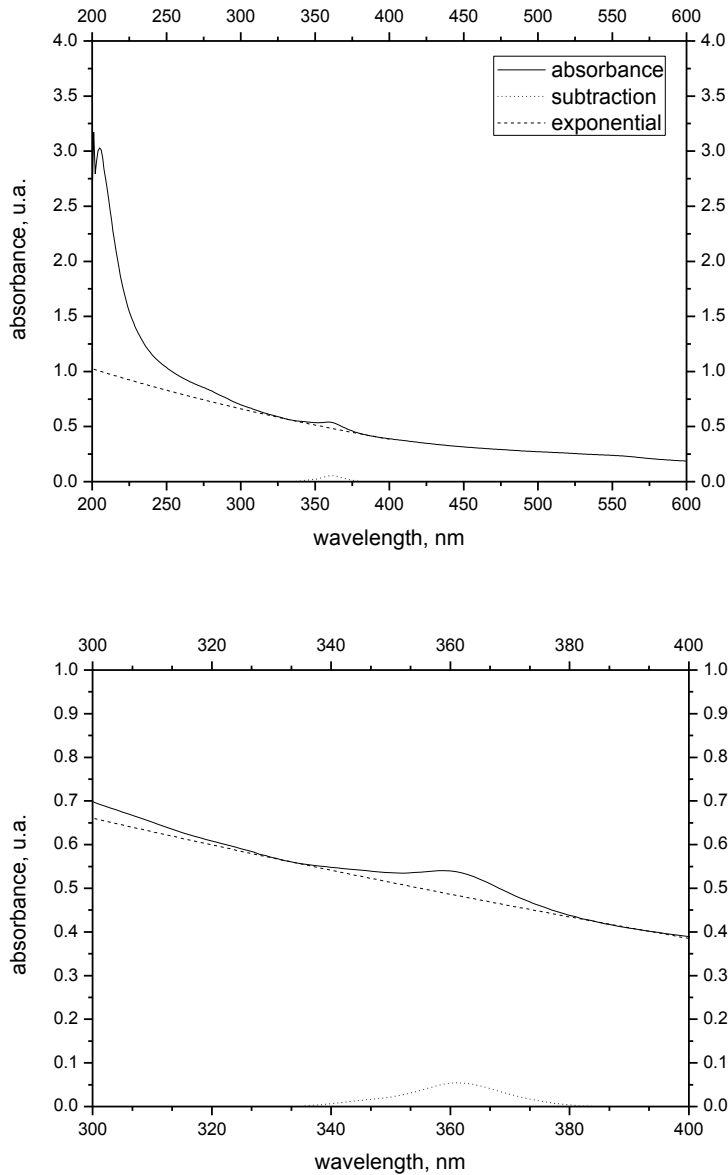


**Figure 60.** Absorbance spectrum (solid line), exponential (dashed line), and curve obtained by subtraction (dotted line), for a system alginate-B12 obtained by atomizing it in the cross-linking solution, drying in a tray-oven with air at 45°C, and then dissolved in a phosphate buffer at pH 7.4. Top: full spectrum; down: particular of spectrum in the range 300-400 nm

Figure 60 shows the spectrum in a phosphate buffer at pH 7.4 of a system of atomized particles containing B12, obtained in the same conditions used for the dripped ones. In this case, the absorbance at 361 nm is 0.54, the value obtained by spectra subtraction is 0.05. Since the values of proportionality constant for the absorbance method and spectra subtraction are not so different (because they are obtained using solutions of pure B12, without any interference of polymer), according to the first method the loaded drug in atomized particles is of an order of magnitude larger than the value measured with the spectra subtraction method.

### *A.1.3 HPLC analysis*

The same solutions of atomized and dripped particles in phosphate buffer at pH 7.4 were also subjected to HPLC analysis, which requires a proper selection of the separation procedure. Also in this case the signal given by the instrument has to be related to the analyte concentration. In particular, the calibration line is obtained by relating the concentration to the area under the curve (signal) evaluated by the mathematical trapezoids method. This area varies in function of the separation procedures, so that the peak of the curve is located at different values of abscissa, i.e. at different retention times.

The first HPLC method (method HPLC-A, Table 14), according to a procedure used in literature [94], stated that all chromatographic separations were carried out at ambient temperature. The mobile phase was methanol/water, 30/70 (v/v), with a flow rate of 0.8 mL/min. The resulting signal, collected at a wavelength of 361 nm, for both dripped and atomized particles in phosphate buffer, was characterized by a double peak, probably due to the interaction between alginate and vitamin B12 (method A, Figure 61). In fact, the eluent solution of methanol/water (30/70) has a pH of about 9. The pKa of vitamin B12 is 7.5 [95] and the pKa of alginate ranges from 3.38 to 3.65 [96], so they both are in a dissociated form. Therefore, the eluent pH was lowered under the pKa of the alginate, to avoid its dissociation, until a pH = 1.6. At this pH, the alginate particles without vitamin B12 dissolved in phosphate buffer, showed a flat signal, unlike solutions of particles containing B12 and solutions of B12 alone.



Initially, a method at pH 1.6 (HPLC-B in Table 14), keeping the flow rate at 0.8 mL/min, gave a retention time of 11.5 min; therefore a bigger flow rate of 1.5 mL/min was used in the definitive method HPLC-C, obtaining a retention time of 3.6 min (Table 14).

**Table 14. Features of the three different HPLC procedures**

HPLC-A	HPLC-B	HPLC-C
methanol/water = 30/70	methanol/water = 30/70	methanol/water = 30/70
pH = 9	pH = 1.6 (using HCl)	pH = 1.6 (using HCl)
flow rate = 0.8 mL·min <sup>-1</sup>	flow rate = 0.8 mL·min <sup>-1</sup>	flow rate = 1.5 mL·min <sup>-1</sup>
wavelength = 361 nm	wavelength = 361 nm	wavelength = 361 nm
retention time = 4.4 min	retention time = 11.5 min	retention time = 3.6 min

An example of the signals given by the instrument with the different separation procedures is shown in Figure 61. In this case the analyzed solution is the phosphate buffer, dripped particles of alginate and B12 are dissolved in. Similar signals for the three procedures were obtained for atomized particles (data not shown).

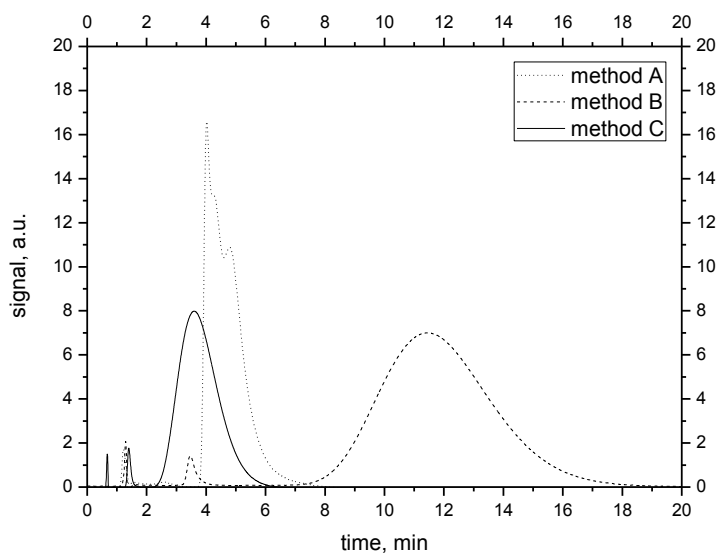


**Figure 61. Signals given by HPLC analysis, using the three different separation procedures**

## A.1.4 Choice of the most reliable method

**Table 15. Comparison among different ways for detection of vitamin B12 in a system containing alginate (particles obtained by dripping)**

	Absorbance measure	Spectra subtraction	HPLC-A	HPLC-B	HPLC-C
<b>B12 in particles<sup>1</sup>, mg</b>	7.53	6.27	4.10	6.46	5.76
<b>B12 lost<sup>2</sup>, mg</b>	3.03	3.14	2.92	2.92	2.92
<b>total B12<sup>3</sup>, mg</b>	10.56	9.41	7.02	9.38	<b>8.68</b>
<b>theoretical B12<sup>4</sup>, mg</b>	8.67	8.67	8.67	8.67	<b>8.67</b>

<sup>1</sup> Value get by dividing the absorbance, the height of Gauss curve, or the area under the curve (depending on the method), by a suitable proportional constant (given by calibration line), and multiplying the so obtained concentration by the volume of buffer solution in which particles are dissolved

<sup>2</sup> Sum of quantity of B12 measured in cross-linking solution and in washing water

<sup>3</sup> Sum of the first and the second row (B12 in particles and B12 lost)

<sup>4</sup> Value obtained by measuring the amount of B12 in the initial solution, then calculating the relative amount in the volume sent to dripping (the volume is calculated multiplying the flow rate by the time of dripping)

**Table 16. Comparison among different ways for detection of vitamin B12 in a system containing alginate (particles obtained by atomization)**

	Absorbance measure	Spectra subtraction	HPLC-A	HPLC-B	HPLC-C
<b>B12 in particles<sup>1</sup>, mg</b>	2.31	0.29	0.42	0.50	0.39
<b>B12 lost<sup>1</sup>, mg</b>	9.20	9.36	9.69	8.37	8.37
<b>total B12<sup>2</sup>, mg</b>	11.51	9.65	10.11	8.87	<b>8.76</b>
<b>theoretical B12<sup>4</sup>, mg</b>	8.67	8.67	8.67	8.67	<b>8.67</b>

<sup>1</sup> Value get by dividing the absorbance, the height of Gauss curve, or the area under the curve (depending on the method), by a suitable proportional constant (given by calibration line), and multiplying the so obtained concentration by the volume of buffer solution in which particles are dissolved

<sup>2</sup> Sum of quantity of B12 measured in cross-linking solution and in washing water

<sup>3</sup> Sum of the first and the second row (B12 in particles and B12 lost)

<sup>4</sup> Value obtained by measuring the amount of B12 in the initial solution, then calculating the relative amount in the volume sent to atomization (the volume is calculated multiplying the flow rate by the time of atomization)

It is worth to note that to make a comparison with the theoretical value of B12, i.e. the total amount of drug in the solution subjected to dripping or atomization, the concentrations of drug lost in the cross-linking solutions (during the cross-linking process) and in the water used for the washing step, have to be measured.

The five check methods were also applied to these two solutions. In Table 15 and Table 16, respectively for dripped and atomized particles, the theoretical value of B12 and the total amount of B12, as the sum of drug loaded in particles and drug lost in cross-linking solution and washing water, were compared for the five methods used for detecting B12 in a system containing alginate. The values obtained from the absorbance measure are very different from the theoretical ones for both kinds of particles. The results from the method of spectra subtraction are nearer to the theoretical values, but it is not very accurate (owing to the resolution limits of the instrument), whereas HPLC appears to be more precise. The most reliable method is the HPLC-C (its features are described in Table 14) as it gives a value of measured B12 which is, especially for dripped particles, the nearest to the theoretical one.



---

---

## **Appendix B**

*In this appendix, the diffusion equation through a sphere for a substance is described.*

---

**B.1 Diffusion in a sphere**

The diffusion equation, restricted to the radial diffusion, for a constant diffusion coefficient is [97]:

$$\frac{\delta C}{\delta t} = \mathcal{D} \left( \frac{\delta^2 C}{\delta r^2} + \frac{2}{r} \frac{\delta C}{\delta r} \right) \quad (\text{B.1})$$

Where:

$C$ : concentration of diffusing substance;

$t$ : time;

$\mathcal{D}$ : substance diffusivity;

$r$ : generic radius in the sphere.

If putting:

$$u = Cr \quad (\text{B.2})$$

The equation (B.1) becomes:

$$\frac{\delta u}{\delta t} = \mathcal{D} \left( \frac{\delta^2 u}{\delta r^2} \right) \quad (\text{B.3})$$

The case of B12 diffusion from gel particles, with a radius  $a$ , can be considered as a system in a non-steady state, with a constant surface concentration  $C_0$ , the boundary conditions are:

$$u = 0, \quad r = 0, \quad t > 0 \quad (\text{B.4})$$

$$u = uC_0, \quad r = a, \quad t > 0 \quad (\text{B.5})$$

$$u = rf(r), \quad t = 0, \quad 0 < r < a \quad (\text{B.6})$$

Moreover, if the sphere is also at a uniform concentration  $C_1$  (as in the case of vitamin B12), the solution is:

$$\frac{C-C_1}{C_0-C_1} = 1 + \frac{2a}{\pi r} \sum_{n=1}^{\infty} \frac{(-1)^n}{n} \sin \frac{n\pi r}{a} \exp(-\mathcal{D}n^2\pi^2 t/a^2) \quad (\text{B.7})$$

The concentration at the centre of the sphere is obtained by imposing the limit of  $r \rightarrow 0$ , i.e. by:

$$\frac{C-C_1}{C_0-C_1} = 1 + 2 \sum_{n=1}^{\infty} (-1)^n \exp(-\mathcal{D}n^2\pi^2 t/a^2) \quad (\text{B.8})$$

Therefore, if  $M_t$  is defined as the total amount of diffusing substance which left the sphere, and  $M_\infty$  the corresponding quantity after infinite

---

time (thus the total amount of substance present in the sphere), the total amount of substance leaving the sphere by diffusion is:

$$\frac{M(t)}{M_{\infty}} = 1 - \frac{6}{\pi^2} \sum_{n=1}^{\infty} \frac{1}{n^2} \exp(-\mathcal{D}n^2\pi^2t/a^2) \quad (\text{B.9})$$

This final diffusion equation can be used to estimate the amount of vitamin B12 diffused through an alginate sphere during preparation, thus, as complementary value, the percentage of loading.





## References

- [1] P. Venkatesan, R. Manavalan, K. Valliappan, Microencapsulation: A vital technique in novel drug delivery system, *Journal of Pharmaceutical Sciences*, 1 (2009) 26-35.
- [2] J. Silva, Effect of drug properties on the release from CAP microspheres prepared by a solvent evaporation method, *Journal of microencapsulation*, 16 (1999) 95-103.
- [3] P. Colombo, P. Catellani, A. Gazzaniga, E. Menegatti, E. Vidale, *Principi di tecnologie farmaceutiche*, Casa Editrice Ambrosiana, Milano, (2004).
- [4] M. Ré, B. Biscans, Preparation of microspheres of ketoprofen with acrylic polymers by a quasi-emulsion solvent diffusion method, *Powder Technology*, 101 (1999) 120-133.
- [5] N. Barakat, A. Ahmad, Diclofenac sodium loaded-cellulose acetate butyrate: Effect of processing variables on microparticles properties, drug release kinetics and ulcerogenic activity, *Journal of microencapsulation*, 25 (2008) 31-45.
- [6] S. Benita, *Microencapsulation: methods and industrial applications*, Informa HealthCare, 2006.
- [7] S. Freitas, H. Merkle, B. Gander, Microencapsulation by solvent extraction/evaporation: reviewing the state of the art of microsphere preparation process technology, *Journal of controlled Release*, 102 (2005) 313-332.
- [8] S. Lyons, S. Wright, Apparatus and method for preparing microparticles, in, 2003.
- [9] J. Herrmann, R. Bodmeier, Biodegradable, somatostatin acetate containing microspheres prepared by various aqueous and non-aqueous solvent evaporation methods, *European Journal of Pharmaceutics and Biopharmaceutics*, 45 (1998) 75-82.
- [10] J. Beyger, J. Nairn, Some factors affecting the microencapsulation of pharmaceuticals with cellulose acetate phthalate, *Journal of Pharmaceutical Sciences*, 75 (1986) 573-578.
- [11] F. Gabor, Ketoprofen-poly (D, L-lactic-co-glycolic acid) microspheres: influence of manufacturing parameters and type of

polymer on the release characteristics, *Journal of microencapsulation*, 16 (1999) 1-12.

[12] Y. Yang, T. Chung, N. Ping Ng, Morphology, drug distribution, and in vitro release profiles of biodegradable polymeric microspheres containing protein fabricated by double-emulsion solvent extraction/evaporation method, *Biomaterials*, 22 (2001) 231-241.

[13] W. Obeidat, J. Price, Preparation and evaluation of Eudragit S 100 microspheres as pH-sensitive release preparations for piroxicam and theophylline using the emulsion-solvent evaporation method, *Journal of microencapsulation*, 23 (2006) 195-202.

[14] H. Chen, J. Wu, H. Chen, Preparation of ethylcellulose microcapsules containing theophylline by using emulsion non-solvent addition method, *Journal of microencapsulation*, 12 (1995) 137-147.

[15] V.S. Mastiholimath, P.M. Dandagi, S.S. Jain, A.P. Gadad, A.R. Kulkarni, Time and pH dependent colon specific, pulsatile delivery of theophylline for nocturnal asthma, *International Journal of Pharmaceutics*, 328 (2007) 49-56.

[16] I. Péter Sipos, Influence of preparation conditions on the properties of Eudragit microspheres produced by a double emulsion method, *Drug Development Research*, 64 (2005) 41-54.

[17] M. Lai, R. Tsiang, Microencapsulation of acetaminophen into poly (L-lactide) by three different emulsion solvent-evaporation methods, *Journal of microencapsulation*, 22 (2005) 261-274.

[18] P. Sansdrap, A. Mo s, Influence of manufacturing parameters on the size characteristics and the release profiles of nifedipine from poly (DL-lactide-co-glycolide) microspheres, *International Journal of Pharmaceutics*, 98 (1993) 157-164.

[19] Y. Maa, C. Hsu, Microencapsulation reactor scale-up by dimensional analysis, *Journal of microencapsulation*, 13 (1996) 53-66.

[20] Y. Maa, C. Hsu, Liquid-liquid emulsification by static mixers for use in microencapsulation, *Journal of microencapsulation*, 13 (1996) 419-433.

[21] B. Amsden, The production of uniformly sized polymer microspheres, *Pharmaceutical research*, 16 (1999) 1140-1143.

[22] H. Liu, Science and engineering of droplets: fundamentals and applications, William Andrew, 2000.

[23] M. Rawat, S. Saraf, Influence of selected formulation variables on the preparation of enzyme-entrapped eudragit S100 microspheres, *AAPS PharmSciTech*, 8 (2007) 289-297.

[24] M. Kitajima, T. Yamaguchi, A. Kondo, N. Muroya, Encapsulation method, in, 1972.

- [25] M. Li, O. Rouaud, D. Poncelet, Microencapsulation by solvent evaporation: State of the art for process engineering approaches, *International Journal of Pharmaceutics*, 363 (2008) 26-39.
- [26] J. Ramstack, Apparatus and method for preparing microparticles using liquid-liquid extraction, in, 2002.
- [27] M. Rickey, J. Ramstack, D. Lewis, Preparation of biodegradable, biocompatible microparticles containing a biologically active agent, in, 2003.
- [28] S. Gouin, Microencapsulation: industrial appraisal of existing technologies and trends, *Trends in Food Science & Technology*, 15 (2004) 330-347.
- [29] C. Wischke, S. Schwendeman, Principles of encapsulating hydrophobic drugs in PLA/PLGA microparticles, *International Journal of Pharmaceutics*, 364 (2008) 298-327.
- [30] J. Coulson, J. Richardson, *Chemical Engineering, Volume 2: Particle Technology and Separation Processes*, Pergamon, (1991).
- [31] A. Stankiewicz, J. Moulijn, *Re-engineering the chemical processing plant: process intensification*, M. Dekker, New York, 2004.
- [32] G. Cravotto, A. Barge, L. Boffa, E. Calcio Gaudino, W. Bonrath, Ultrasound-microwave coupling: an efficient tool for chemical-process intensification, in, *GPE-EPIC, 2nd International Congress on Green Process Engineering, 2nd European Process Intensification Conference*, 2009.
- [33] B. Redding Jr, Apparatus and method for making microcapsules, in, 1993.
- [34] G. Alisch, E. Brauneis, B. Pirstadt, N. Iffland, E. Brandau, Process and plant for the production of spherical alginate pellets, in, 1995.
- [35] B. Amsden, R. Liggins, Methods for microsphere production, in, 2001.
- [36] D. Bomberger, P. Catz, M. Smedley, P. Stearns, System and method for producing drug-loaded microparticles, in, 2002.
- [37] J. Gibson, R. Holl, A. Tipton, Emulsion-based processes for making microparticles, in, 2002.
- [38] P. Herbert, M. Healy, Production scale method of forming microparticles, in, 2004.
- [39] M. Tyo, Y. Hsu, M. Hedley, Continuous-flow method for preparing microparticles, in, 2004.
- [40] J. Piechocki, D. Kyle, Continuous spray-capture production system, in, 2009.

- [41] T. Brandau, Preparation of monodisperse controlled release microcapsules, *International Journal of Pharmaceutics*, 242 (2002) 179-184.
- [42] R. Pareta, M. Edirisinghe, A novel method for the preparation of biodegradable microspheres for protein drug delivery, *Journal of The Royal Society Interface*, 3 (2006) 573.
- [43] M. Chang, E. Stride, M. Edirisinghe, Controlling the thickness of hollow polymeric microspheres prepared by electrohydrodynamic atomization, *Journal of The Royal Society Interface*, 7 (2010) S451.
- [44] Y. Lee, F. Mei, M. Bai, S. Zhao, D. Chen, Release profile characteristics of biodegradable-polymer-coated drug particles fabricated by dual-capillary electrospray, *Journal of controlled Release*, (2010).
- [45] A. Dalmoro, A.A. Barba, G. Lamberti, M. d'Amore, Intensifying the microencapsulation process: Ultrasonic atomization as an innovative approach, *European Journal of Pharmaceutics and Biopharmaceutics*, (2012).
- [46] A. Patist, D. Bates, Ultrasonic innovations in the food industry: From the laboratory to commercial production, *Innovative food science & emerging technologies*, 9 (2008) 147-154.
- [47] D. Ensminger, F. Stulen, *Ultrasonics: data, equations, and their practical uses*, CRC Press, 2009.
- [48] B. Avvaru, M. Patil, P. Gogate, A. Pandit, Ultrasonic atomization: effect of liquid phase properties, *Ultrasonics*, 44 (2006) 146-158.
- [49] R. Rajan, A. Pandit, Correlations to predict droplet size in ultrasonic atomisation, *Ultrasonics*, 39 (2001) 235-255.
- [50] K. Park, Y. Yeo, Microencapsulation using ultrasonic atomizers, in, 2003.
- [51] L. Rodriguez, N. Passerini, C. Cavallari, M. Cini, P. Sancin, A. Fini, Description and preliminary evaluation of a new ultrasonic atomizer for spray-congealing processes, *International Journal of Pharmaceutics*, 183 (1999) 133-143.
- [52] N. Ashgriz, *Handbook of Atomization and Sprays: Theory and Applications*, Springer, 2011.
- [53] B. Bittner, T. Kissel, Ultrasonic atomization for spray drying: a versatile technique for the preparation of protein loaded biodegradable microspheres, *Journal of microencapsulation*, 16 (1999) 325-341.
- [54] S. Freitas, H. Merkle, B. Gander, Ultrasonic atomisation into reduced pressure atmosphere--envisaging aseptic spray-drying for microencapsulation, *Journal of controlled Release*, 95 (2004) 185-195.

- [55] P. Luz, A. Pires, O. Serra, A low-cost ultrasonic spray dryer to produce spherical microparticles from polymeric matrices, *Química Nova*, 30 (2007) 1744-1746.
- [56] P. Burke, L. Klumb, J. Herberger, X. Nguyen, R. Harrell, M. Zordich, Poly (lactide-co-glycolide) microsphere formulations of darbepoetin alfa: spray drying is an alternative to encapsulation by spray-freeze drying, *Pharmaceutical research*, 21 (2004) 500-506.
- [57] C. Berkland, E. Pollauf, D. Pack, K. Kim, Uniform double-walled polymer microspheres of controllable shell thickness, *Journal of controlled Release*, 96 (2004) 101-111.
- [58] Y. Yeo, K. Park, A new microencapsulation method using an ultrasonic atomizer based on interfacial solvent exchange, *Journal of controlled Release*, 100 (2004) 379-388.
- [59] R. Graves, D. Poole, R. Moiseyev, L. Bostanian, T. Mandal, Encapsulation of Indomethacin Using Coaxial Ultrasonic Atomization Followed by Solvent Evaporation, *Drug development and industrial pharmacy*, 34 (2008) 419-426.
- [60] J. Legako, N. Dunford, Effect of Spray Nozzle Design on Fish Oil–Whey Protein Microcapsule Properties, *Journal of Food Science*, 75 (2010) E394-E400.
- [61] L. Pilon, H. Berberoglu, Method and apparatus for liquid microencapsulation with polymers using ultrasonic atomization, in, 2005.
- [62] H. Liu, *Science and Engineering of Droplets:: Fundamentals and Applications*, William Andrew, 1999.
- [63] R.J. Lang, Ultrasonic atomization of liquids, *The journal of the acoustical society of America*, 34 (1962) 6-8.
- [64] K.A. Ramisetty, A.B. Pandit, P.R. Gogate, Investigations into ultrasound induced atomization, *Ultrasonics Sonochemistry*, (2012).
- [65] A.A. Barba, M. d'Amore, S. Cascone, G. Lamberti, G. Titomanlio, Intensification of biopolymeric microparticles production by ultrasonic assisted atomization, *Chemical Engineering and Processing: Process Intensification*, 48 (2009) 1477-1483.
- [66] [www.sono-tek.com](http://www.sono-tek.com), in.
- [67] [www.verderflex.com](http://www.verderflex.com), in.
- [68] [www.watson-marlow.com](http://www.watson-marlow.com), in.
- [69] R.A. Arterburn, The sizing and selection of hydrocyclones, *Design and Installation of Comminution Circuits*, (1982) 592-607.
- [70] W. Yu, H. Song, G. Zheng, X. Liu, Y. Zhang, X. Ma, Study on membrane characteristics of alginate-chitosan microcapsule with cell growth, *Journal of Membrane Science*, 377 (2011) 214-220.

- [71] M. George, T.E. Abraham, Polyionic hydrocolloids for the intestinal delivery of protein drugs: alginate and chitosan--a review, *Journal of Controlled Release*, 114 (2006) 1-14.
- [72] H. Zhang, H. Wang, J. Wang, R. Guo, Q. Zhang, The effect of ionic strength on the viscosity of sodium alginate solution, *Polymers for Advanced Technologies*, 12 (2001) 740-745.
- [73] W. Gombotz, S. Wee, Protein release from alginate matrices, *Advanced Drug Delivery Reviews*, 31 (1998) 267-285.
- [74] C. DeRamos, A. Irwin, J. Nauss, B. Stout, <sup>13</sup>C NMR and molecular modeling studies of alginic acid binding with alkaline earth and lanthanide metal ions, *Inorganica chimica acta*, 256 (1997) 69-75.
- [75] H. Tønnesen, J. Karlsten, Alginate in drug delivery systems, *Drug development and industrial pharmacy*, 28 (2002) 621-630.
- [76] G. Fundueanu, C. Nastruzzi, A. Carpov, J. Desbrieres, M. Rinaudo, Physico-chemical characterization of Ca-alginate microparticles produced with different methods, *Biomaterials*, 20 (1999) 1435.
- [77] M.S. Shoichet, R.H. Li, M.L. White, S.R. Winn, Stability of hydrogels used in cell encapsulation: An in vitro comparison of alginate and agarose, *Biotechnology and bioengineering*, 50 (1996) 374-381.
- [78] A. Dalmoro, A.A. Barba, G. Lamberti, M. Grassi, M. d'Amore, Pharmaceutical applications of biocompatible polymer blends containing sodium alginate, *Advances in Polymer Technology*, (2012).
- [79] E.S. Chan, B.B. Lee, P. Ravindra, D. Poncelet, Prediction models for shape and size of ca-alginate macrobeads produced through extrusion-dripping method, *Journal of colloid and interface science*, 338 (2009) 63-72.
- [80] E. Pasut, R. Toffanin, D. Voinovich, C. Pedersini, E. Murano, M. Grassi, Mechanical and diffusive properties of homogeneous alginate gels in form of particles and cylinders, *Journal of Biomedical Materials Research Part A*, 87 (2008) 808-818.
- [81] Sigma-Aldrich, in.
- [82] S.P. Stabler, R.H. Allen, Vitamin B12 deficiency as a worldwide problem, *Annu. Rev. Nutr.*, 24 (2004) 299-326.
- [83] F. Aranda, A. Coutinho, M. Berberan-Santos, M. Prieto, J. Gomez-Fernandez, Fluorescence study of the location and dynamics of  $\alpha$ -tocopherol in phospholipid vesicles, *Biochimica et Biophysica Acta-Biomembranes*, 985 (1989) 26-32.

- [84] E.F. Bell, History of vitamin E in infant nutrition, *The American Journal of Clinical Nutrition*, 46 (1987) 183-186.
- [85] M. Simonoska Crcarevska, M. Glavas Dodov, K. Goracinova, Chitosan coated Ca-alginate microparticles loaded with budesonide for delivery to the inflamed colonic mucosa, *European Journal of Pharmaceutics and Biopharmaceutics*, 68 (2008) 565-578.
- [86] A.A. Barba, S. Chirico, A. Dalmoro, G. Lamberti, Simultaneous measurement of theophylline and cellulose acetate phthalate in phosphate buffer by uv analysis, *Can J Anal Sci Spectros*, 53 (2009) 249-253.
- [87] T.W. Wong, L.W. Chan, S.B. Kho, P.W. Sia Heng, Design of controlled-release solid dosage forms of alginate and chitosan using microwave, *Journal of controlled Release*, 84 (2002) 99-114.
- [88] R.E. Mardziah, T.W. Wong, Effects of microwave on drug-release responses of spray-dried alginate microspheres, *Drug development and industrial pharmacy*, 36 (2010) 1149-1167.
- [89] A. Metaxas, R.J. Meredith, *Industrial microwave heating*, Inst of Engineering & Technology, 1983.
- [90] R.E. Mudgett, Microwave properties and heating characteristics of foods, *Food Technology*, 40 (1986).
- [91] C.M. Sabliov, C. Fronczek, C. Astete, M. Khachatryan, L. Khachatryan, C. Leonardi, Effects of temperature and UV light on degradation of  $\alpha$ -tocopherol in free and dissolved form, *Journal of the American Oil Chemists' Society*, 86 (2009) 895-902.
- [92] T. Pongjanyakul, S. Puttipipatkachorn, Xanthan–alginate composite gel beads: Molecular interaction and in vitro characterization, *International Journal of Pharmaceutics*, 331 (2007) 61-71.
- [93] A.A. Barba, M. d'Amore, S. Cascone, G. Lamberti, G. Titomanlio, Intensification of biopolymeric microparticles production by ultrasonic assisted atomization, *Chemical Engineering and Processing: Process Intensification*, 48 (2009) 1477-1483.
- [94] H.B. Li, F. Chen, Y. Jiang, Determination of vitamin B12 in multivitamin tablets and fermentation medium by high-performance liquid chromatography with fluorescence detection, *Journal of Chromatography A*, 891 (2000) 243-247.
- [95] E.L. SMITH, K. FANTES, S. BALL, J. WALLER, W. EMERY, B12 Vitamins (Cobalamins), (1951).
- [96] Y. Xu, C. Zhan, L. Fan, L. Wang, H. Zheng, Preparation of dual crosslinked alginate-chitosan blend gel beads and in vitro controlled

release in oral site-specific drug delivery system, *International Journal of Pharmaceutics*, 336 (2007) 329-337.

[97] J. Crank, *The mathematics of diffusion*, (1979).



## CURRICULUM VITAE

Ing. Annalisa Dalmoro was born in 01/11/1984. She achieved the bachelor degree in Chemical Engineering, cum laude, in 2006, with a thesis entitled “Analysis of transport phenomena in matrices of swellable hydrogels”. Then she gained the Master Degree in Chemical Engineering, cum laude, in 2009 with a thesis entitled “Enteric micro-particles coated with smart polymers for controlled drug delivery applications”.

In the same year she started her Ph.D. study, described in this thesis, in Science and technologies for chemical, pharmaceutical, and food industry - curriculum Chemical Engineering. She produced several papers, of which some were published on international journals; the remaining being communications to international conferences, and papers published on national journals.

### *Publications:*

1. Barba A.A.; **Dalmoro A.**; d'Amore M.; (2012), “Microwave assisted drying of cellulose derivative (HPMC) granular solids”, in press on Powder Technology;
2. Barba A.A.; **Dalmoro A.**; d'Amore M.; Lamberti G.; “Controlled release of drugs from microparticles produced by ultrasonic assisted atomization based on biocompatible polymers”, Chem. Biochem. Eng. Q., 26(4) 345-354 (2012);
3. Barba A.A.; **Dalmoro A.**; d'Amore M.; Lamberti G.; “In vitro dissolution of pH sensitive micro-particles for colon-specific drug delivery”, in press on Pharmaceutical Development and Technology;

4. Barba A.A.; **Dalmoro A.**; d'Amore M.; (2012) "An engineering approach to biomedical sciences: advanced strategies in drug delivery systems production", *Translational Medicine @ UniSa*, 4 (1) 5-11 (2012);
5. **Dalmoro A.**; Barba A.A.; Lamberti G.; Grassi M.; d'Amore M.; "Pharmaceutical applications of biocompatible polymer blends containing sodium alginate", *Advances in Polymer Technology*, 31(3) 219-230 (2012);
6. **Dalmoro A.**; Barba A.A.; Lamberti G.; d'Amore M.; "Intensifying the microencapsulation process: Ultrasonic atomization as an innovative approach", *European Journal of Pharmaceutics and Biopharmaceutics*, 80 471-477 (2012);
7. **Dalmoro A.**; Lamberti G.; Titomanlio G.; Barba A.A.; d'Amore M.; "Enteric Micro-Particles for Targeted Oral Drug Delivery", *AAPS PharmSciTech*, 11(4) 1500-1507 (2010);
8. **Dalmoro A.**; Barba A.A.; d'Amore M.; Lamberti G.; "Micro-Systems Production: A Promising New Technique with Low Energy Consumption", *Scientia Pharmaceutica*, 78 (3) 670-670 (2010);
9. **Dalmoro A.**; Villano O.; Barba A.A.; Lamberti G.; "Dosare dove serve", *NCF-Notiziario Chimico E Farmaceutico*, 49 (4) 112-114 (2010);
10. Barba, A.A.; **Dalmoro, A.**; De Santis, F.; Lamberti, G. "Synthesis and characterization of P(MMA-AA) copolymers for targeted oral drug delivery", *Polymer Bulletin*, 62(5) 679-688 (2009)
11. Barba, A.A.; Chirico, S.; **Dalmoro, A.**; Lamberti, G. "Simultaneous measurement of Theophylline and Cellulose Acetate Phthalate in Phosphate Buffer by UV analysis", *Canadian Journal of Analytical Sciences & Spectroscopy*, 53(6) 249-253 (2009)
12. Chirico S., **Dalmoro A.**, Lamberti G., Russo G., Titomanlio G., "Analysis and modeling of swelling and erosion behavior for pure HPMC tablet", *Journal of Controlled Release*, 122 (2) 181-188 (2007)

***Proceedings:***

**Dalmoro A.**; Barba A.A.; Lamberti G.; d'Amore M., Sistemi particellari shell-core prodotti via atomizzazione assistita da ultrasuoni, presented to Convegno *GRICU 2012-Ingegneria chimica: dalla nanoscala alla macroscala*, 16<sup>th</sup>-19<sup>th</sup> September 2012, Montesilvano (PE) (Italy) - *SPEAKER*

Cascone S.; **Dalmoro A.**; Lamberti G.; Barba A.A., Metodi innovativi di preparazione e testing per sistemi farmaceutici, presented to Convegno *GRICU 2012-Ingegneria chimica: dalla nanoscala alla macroscala*, 16<sup>th</sup>-19<sup>th</sup> September 2012, Montesilvano (PE) (Italy) - *SPEAKER*

**Dalmoro A.**; d'Amore M.; Barba A.A., Shell-core particles production by coaxial double channel device, presented to 8<sup>th</sup> *World Meeting on Pharmaceutics, Biopharmaceutics and Pharmaceutical Technology*, 19<sup>th</sup>-22<sup>nd</sup> March 2012, Istanbul (Turkey) - *SPEAKER*

Galdi I.; **Dalmoro A.**; Lamberti G.; Titomanlio G.; Barba A.A.; d'Amore M.. "Modeling of the controlled drug release from solid matrices based on swellable/erodible polymeric hydrogels", presented to 19<sup>th</sup> *International Congress of Chemical and Process Engineering CHISA 2010 and the 7<sup>th</sup> European Congress of Chemical Engineering ECCE-7*, 28<sup>th</sup> August – 1<sup>st</sup> September 2010, Prague (Czech Republic) - *SPEAKER*

**Dalmoro A.**; Galdi I.; Lamberti G.; Titomanlio G.; Barba A.A.; d'Amore M.. "Targeted oral drug delivery by pH-sensitive microparticles", presented to 19<sup>th</sup> *International Congress of Chemical and Process Engineering CHISA 2010 and the 7<sup>th</sup> European Congress of Chemical Engineering ECCE-7*, 28<sup>th</sup> August – 1<sup>st</sup> September 2010, Prague (Czech Republic) - *SPEAKER*

Galdi I.; **Dalmoro A.**; Lamberti G.; Titomanlio G.; Barba A.A.; d'Amore M. "Swelling, erosion and drug release in hydrogel based solid matrices", presented to 7<sup>th</sup> *World Meeting on Pharmaceutics, Biopharmaceutics and Pharmaceutical Technology*, 8<sup>th</sup>-11<sup>th</sup> March 2010, Valletta (Malta) - *SPEAKER*

**Dalmoro A.**; Galdi I.; Lamberti G.; Titomanlio G.; Barba A.A.; d'Amore M. "PH-sensitive microparticles for enteric drug delivery by solvent evaporation from double emulsion", presented to *7<sup>th</sup> World Meeting on Pharmaceutics, Biopharmaceutics and Pharmaceutical Technology*, 8<sup>th</sup>-11<sup>th</sup> March 2010, Valletta (Malta) - *SPEAKER*

Barba A.A., Chirico S., **Dalmoro A.**, Galzerano B., Lamberti G., "Water and drug mass fraction profiles in HPMC/TP matrices", presented to *36<sup>th</sup> Meeting of Controlled Release Society*, 18<sup>th</sup>-22<sup>nd</sup> July 2009, Copenhagen (Denmark) - *SPEAKER*

Barba A.A., D'Amore M., **Dalmoro A.**, Lamberti G., Titomanlio G., "Enteric coated micro-particles for targeted and controlled release", presented to *36<sup>th</sup> Meeting of Controlled Release Society*, 18<sup>th</sup>-22<sup>nd</sup> July 2009, Copenhagen (Denmark) - *SPEAKER*

Chirico S., **Dalmoro A.**, Lamberti G., Russo G., Titomanlio G., "Radial water up-take in pure HPMC tablet analysis and model prediction", proceedings of Pharmaceutical Sciences World Congress, 22<sup>th</sup> -25<sup>th</sup> April 2007, Amsterdam (Netherlands)

## ***Acknowledgments***

*I would like to thank all the people who helped and supported me during these years of my Ph.D-experience.*

*A warm thanks to my supervisors for giving me the opportunity to carry out an interesting and pleasant work. In particular, much gratitude to prof. Matteo d'Amore for being a valuable reference point thanks to his knowledge, experience and humanity. A special "Thanks" to prof. Anna Angela Barba, who was not only a coach and a guide, but especially a friend and a confidant, the best I could hope!*

*Thanks also to prof. Gaetano Lamberti for having taught me love for research and for his continuous presence, only apparently offstage, but ever comforting.*

*I gratefully acknowledge prof. Giuseppe Titomanlio, especially for our sketch about my final Ph.D. presentation, the pharmacists and "the balance is not closed"!*

*I want to express my gratitude to my scientific referees, prof. Roland Bodmeier and prof. Nadia Passerini, for their availability to take part of my scientific committee and for their valuable suggestions.*

*A great thanks to my PhD-mate, Sara, for sharing the good and the bad situations, "the corner of mess-ups", the Gricu experience and the trips all over the Europe!*

*Thanks also to Valentina: we shared troubles and happiness since bachelor degree up to this important goal.*

*This Ph.D. has given me the opportunity to meet nice people for funny moments: the Gricu-mates...some of them became "my business partners".*

*Many thanks go to my two Sisters, Barbara & Monica: the lab T5a brought us together and it made us inseparable.*

*A kind thanks to the girls of lab. Impianti & Processi, who cheered up the work in the lab, and not only!!! Especially thanks to the “mad group” composed of Amanita, Clara, Enza, Giovanna, Margherita e Michela, headed by Giovanna: in her discovered an Authentic friend! I can't forget the two official “blighters” of the lab, Peppe and Marco, who made lighter work days with our coffees and lunches.*

*Here I come to the most important people of my life: my parents...thanks to them I have become what I am nowadays, and Gianni, who always supported me in everything, giving me serenity and love.*

*Finally I thank all the people with whom I have shared experiences, "mess-ups", a coffee, a pizza or a chat.*

*Simply thanks again to people who have believed and still believe in me...*

